REPORT DOCUMENTATION PAGE	Form Approved OMB No. 0704-0188

1. AGENCY USE ONLY *(Leave blank)*	2. REPORT DATE	3. REPORT TYPE AND DATES COVERED
	15 Dec 03	THESIS

4. TITLE AND SUBTITLE
"VALIDATION OF THE PARAMATERIZED REAL-TIME IONOSPHERIC SPECIFICATION MODEL (PRISM)"

5. FUNDING NUMBERS

6. AUTHOR(S)
LT ROBERT PULLIAM C

7. PERFORMING ORGANIZATION NAME(S) AND ADDRESS(ES)
OHIO STATE UNIVERSITY

8. PERFORMING ORGANIZATION REPORT NUMBER
CI02-230

9. SPONSORING/MONITORING AGENCY NAME(S) AND ADDRESS(ES)
THE DEPARTMENT OF THE AIR FORCE
AFIT/CIA, BLDG 125
2950 P STREET
WPAFB OH 45433

10. SPONSORING/MONITORING AGENCY REPORT NUMBER

11. SUPPLEMENTARY NOTES

12a. DISTRIBUTION AVAILABILITY STATEMENT
Unlimited distribution
In Accordance with AFI 35-205/AFIT Sup 1

DISTRIBUTION STATEMENT A
Approved for Public Release
Distribution Unlimited

12b. DISTRIBUTION CODE

13. ABSTRACT *(Maximum 200 words)*

20040105 018

14. SUBJECT TERMS

15. NUMBER OF PAGES
115

16. PRICE CODE

17. SECURITY CLASSIFICATION OF REPORT	18. SECURITY CLASSIFICATION OF THIS PAGE	19. SECURITY CLASSIFICATION OF ABSTRACT	20. LIMITATION OF ABSTRACT

VALIDATION OF THE PARAMATERIZED REAL-TIME IONOSPHERIC SPECIFICATION MODEL (PRISM)

A Thesis

Presented in Partial fulfillment of the Requirements for

The Degree Masters of Science in the

Graduate School of The Ohio State University

By

Robert Charles Pulliam, B.S.

*****

The Ohio State University
2003

Masters Examination Committee:

Dr. Jeff Rogers, Advisor

Dr. Jay Hobgood

Approved by

_____

Advisor
Department of Atmospheric Sciences

ABSTRACT

The earth's ionosphere between 60km and 1000km altitude contains a significant amount of partially ionized plasma that affects the propagation of radio waves. This plasma is created when extreme ultraviolet (EUV) light from the sun strips electrons from the neutral molecules in the Earth's atmosphere. The ionosphere's free electron density is highly variable and often unstable and can adversely affect Department of Defence systems which rely on radio wave propagation. These effects include: inaccurate position readings from GPS satellites, communication disturbances, and communication outages. The Air Force Research Laboratory has developed a Parameterized Real-time Ionospheric Specification Model (PRISM) that specifies the density of free electrons in the ionosphere on a global scale. This research will focus on validating PRISM using data from GPS satellites, the Digital Portable Sounding (DPS) network, and TOPEX/Poseidon data. In order to do a complete performance analysis, several time periods (3-6 weeks) of varying solar activity will be selected. Once these periods are selected PRISM will be initialized two different ways. The first initialization will be made without any real time input data and the output will be purely PRISM climatology. As for the second initialization PRISM will be given the real time data that the Air Force Weather Agency uses and the output will be an

adjusted climatology. Once these two sets of PRISM runs are complete they will be compared to the validation data and an analysis of the improvement gained by using the input data can be made. Additionally, the performance of PRISM at different solar activities, times of the day, and varying latitudes will be explored.

Dedicated to my wife

ACKNOWLEDGMENTS

I would like to express my sincere thanks to Dr. Dwight Decker (Air Force Research Lab), & Dr. Patricia Doherty (Boston College) for the data and guidance throughout this research project. They provided, advice, resources and insight that helped me tremendously throughout this research. Without their assistance this project would have not been possible. I would also like to thank my advisor Dr. Jeff Rogers for his patience and genuine interest in this project. His flexibility in allowing me to pursue a research topic outside his area of expertise is most appreciated.

I would also like to extend thanks to all the faculty in the Atmospheric Sciences Department, Dr. Rogers, Dr Hobgood, and Dr. Arnfield for their willingness to work with the time the Air Force has allowed for me to get my degree. This has truly been one of the most challenging and rewarding experiences of my life. The knowledge gained at Ohio State will help me go far in my Air Force career in being a successful weather officer.

Most importantly, I would like to thank my wife, [redacted], who has gone out of her way in supporting me though this time consuming effort. Without her support this would have not been possible.

VITA

[redacted]	Born – Duluth, Minnesota
May 1999	B.S. Physics, University of Wisconsin Commissioned in the US Air Force
June 1999	Married [redacted]
1999-2002	Space Forecasting Test Manager USAF, Space Vehicles Directorate Hanscom AFB, Lexington, MA
2002-Present	Graduate Student/Air Force Officer The Ohio State University Columbus, OH

PUBLICATIONS

1. R. C. Pulliam, R. Rybski, "Asteroid Detection System", National Conference for Undergraduate Research, Salisbury, Maryland, Apr 1998.

2. R. C. Pulliam, R. Rybski, "Asteroid Detection System", National Conference for Undergraduate Research, Salisbury, Maryland, Apr 1999.

3. R. C. Pulliam, W. Borer, "PRISM Validation Study", Proceedings of the 2000 Space Weather Conference, Boulder CO, May 2000.

4. R. C. Pulliam, W. Borer, D. Decker, P. Doherty, "Operational Ionosphere Model Validation", Proceedings of the American Institute of Aeronautics and Astronautics Space 2000 Conference & Exposition, Paper #A00-42948, Long Beach, CA, Sep 2000.

5. R. C. Pulliam, W. Borer, "PRISM Validation Study - Update", Proceedings of the 2001 Space Weather Conference, Boulder CO, May 2001.

FIELDS OF STUDY

Major Field:	Space & Tropospheric Weather
Minor Fields:	Physics, Astronomy, & Math

TABLE OF CONTENTS

LIST OF TABLES

LIST OF FIGURES

Chapter 1

Introduction

1.1 The Ionosphere

The ionosphere is the region of charged particles surrounding Earth between the altitudes of 60km – 1000km and is created by the ultraviolet (UV) radiation from the Sun [Jursa, 1985]. This process is called photo ionization which produces the following reactions:

$$O_2 + photon \rightarrow O_2^+ + e^-$$
$$O + photon \rightarrow O^+ + e^-$$
$$N_2 + photon \rightarrow N_2^+ + e^-$$

Since the ionosphere is created by the sun's UV radiation the density is dependent on the time of day. So after sunset photo ionization stops and the free electrons begin to recombine with the O_2, O, N_2, ions [Tascione, 1994]. This recombination often eliminates some layers of the ionosphere completely. The distribution of the ionosphere is best described by the continuity equation:

$$\frac{\Delta N_e}{\Delta t} = P - L + T$$

- $\frac{\Delta N_e}{\Delta t}$ = Rate of change in the density of electrons with time
- P = Production rate of electrons from UV radiation.
- L = Loss rate of free electrons from recombination.
- T = Transport rate at which electrons are transported into or out of the volume.

The production rate (P term) is the daytime source for creating the ionosphere and during the night recombination (L term) attributes to decreasing the density of the ionosphere. The transport term represents the

movement of electrons from one area to another caused by plasma drift. Plasma drift occurs when ions move from an area of higher density to a region of lower density. This drift can come from several factors such as gravity, neutral winds, and the earth's magnetic field. The variability of this drift is dependent on the altitude because the density of the ionosphere varies with height.

The ionosphere is also considered to be a plasma. A plasma is composed of a collection of discrete ionized particles. However not every collection of charged particles qualifies as a plasma, as certain criteria must be met. Over large length scales, the medium must be electrically neutral. For a plasma composed of electrons and protons, electrons are attracted toward protons and repulsed from other electrons by electrostatic forces. So at a certain distance from a charged particle, its charge can no longer be seen due to the shielding, or screening, of the other charged particles around it. This distance is called the Debye length (l_D), which is defined by the following equation:

$$l_D^2 = kTe_o/nq^2$$

- l_D = Debye length
- k = Boltzman constant
- T = Temperature
- e_o = the permittivity of free space
- n = the plasma number density
- q = the unit electric charge.

Within a sphere of this radius, there are

$$N_D = 4\ \pi\ n\ l_D^3$$

other charged particles. An ionized gas is termed a plasma when:

$$g = 1/N_D << 1$$

·g is called the plasma parameter.

This plasma parameter depends on the charged particle density and the average energy of the particles measured by the temperature. In the ionosphere, g ranges from 10^{-4} to 10^{-6}. So considering the ionosphere a plasma is certainly valid.

Earth's ionosphere is divided into several regions designated by the letters D, E, F (Figure 1.1). These regions may be further divided into several regularly occurring layers, such as F1 and F2. Historically, these divisions arose from the successive plateaus observed in the electron number density. Distinct ionospheric regions develop because (1) the solar spectrum deposits energy at different heights depending on absorption characteristics of the atmosphere, (2) the physics of recombination depends on the density, which exponentially decreases with height, and (3) the composition of the atmosphere changes with height. Thus the main ionospheric regions can be associated with different governing physical processes. In figure 1.2 you can see the dominating molecules as a function of height [Canck, 2002].

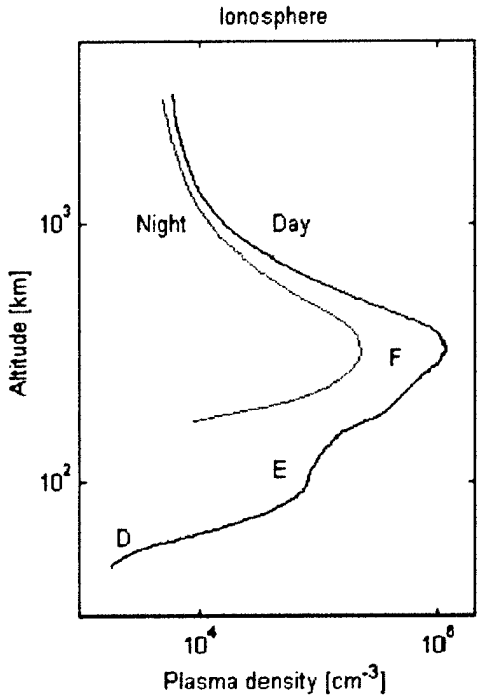

Figure 1.1: Plasma Density [cm^{-3}] with Height [km].

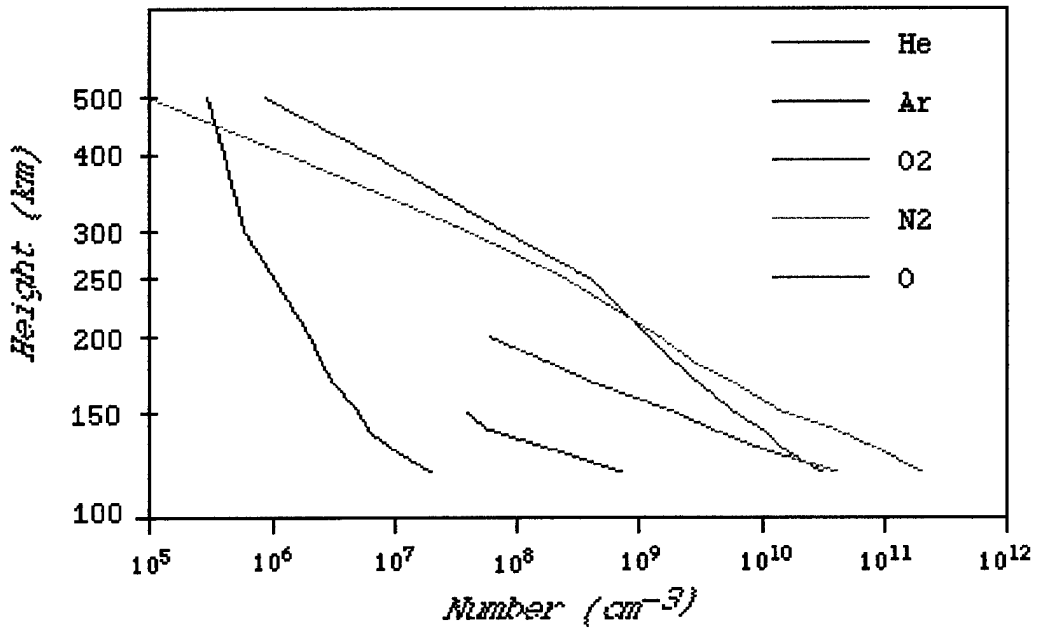

Figure 1.2: Molecule Species with Height

1.1.1 D Region

The D region is the region of the ionosphere that is approximately 60km to 90km above the surface of the earth. The charged particle number density ranges from between 10^2 to 10^4 cm^{-3} during the day and completely vanishes during the night due to recombination. During sunrise ions are formed by the ionization of atmospheric neutrals by the Extreme Ultra Violet (EUV) radiation (.1-.11um). Due to the relatively high ambient atmospheric pressure, many negative ions are produced by electron attachment to atomic and molecular neutrals. Positive and negative ions of N_2, O_2, and O are dominant constituents.

1.1.2 E Region

The E region lies between an altitude of 90 and 150 km above the earth. The electron densities range on average between 10^5 cm^{-3} (in the daytime) to 10^4 cm^{-3} (at night). Ions in this region are mainly O, O_2^+, and N_2^+, formed by EUV radiation below .11um. Other subdivisions, isolating separate layers of irregular occurrence within this region, are also labeled with an E prefix, such as the thick layer, E2. Unlike the D region, the E region can persist throughout the night as a result of dense patches of ionization called Sporadic E. Upward propagating gravity waves and tides collect this ionization into thin, downward propagating layers of enhanced ionization which can occur at all latitudes [Hargreaves, 1992]. The presence of the nighttime E region and sporadic E are thought to be due to electron and meteor bombardment from space.

1.1.3 F Region

The region above about 150 km is known as the F region. This region is often divided into the F1 and F2 regions. The F1 region (150km to 200km) has a maximum electron number density of a few times 10^5 cm^{-3} at about 200 km altitude, and the density of the F2 region varies between 10^6 and 10^5 cm^{-3} between day and night respectively. The altitude of maximum electron density in the F2 region is roughly 350 km. This peak is highly variable depending upon daily, seasonal, and sunspot-cycle variations. It is important to note that even at this maximum, the charged particle number density is less than the number density of neutral atmospheric gas; electron density ~ 10^6 cm^{-3} , while neutral number density ~ 10^9 cm^{-3}. The F region is formed by ionization of atomic oxygen by Lyman emissions and by emission lines of He. In the lower part of the F region, O^+ ions readily transfer charge to neutrals forming N_2^+. In the F2 region, O^+ remains the dominant ion.

1.1.4 Latitude and Local Time Variations

Not only does the ionosphere vary with altitude, but it also varies with latitude, local time, and season. These variations are largely dependent on solar zenith angle, which controls the amount of photoionization (appendix G contains a sample PRISM TEC output for 24 hours). The response of the ionosphere to sunrise and sunset is very rapid; electron densities can increase/decrease by two orders of magnitude within an hour of dawn/dusk, revealing the dependencies on zenith angle. A dependence on latitude is because as the northern hemisphere enters into its winter months and the solar zenith angle increases, the photoionization rate drops resulting in a

decrease in electron density. Additionally, ionization due to particle precipitation demonstrates electron content dependence on latitude. Particle precipitation happens when charged particles follow the earth's magnetic field lines and bombard the high latitude ionosphere resulting in large electron production rates in the high latitudes.

Other phenomena that influence the electron content of the ionosphere are the Sudden Ionospheric Disturbance, the Appleton Anomaly, and the Mid-latitude F2 Winter Anomaly. The Sudden Ionospheric Disturbance occurs within minutes of a strong solar flare. The X-rays emitted from the flare lead to a large ionization of the ionosphere and is normally about an hour of duration. The Appleton Anomaly (or Equatorial Anomaly) is high concentrations of electrons on either side of the geomagnetic equator in the post sunrise sector (+/- 15 degrees magnetic latitude). The Mid-latitude F2 Winter Anomaly is the transport of plasma by neutral winds from the summer hemisphere to the winter hemisphere causing the daytime F2 peak electron density in wintertime to be as much as four times greater than the density in the summertime hemisphere. The Winter Anomaly occurs during solar maximum conditions and is most apparent between 45-55 north magnetic latitude.

The eleven-year solar cycle also influences the ionosphere. During periods of high solar activity there is an increase in the number of high energetic particles discharged from the sun, which increases particle precipitation. Particles precipitating can increase ionization by an order of magnitude from solar minimum to solar maximum. Also during periods of

high solar activity there is an increase in the number and strength of geomagnetic storms. However geomagnetic storms are observed during quiet solar conditions too [Tascione, 1994].

1.2 Introduction to PRISM

PRISM is comprised of two components, a Parameterized Ionospheric Model (PIM), and a Real Time Adjustment (RTA) algorithm [Daniell and Brown, 1995]. PIM is a global specification of ionospheric free electron densities that was created from curve fits to the output fields of several theoretical ionospheric models. This description of the ionosphere's average behavior is referred to as climatology. The inputs for PIM are: solar activity (F10.7) which is a measure of the sun's radiation at a wavelength of 10.7cm, magnetic activity (Kp) which is an indicator of the general level of magnetic field strength variations measured at the Earth's surface, and the strength of the sun's interplanetary magnetic field (IMF) vectors B_y and B_z measured by a Magnetometer aboard the Advanced Composition Explorer (ACE) satellite. The output of PIM is a global 3-dimensional specification of electron densities which includes the ionosphere's E-region (~90-155km) and the F2-region (~250-1000km), critical frequencies of the E and F2 region (foF2) where the critical frequencies are the highest HF frequency able to be reflected by the layer without penetrating it, and heights of the E layer and F2 layer. Variations in the critical frequency are caused by variations in the density of the ionosphere. A larger density (or higher TEC value) will reflect a higher wavelength than smaller density. As for the output, the electron densities from PIM and PRISM are available in two formats: (1) gridded output on a

regional or global grid in geographic or geomagnetic latitude and longitude, (2) output at a set of user specified points in geographic coordinates on the Earth's surface.

1.2.1 PIM

The parameterised database was generated using an ensemble of four separate physical models: (1) a low latitude F layer model (LOWLAT), (2) a mid latitude F layer model (MIDLAT), (3) a combined low and middle latitude E layer model (ECSD), and (4) a high latitude E and F layer model (TDIM). All four models are based on a tilted dipole representation of the geomagnetic field and a corresponding magnetic coordinate system. In addition, information on heat transport, thermospheric winds and plasma drift velocities were incorporated into these models. From running these four models a parameterised representation of the ionosphere database was developed. This process took into account different geomagnetic conditions (Kp), solar activity (F10.7), universal times, Interplanetary Magnetic Field (IMF) By direction, geomagnetic latitudes and longitudes, and days of the year. Since it would take a long time and a large amount of computer memory in order to account for every possible combination of these parameters these models were run for a relatively small number of possible conditions [Daniell and Brown, 1995]. This parameterisation was accomplished in a two-step process. First, the models were used to generate a number of databases for a discrete set of varying solar activity. Each of these databases consisted of ion density profiles on a discrete grid of latitudes and longitudes for a twenty-four hour period. Second, in order to reduce the

storage requirements the databases were approximated with semi-analytic functions. The tables below shows the values used in generating these databases as well at the grid resolution used.

Model	Solar activity F10.7	Magnetic activity Kp	IMF By	Day of the year	Databases
LOWLAT	70, 130, 210	N/A	N/A	80, 172, 264, 355	36a
MIDLAT	70, 130, 210	1, 3.5, 6	N/A	80, 172, 264, 355	54b
ECSD	70, 130, 210	1, 3.5, 6	N/A	80, 172, 264, 355	54c
TDIM	70, 130, 210	1, 3.5, 6	+,-	80, 172, 264, 355	324d

a. 3 seasons X 3 solar activities X 4 longitude sectors
b. 3 seasons X 3 solar activities X 3 magnetic activities X 2 hemispheres
c. 3 seasons X 3 solar activities X 3 magnetic activities X 2 species
d. 3 seasons X 3 solar activities X 3 magnetic activities X 2 By's X 3 species X hemispheres.

Table 1.1: Geophysical Parameter Values

Model	Magnetic Latitude	Magnetic Longitude	UT (Magnetic Local time [MLT])
LOWLAT	-32 to 32 in 2 deg steps	30, 149, 250 and 329	MLT: 0-23.5 in .5 hour steps
MIDLAT	30 to 74 and –30 to –74 in 4 deg steps	0 to 345 in 15 deg steps	MLT: 1-23.5 in 2 hour steps
ECSD	-76 to 76 in 4 deg steps	0 to 345 in 15 deg steps	MLT: 1-23.5 in 2 hour steps
TDIM	51 to 89 and –51 to 89 in 2 deg steps	Magnetic Local Time .5- 23,5 in 1 hr steps	MLT: 1-23.5 in 2 hour steps

Table 1.2: Horizontal Grid Resolution used for Climatology

1.2.2 The Low Latitude F Layer Model

The low latitude F region model (LOWLAT) was originally developed by Anderson, [1973]. It is designed to solve the diffusion equation for O+ along a magnetic flux tube. Normally, the entire flux tube is calculated with chemical equilibrium boundary conditions at both feet of the tube. A large number of flux tubes must be calculated in order to build up an altitude profile. Since heat transport is not included in this model, ion and electron temperature models must be used. The LOWLAT model makes use of the of the ion and electron temperatures by a model developed by Brace and Theis [1981] and the Horizontal Wind Model (HWM) of Hedin [1988] for the thermospheric winds.

The critical feature incorporated in the low latitude model is the dynamo electric field. The horizontal component of this field drives upward convection due to the earth's electric and magnetic field, and this can significantly modify profile shapes and densities. This phenomenon is responsible for the equatorial anomaly, crest in the ionisation on either side of the magnetic equator at ± 15 to 20 degrees magnetic latitude. In the current version of PRISM the ExB vertical drift used for these calculations was based on the empirical models derived form data from the Atmospheric Explorer-E satellites [Fejer, 1995]. Which are consistent with the drifts measured at Jicamarca, Peru but include longitudinal variations as well.

1.2.3 The Mid latitude F Layer Model

The mid latitude F region model (MIDLAT) is the same as the low latitude version, except that the dynamo electric field is not included.

Complete flux tubes are followed, but neither horizontal nor vertical convection is included. The computer resource requirement of MIDLAT are far less that those of LOWLAT. As long as the boundary between low and middle latitudes is chosen so that the electric field is negligible on the boundary flux tubes, the two models give identical results at the boundary ensuring continuity across that boundary. For the PRISM development the same temperature model [Brace and Theis, 1981] and the same thermospheric wind model [Hedin, 1988] were used.

1.2.4 The Low and Midlatitude E Layer Model

The low and mid-latitude E region model (ECSD) was developed by Dwight T. Decker and John R. Jasperse and incorporate photoelectrons calculated using the continuous slowing down (CSD) approximation [Jasperse, 1982]. Ion concentrations are calculated assuming local chemical equilibrium. A small nighttime source is included to ensure that an E layer is maintained throughout the night.

1.2.5 The High Latitude Model

The high latitude model (incorporating both E and F layers) is the Utah State University (USU) Time Dependent Ionosphere Model (TDIM). This model is similar to the low and middle latitude models except that the flux tubes are truncated and a flux boundary condition is applied at the top. In addition, the flux tubes move under the influence of the high latitude convection electric field. In the low latitudes, because the magnetic field is mainly horizontal, the effect of the electric field is mainly vertical, and the electric-field-driven convection is horizontal. TDIM includes an E layer model that

incorporates the effects of ionisation by precipitating auroral particles. The ion production rates used were calculated using the B3C electron transport code [Strickland, 1994] and incident electron spectra representative of DMSP SSJ/5 data. The characteristics of the electron spectra were taken from the Hardy [1987] electron precipitation model.

1.2.6 PRISM's RTA Algorithm

The availability of real time data permits operation of PRISM's RTA algorithm that adjusts the model output to fit the real time measurements. The real time data include: density profile parameters (foF2=density of F2 layer, hmF2=height of the F2 layer, foE=density of E layer and hmE=height of the E layer), total electron content (TEC) which is the line integral of electron density from the receiver to the satellite (1 TEC unit = $10^{16}/m^2$), and a variety of in situ plasma and precipitating particle measurements from the Defence Meteorological Satellite Program (DMSP). The amount the RTA algorithm modifies the PIM output profiles to match the data is determined by the following weighting function:

$$W(lat,lon)=1/d_n(lat,lon) \qquad d_n(lat,lon) = .5[1-\cos\Upsilon_n(lat,lon)]$$

Where d_n is the distance between the data point and the point to be adjusted in PIM, lat and lon are the latitude and longitude, respectively, and Υ is the angle of separation between the two points with respect to the center of the Earth. Figure 1.3 below show the data flow in the operation of PRISM.

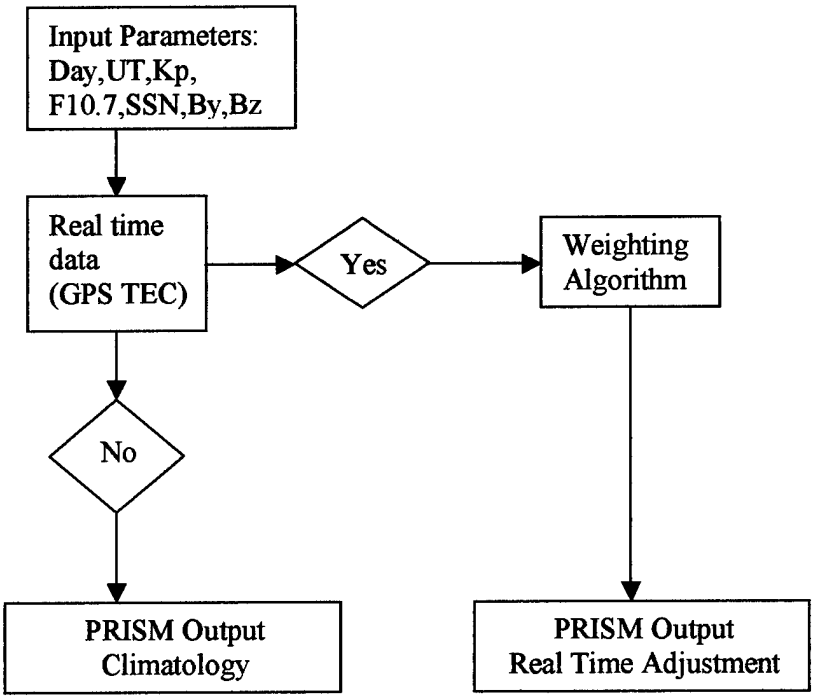

Figure 1.3: Operation of PRISM

Chapter 2

The Validation of PRISM

2.1 Past Validation

A previous validation of PRISM was conducted by Pulliam [2000] and focused on determining the improvement gained when running PRISM with real time GPS data. In this study data were processed and quality controlled from sixty-two dual frequency GPS stations from the International GPS Service (IGS) network for a one week period of quiet magnetic activity (13 Jan 00 - 19 Jan 00). Thirty-seven of these stations were selected as inputs for PRISM while the remaining twenty-five were used as ground truth for the validation. By using the Receiver Independent Exchange (RINEX) data from the GPS receivers the Total Electron Content (TEC) values were calculated from the differential group delay and phase advance measurements routinely made by the receivers which monitor the L1 (1575.42 MHz) and L2 (1227.6 MHz) frequencies of GPS satellites. Since the GPS signal is a time-encoded transmission, the time of flight for each of these signals can be calculated. By comparing these two time of flight measurements it is then possible to calculate the refraction of the GPS signal caused by the ionosphere. This result is then converted to a slant TEC measurement along the line of sight (LOS) from the receiver to the satellite. Where a TEC unit is the line integral of electron density from the receiver to the satellite (1 TEC unit = $10^{16}/m^2$). However, in order to use these measurements for PRISM inputs, they must first be converted to vertical equivalent TEC (VETEC). This conversion assumes that the height of the ionosphere is 400km. The formula for this

conversion is: VETEC = (Slant TEC) x cos[arcsin(.94092 x cos(Elevation angle))]. Where the elevation angle is the angle from the horizon to the satellite. Figure 2.1 shows the geometry of this conversion.

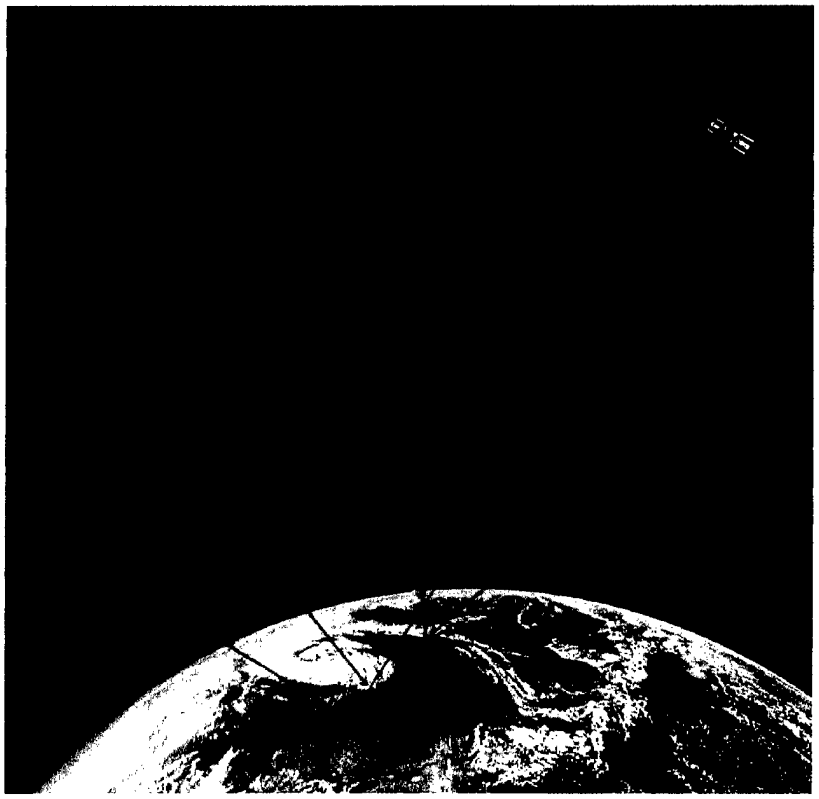

Figure 2.1:Convertion from Slant TEC to Vertical Equivalent TEC (VETEC)

The distribution of the IGS stations used in this study are represented in Figures 2.2 and 2.3. The triangles represent the location of the input stations and the asterisks represent the location of the ground truth stations.

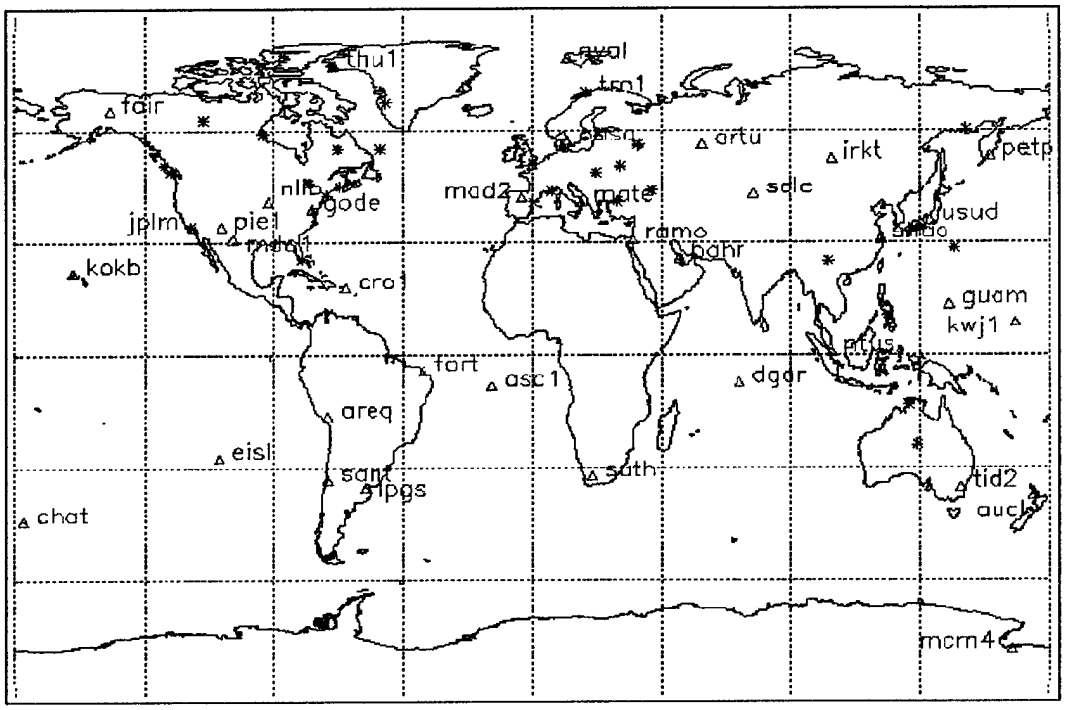

Figure 2.2: Distribution of the Input GPS Stations for PRISM.

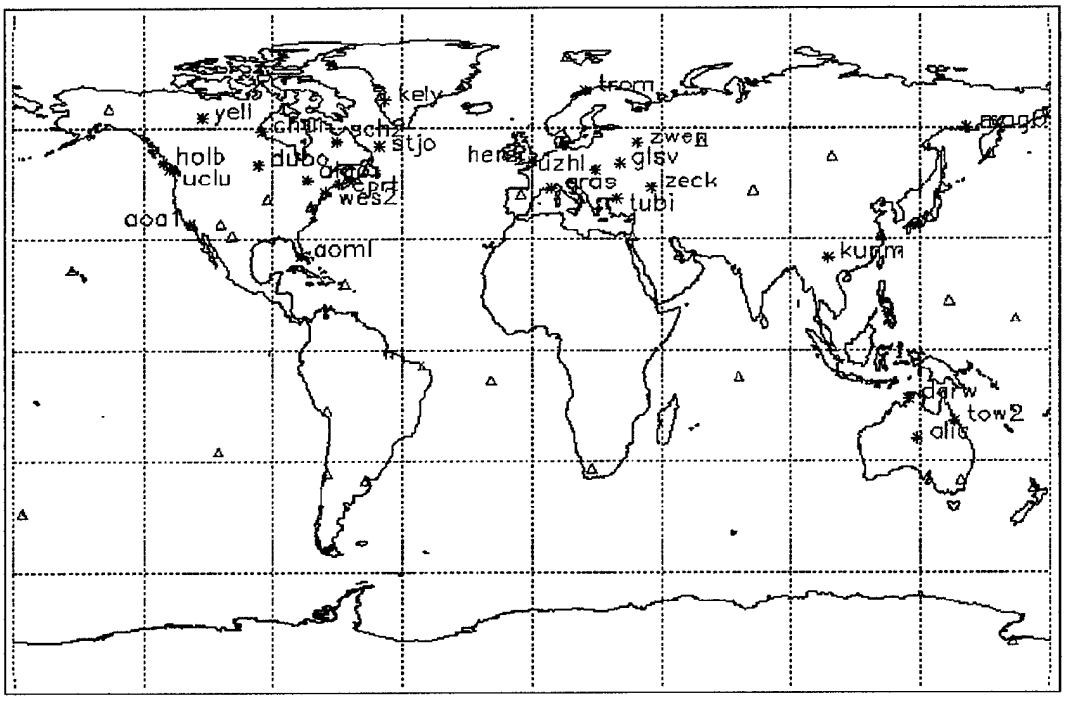

Figure 2.3: Distribution of the GPS Ground Truth Stations for PRISM.

2.1.1 Validation Method:

PRISM was run twice for the 1 week period at hourly intervals to produce two different global 3-dimensional ionospheric specifications. The first run was done with no input data and produced a PIM output based only on climatology. In the second run, PRISM was given the TEC data from the thirty-seven input stations to produce an adjusted climatology output. Figure 2.4 is an example of the TEC data used and shows its diurnal pattern. The variation in the individual station maximum is due to the stations magnetic latitude. For example station AREQ which is in Peru is peaking near 100 TEC units, and ARTU at a higher latitude is around 40 TEC units.

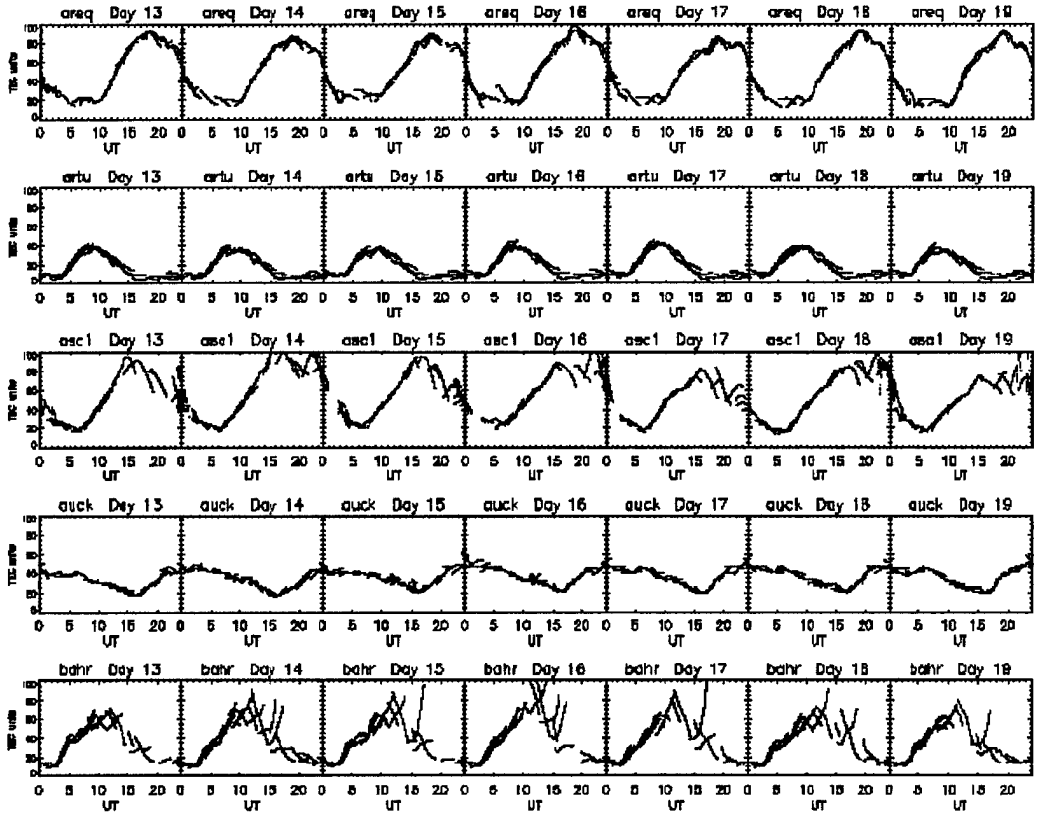

Figure 2.4: Processed Data from the GPS Receivers.

For the validation the ground truth slant TECs (STEC) were compared to PRISM's STECs. The PRISM STEC was calculated by integrating along the ground truth LOS through PRISM's 3-dimensional electron density specification from an altitude of 90km to 1600km. This comparison was done on both PRISM runs for all STEC values for all ground truth stations. From these results it was determined how much the input data improved the accuracy of the model with respect to the ground truth.

2.1.2 The Results.

The major objective of this study is to compare the PRISM STEC (model value) with the ground truth STEC (GPS measured value). Figure 2.5 shows the difference between (PRISM's STEC) minus (Ground truth STEC) vs number of occurrences (individual measurements). The errors are expressed in TEC units . The solid line represents the PRISM runs with no input data (climatology), and the dashed line represents the PRISM runs with the input data. Each of these station's summary plots show a significant improvement when PRISM is given the thirty-seven stations of data. Both the large positive and negative errors were reduced and there is a larger number of these differences centered around zero. Figure 2.6 shows the PRISM outputs compared with the input slant TEC data. This was done to gain confidence in PRISM's ability to assimilate the real time data and to assess how well PRISM was able to reproduce the slant TEC when given VETEC.

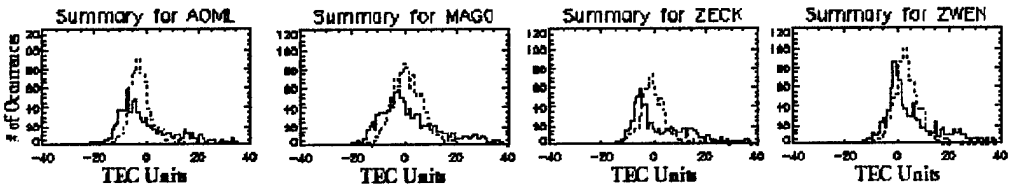

Figure 2.5: Station Summary Plots (PRISM vs Ground Truth)

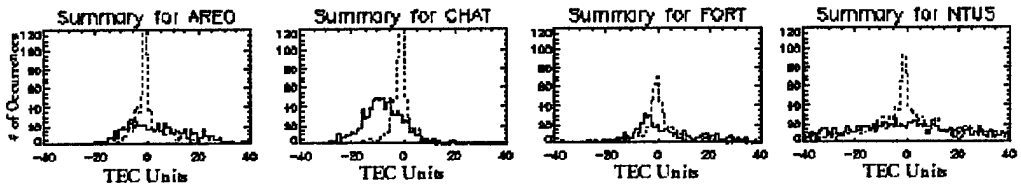

Figure 2.6: PRISM Output Compared to the Input Data.

As seen from this diagram the model does a very good job at assimilating the data. However a closer look was taken on this data because a perfect assimilation would represent a delta function. When doing this it was noticed that 90% of the larger error came from data that had a very low elevation angle, which is the angle of the GPS satellite with respect to the horizon. This error is thought to be caused by multi-path interference caused by obstacles on the surface. So to eliminate this error from this study the elevation was limited to 45 degrees and greater. In Figure 2.7 all the summary plots of the stations were combined in one concise plot. The addition of input data into PRISM results in an overall improvement in the error distribution. However, the detail as to how the individual ground truth stations are affected is lost in this display.

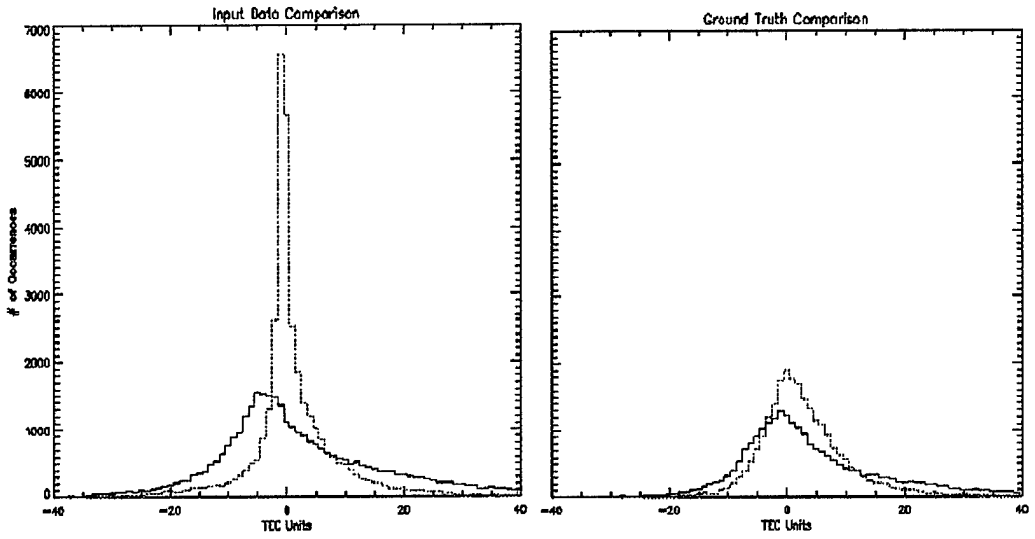

Figure 2.7: Input data and ground truth comparisons.
The dashed line represents the PRISM run with input data.
The solid line represents the PRISM run with no input data

2.1.3 Summary and Conclusion

In this study more than 150,000 measured STECs were made from sixty-two globally distributed IGS receivers during this one week period in January. Thirty-seven of these receivers were used as inputs in PRISM. The remaining twenty-five, were set aside to be used as ground truth. In this validation effort PRISM was run two ways:

Run 1 = PRISM run with no input data (climatology).

Run 2 = PRISM run with the thirty-seven stations (RTA).

In the first PRISM run, the only model inputs were the date, F10.7, Kp, and By and Bz components. However for the second PRISM run the GPS vertical TEC data were also given to PRISM to do the RTA. With these two sets of runs a comparison was made to determine the improvement when input data was used. The results of this comparison showed an overall improvement when the RTA was made to the input data. Figure 2.8 summarizes the TEC specification improvements in TEC units for each GPS receiver.

Overall, the average standard deviation of the TEC error when compared to the ground truth data was reduce by 6.1 TEC units (44% improvement over climatology), the mean error was reduced by 2.3 TEC units (39% improvement over climatology), and the root mean square (RMS) error was reduce by 6.4 TEC units (42% improvement over climatology) during this validation time period. However, the most striking results came from the station by station analysis (Figure 2.8). For the majority of the mid latitude station the errors were usually

cut in half with the use of the input data, although a few stations showed little to no improvement. By looking at these three stations closer (KELY, YELL, TROM) three conclusions were drawn. The first was that the model with no input data did fairly well in the station's region and input data did not really have an effect. Secondly, the model is slightly misplacing a TEC gradient, or that the slant to vertical conversion is either over or under estimating the input VETEC which would incorrectly adjust the model. Lastly is the fact that these stations are all in the high latitude region. This region of the ionosphere is highly dynamic which makes it very difficult to model. So PRISM may not be the first choice in models for high latitudes. For this region a physics based model may be more appropriate.

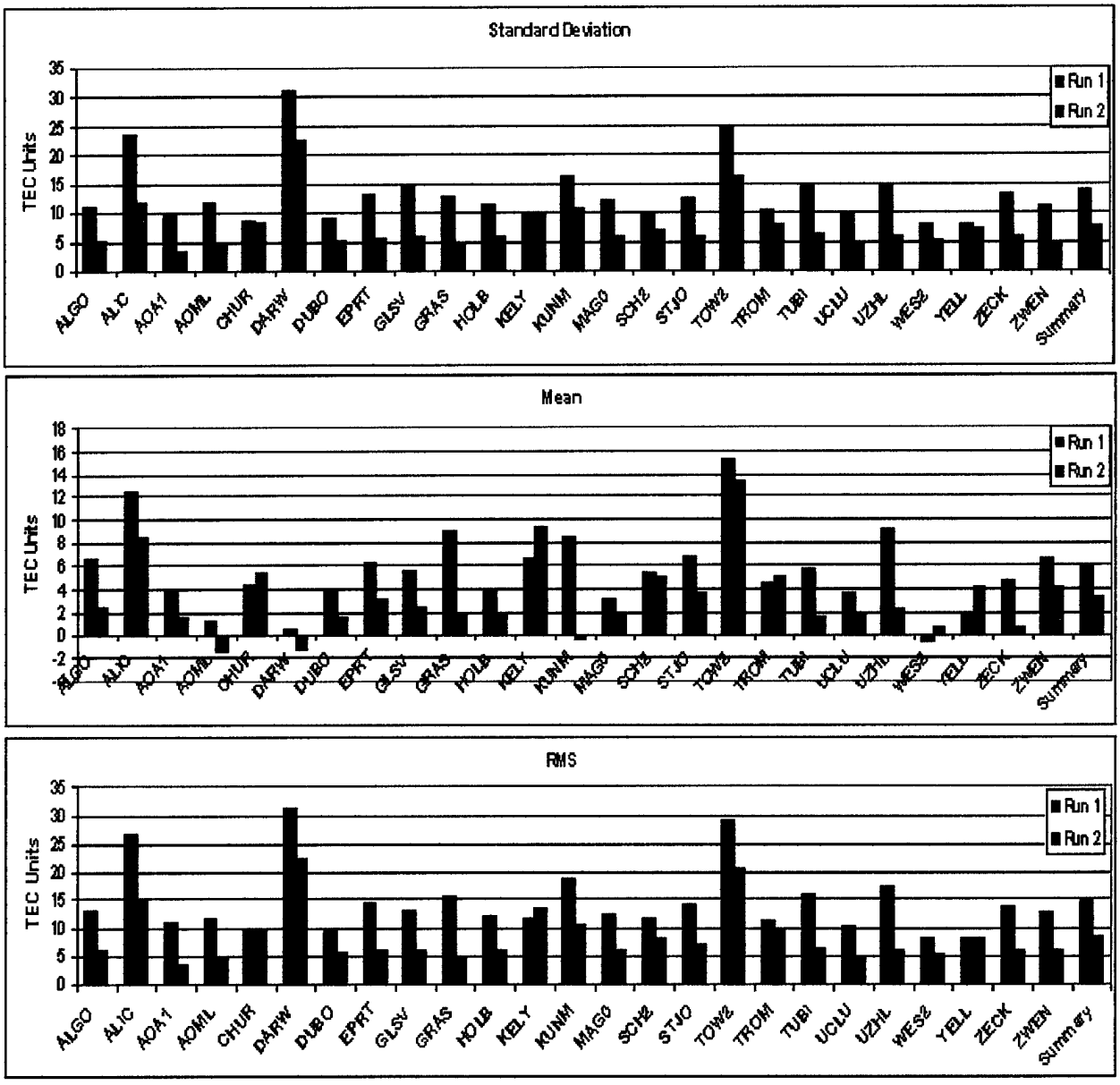

Figure 2.8: Statistics for the Ground Truth Summary Plots for PRISM.

2.2 This Validation

2.2.1 Introduction

In this validation PRISM was set up to run hourly to produce electron densities on a global grid (a partial PRISM output is in appendix F). PRISM has a maximum resolution of two degrees by two degrees. However, in order to reduce the computation time and hard drive space, the resolution was set to four degrees by four degrees. For each of the grid points PRISM computes the electron density at fifty different altitude levels. Table 2.1 below shows the altitudes used for this study.

90	160	290	750
95	170	300	800
100	180	320	850
105	190	340	900
110	200	360	1000
115	210	380	1100
120	220	400	1200
125	230	450	1300
130	240	500	1400
135	250	550	1500
140	260	600	1600
145	270	650	
150	280	700	

Table 2.1: PRISM Altitude Profile in Kilometers

A finer altitude resolution was used for the lower levels of the ionosphere due to the greater variability in this region. The lower ionosphere has the greatest electron density.

PRISM was run twice at hourly intervals during the period of February 4 2002 (day 35) – July 19 2002 (day 200). The first run was done with no input data (only Kp, Day, UT, F10.7, SSN, By and, Bz) which produced a PRISM output based only on climatology (CLM). In the second run, PRISM was given the GPS TEC data used by the Air Force Weather Agency (AFWA) to run PRISM in real time to produce an adjusted climatology output (RTA). This GPS data are provided by the Jet Propulsion Lab in Pasadena CA from a sub set of their global network of GPS stations operating in real time. The figure below shows the locations of these GPS stations.

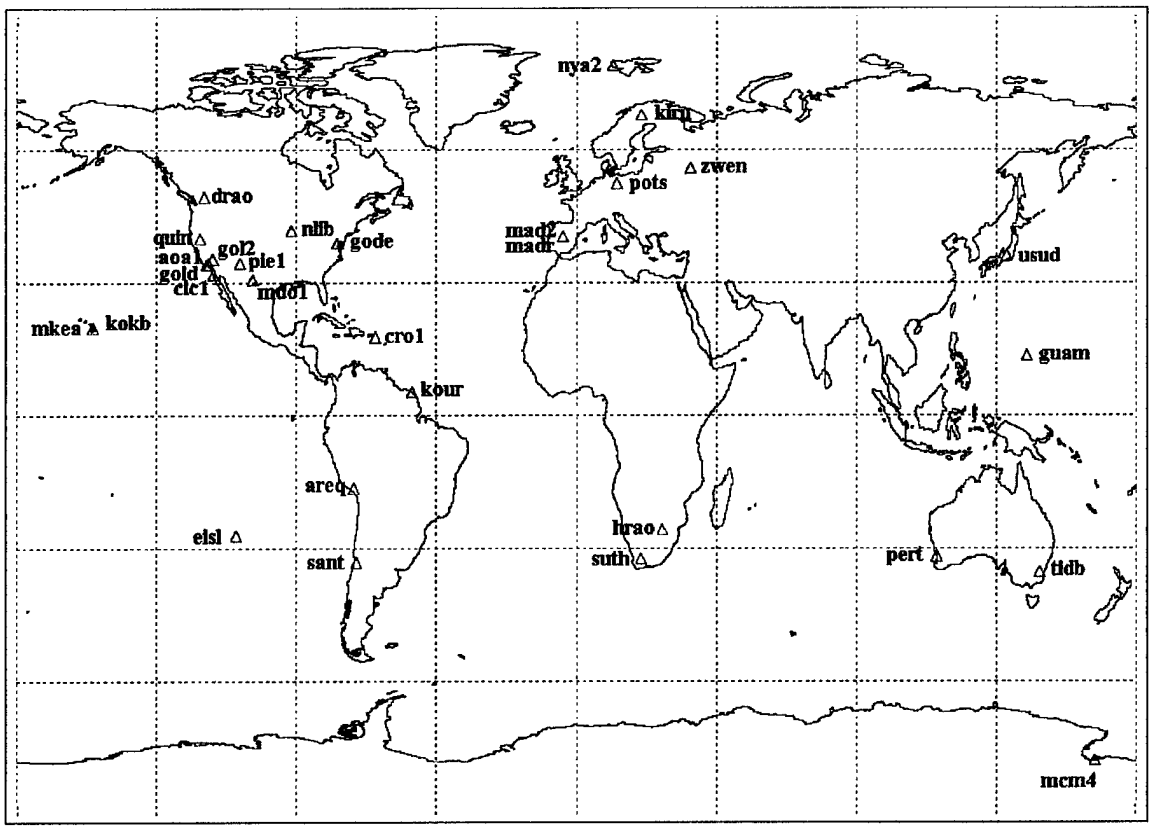

Figure 2.9: Distribution of GPS Stations

The first step in the validation is to look at the quality and consistency of the GPS data given to PRISM. To do this the TEC data were plotted for each station for every day. This resulted in 165 daily plots for each of the thirty stations. Appendex A contains a sample of these plots for station PERT which is located in Australia. A summary of the station inconsistencies is listed in table 2.2.

Station	Findings
aoa1	Excellent, S: 55, 90,106 M: 57
Areq	Fair, S:35-72,77 M:44-46,64,89,90
cic1	Good, S:56,60,65,69,77,106,126,141,157,186 M:48,200
cro1	Excellent, S: 65,77,106,153,187,186 M: 200
Drao	Good, S:46,65,77,61,62,106,125,153,157,167,186
Eisl	Poor - many days very sparse, M:57-59,60,134-143,147,148,187,200
Gode	Poor - many days very sparse, M: 47,56,69,81,82,90-106,113,124-129,166,200
gol2	Excellent, S:77,106,107,186 M:
Gold	Excellent, S:106,153,167,186
Guam	Good - data other than gaps, S:65,77,142,143,154 M:130-141,147-153,166,185-200
Hrao	Good, S:65,77,106,127,167,186 M:200
Jplm	Excellent, S:106,186
Kiru	Fair, S:52,65,77,82-84,106,153,157,167,178,186,189 M:61,62,81,132
Kour	Many days very sparse, M:35,37,41,62,81,86,91-93,131,132,167,168
Mad2	Excellent, S:73,74,106,157,186
Madr	Excellent, S:65,77,106,153,157,186
Mcm4	Fair - many days very sparse, M:41,179-181,200 (not to bad for high lat station)
mdo1	Excellent, S:77,106,129,162 M:163,186,189,200
Mkea	Excellent, S:58,77,106,153,157,167,180,186 M:200
Nlib	Good, S:65,77,99-102,106,111,112 M:200
nya2	Excellent, S:77,106,107,157, M:90-92
Pert	Excellent, S:50-52,61-63,106,107,132,157,178,186-189 M:118
pie1	Excellent, S:45,70,77,78,106,157,186 M:69,200
Pots	Excellent, S:65,77,81,82,106,153,157,167,186,189
Quin	Fair many missing days, S:46, 77,78,102,134,153,154 M:48-63,103-133,166-200
Sant	Excellent, S:38,39,55,77,106,115,153,157,158,167,186
Suth	Poor, M:58-90
Tidb	Excellent, S:65,77,98,106,135,153,157,186
Usud	Good,S:46,65,77,82,106,157,187,186 M:48-54
Zwen	Excellent,S:51,65,77,61,62,106,121,125,183,157,187,186

Table 2.2: Input Data Quality by Day Number (S=Sparse data, M=Data Missing)

From this analysis it was determined that the overall quality of the data was quite good. There are no large outlying TEC data values that would cause the RTA algorithm to falsely adjust the model. However there were a few days

[77,106,157,186] where most of the stations had very sparse data. The sparseness of the data would produce a PRISM output file very similar to the climatology output file and would affect the results of the validation. So these days were removed from the validation. Also, there was a few days that most of the stations didn't have data at all and they are as follows: [42, 47, 55, 56, 68, 75, 76, 166, 185, 200]. These days were also removed. Figure 2.10 shows the data quality spatially for the remaining days used in this study. The station locations are color coded to correspond to the data quality for each individual GPS receiver.

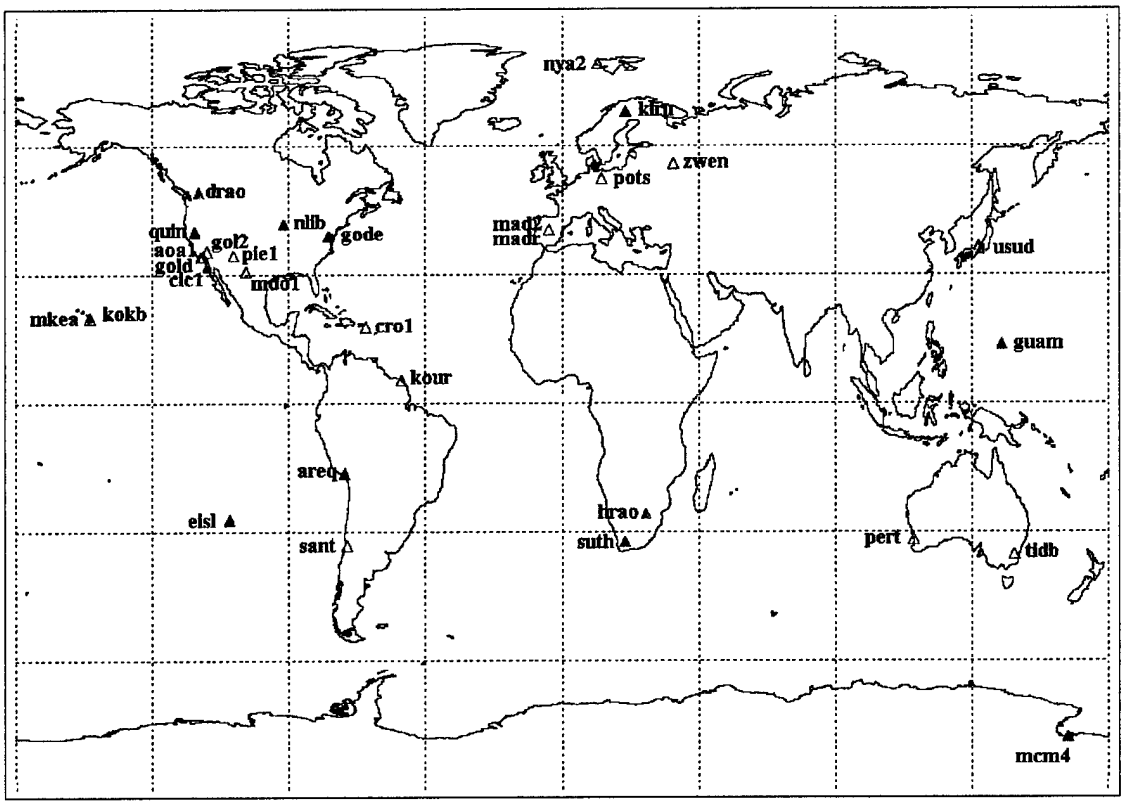

Figure 2.10: Station Quality Map (Blue=Excellent, Green=Good, Fair=Purple, Red=Poor)

With these two sets of PRISM runs (CLM &, RTA) a comparison will be made to the TOPEX validation data. By comparing the RTA comparison to the CLM comparison an assessment can be made of the improvement gained by using the GPS input data. This study will also greatly expand upon the past validation, which only looked at the improvement of the overall error when running the model with GPS data for a week of quiet solar activity. It should also be noted that the previous validation data were limited primarily to the mid latitude region. However, this study does a more detailed study by examining the errors as a function of magnetic latitude (low, mid, and some high latitudes) and local time and how they vary during periods of differing solar activities. By doing this a performance analysis can be made of PRISM which will be invaluable to both the forecaster and the model developer. By knowing the strengths and weaknesses of PRISM the forecaster can apply the appropriate confidence level to the model output. This research will also provide the Air Force Research Lab model developers with the insight to make improvements to the next version of PRISM and establish a bench mark for the future generation of ionospheric models.

2.2.2 Validation Data

The data used for the validation are from the TOPEX/Poseidon mission (1992) which is a joint endeavor between NASA and the French space agency, Centre National d'Etudes Spaatiales (CNES), designed to study global ocean

dynamics. This satellite has an orbit of 1336 km, and an inclination of 66 degrees. The time to complete one orbit is approximately 112 minutes, and it has an orbital speed of 7.2 km/s. This provides world wide (over-ocean) coverage of vertical TEC within a longitude range of 0 to 360 degrees and a latitude range of –66 to 66 degrees. There are 127 revolutions in a TOPEX cycle, which covers the same surface tracks every 10 days. The instrument used to get the TEC data is a dual frequency altimeter (C Band 5.3 GHz, Ku Band 13.6 GHz) that takes measurements at a rate of one per second. The measurement range is given by:

$$R_{measured} = R_{true} + \Delta R_{ionosphere} + \Delta R_{other}$$

where R_{true} is the true range, $\Delta R_{ionosphere}$ is the ionospheric range error at the frequency C or Ku, and ΔR_{other} are the range errors due to other frequency dependent and non frequency dependent sources. The range error , $\Delta R_{ionosphere}$ (centimeters), has the form b_C / f_C^2 or b_{Ku} / f_{Ku}^2 where b_i equals 40.3 $TEC_{vertical}$ with f_i expressed in gigahertz. The measured range equations for C and Ku bands provide an expression for the differential ionospheric correction:

$$\Delta R_{ionosphere} = [40.3 TEC_{vertical}][(f_{Ku}^2 - f_C^2)/ f_C^2 f_{Ku}^2]$$

The vertical TEC follows as:

$$TEC_{vertical} = \Delta R_{ionosphere}[f_C^2 f_{Ku}^2 /(f_{Ku}^2 - f_C^2)40.3]$$

One TEC unit (TECU) (10^{16} el/m^2) corresponds to 12.17mm range error at the given TOPEX altimeter frequencies [Vladimer, 1999].

2.2.3 TOPEX Limitations

The TOPEX data have some limitations when being used to study vertical TEC and they are as follows.

1. A study done by Callahan [1993] and Imel [1994] estimated the error in this data to be about 3 TECU. However in this study the TOPEX data will be regarded as truth.
2. Another limitation is that the data do not obtain measurements over land. This will produce large gaps in coverage over the continents.
3. Because of the 66 degree inclination of the orbit a large portion of the high latitude is not sampled. However for this study the major focus is the low and mid latitudes so this shouldn't be an issue in this research.

2.2.4 TOPEX Data Used for This Study

TOPEX data from February 4th 2002 (day 35) – July 19 2002 (day 200) were provided by Dr. Patricia Doherty at Boston College. The raw altimeter data are first converted to vertical TEC data as outlined in the previous discussion. The

figure below shows an example of a single pass that is for February 4th (Day 35) from UT 20:56 to UT 21:49 along with a PRISM plot of the TEC at 2100 UT.

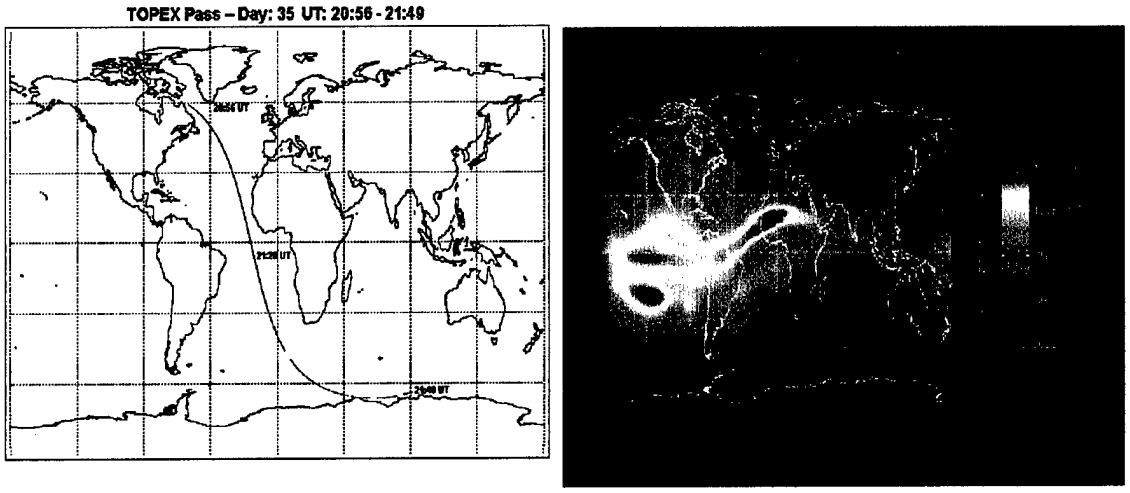

Figure 2.11: Sample Single TOPEX pass for Day 35 and the corresponding TEC plot.

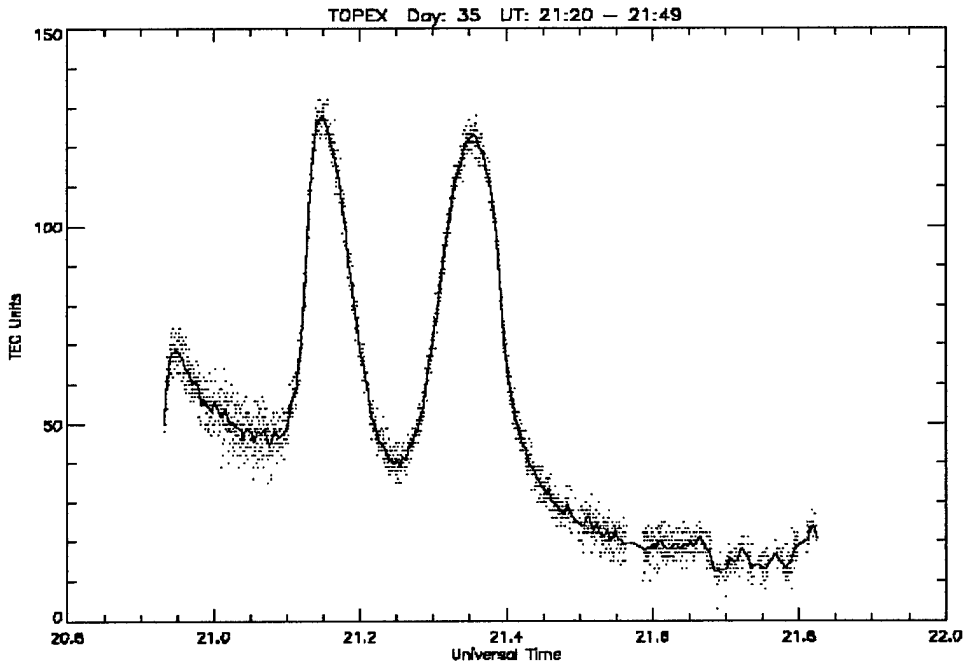

Figure 2.12: Data Smoothing (Black=1 second data, Blue=12 second average)

Figure 2.12 is the plot of the TEC for this TOPEX pass. This figure demonstrates the smoothing that was done in order to reduce some of the noise in the TOPEX data. For the smoothing, the 1 second data are averaged over 12 seconds, which converts the point measurement of vertical TEC to a 12 second average TEC value. This averaging corresponds to a distance of 86.4 km. The latitudes and longitudes of this 1-second data were also averaged to produce a corresponding 12-second average position. Since the PRISM resolution is only 4x4 degrees this averaging will not have an effect in the results and will greatly aide in reducing the number of comparisons. Finally, to get an idea of the TOPEX data coverage the ground track for day 35 from 0000 UT to 2359 UT was plotted on a world map (Figure 2.13).

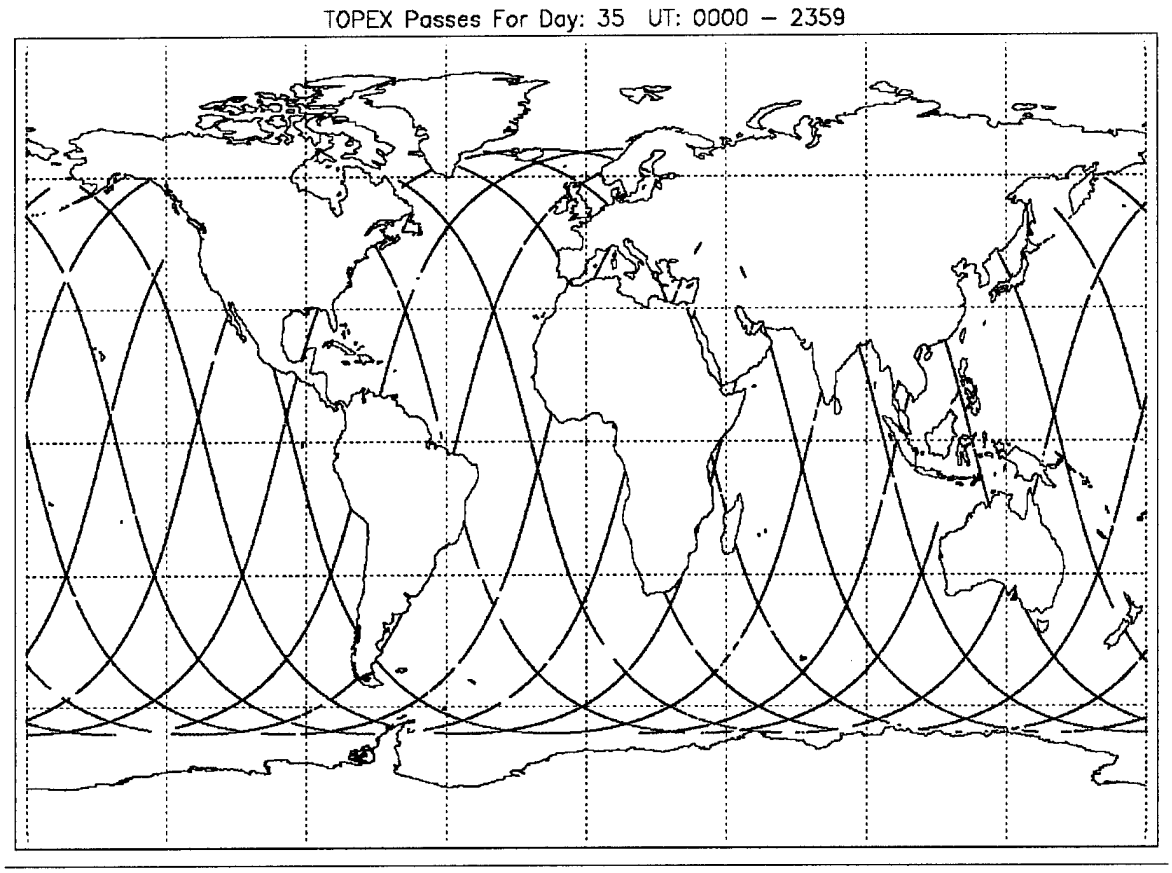

Figure 2.13: Example of TOPEX Ground Tracks for One Day

2.2.5 Method

For the actual validation the two sets of PRISM runs will be organized into two 3 dimensional arrays to assist in the comparison to the TOPEX data. One array will be for the climatology run (CLM) and the other will be for the real time adjustment run (RTA) with GPS data. The dimensions of each array will be longitude (180), latitude(90), UT(24), and the corresponding value will be TEC. Then an interpolation will be made along these three dimensions for every 12-second point of TOPEX TEC data and the PRISM TEC value will be obtained.

Also, by using the latitude and longitude of the TOPEX data the distance to the closest driver station will also be calculated. This comparison looks at the GPS input file used in the RTA run to determine which stations were present at that time to do the distance calculation. In order to automate this comparison an IDL program was written called TOPEX_Comparison6.pro (See Appendix B). This program takes one day of data and creates an output file containing the comparison data. Figure 2.14 shows how this program does the comparison. To get an idea of the amount of data processed by this program, Table 2.3 lists the data used for one day of data (day 35). The output of this program is one file containing all the TOPEX comparisons for one day, and it is this file that will be used for the error analysis. These daily files are on average only .45 [Mb]. So over the entire validation period this program takes 12045 files (20349MB) and converts it to 165 (74.25MB) files for the analysis. In appendix C you can see a sample page of one of these files. Table 2.4 shows the content contained in each of these 165 daily comparison files.

Input Files	# of Files	Avg. Size [Mb]	Total Size [Mb]
PRISM CLM Files	24	2.557	61.368
PRISM RTA Files	24	2.557	61.368
PRISM Driver Data	24	.015	.36
TOPEX Data	1	.230	.23
TOTAL	73	5.359	123.326

Table 2.3: TOPEX_Comparison6.pro Input File Sizes.

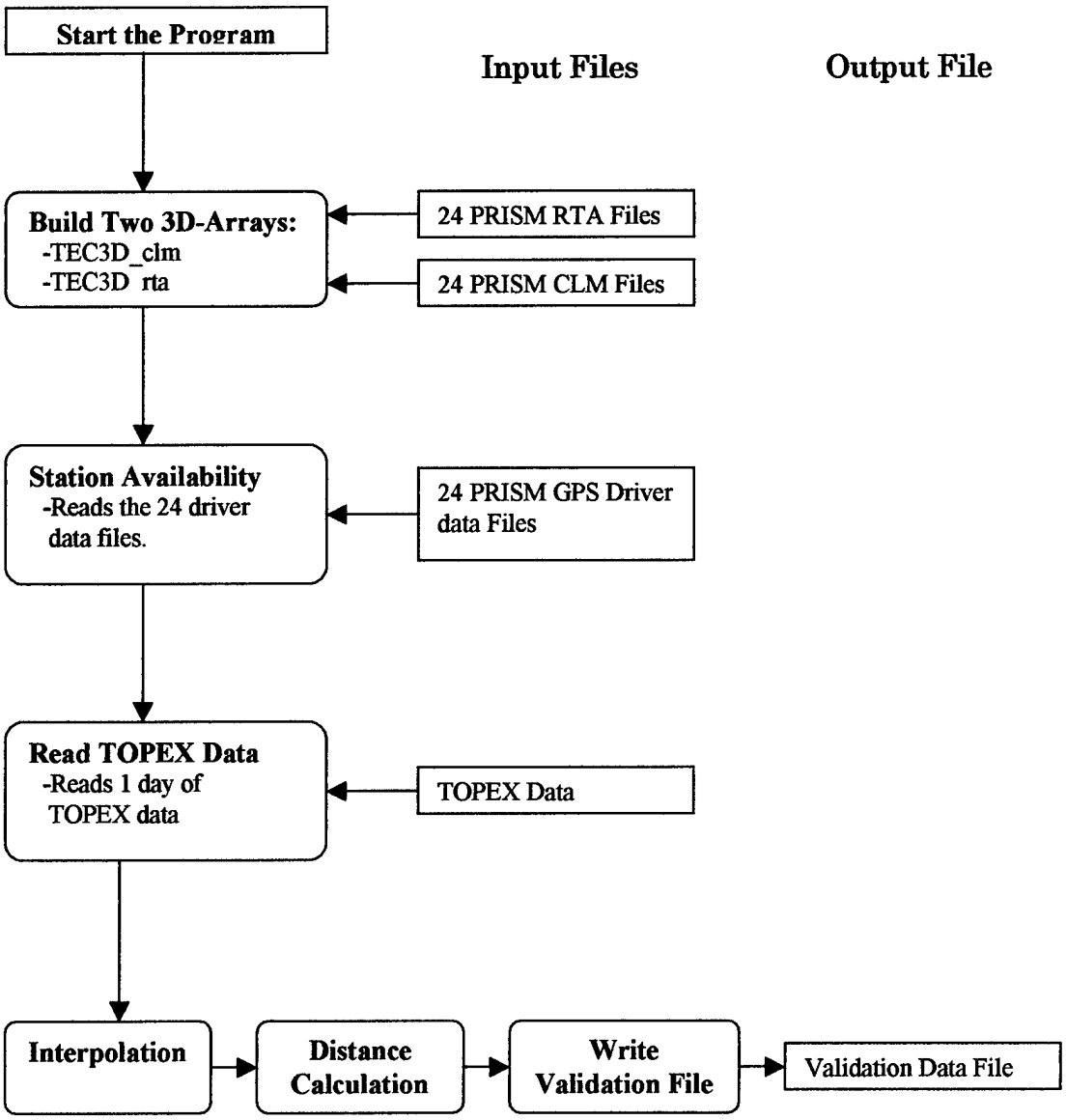

Figure 2.14: TOPEX_Comparison6.pro Flow Chart

Variable	Discription
Day	-Day of observation.
UT	-Universal time at the point measurement.
LT	-Local time at the point measurement.
Lat	-Latitude of the point measurement.
Lon	-Longitude of the point measurement.
Mag lat	-Magnetic latitude of the point measurement.
Mag Lon	-Magnetic longitude of the point measurement.
TOPEX TEC	-TEC measured by the TOPEX altimeter at a point.
STDDEV	-The standard deviation caused by the 12 second averaging.
CLM TEC	-PRISM Climatology (no GPS data) TEC value at the point.
RTA TEC	-PRISM Real Time Adjustment (with GPS data) TEC value at the point.
Distance	-Distance to the closest GPS station from the TOPEX measurement.
Station Lat	-The closest station Latitude.
Station Lon	-The closest station Longitude.
Station	-The name of the closest station.

Table 2.4: TOPEX_Comparison6.pro Output File Variables.

Chapter 3

The Results

3.1 Local Time Analysis

In doing this analysis the error distributions were sorted by local time. In Figure 3.1 the error for the climatology and the RTA runs were plotted with respect to local time. A further subdivision was made by magnetic latitude to see the contribution of error made by each of the individual models within PRISM (LOWLAT, MIDLAT, HIGHLAT). Table 3.1 shows how the subdivisions were binned.

Model	Magnetic Latitude Range
LOWLAT	$-32 \leq Value \leq 32$
MIDLAT	$32 < Value < 51$ and $-51 < Value < -32$
HIGHLAT	$Value \geq 51$ and $Value \leq -51$

Table 3.1 Magnetic Latitude Range for Comparisons

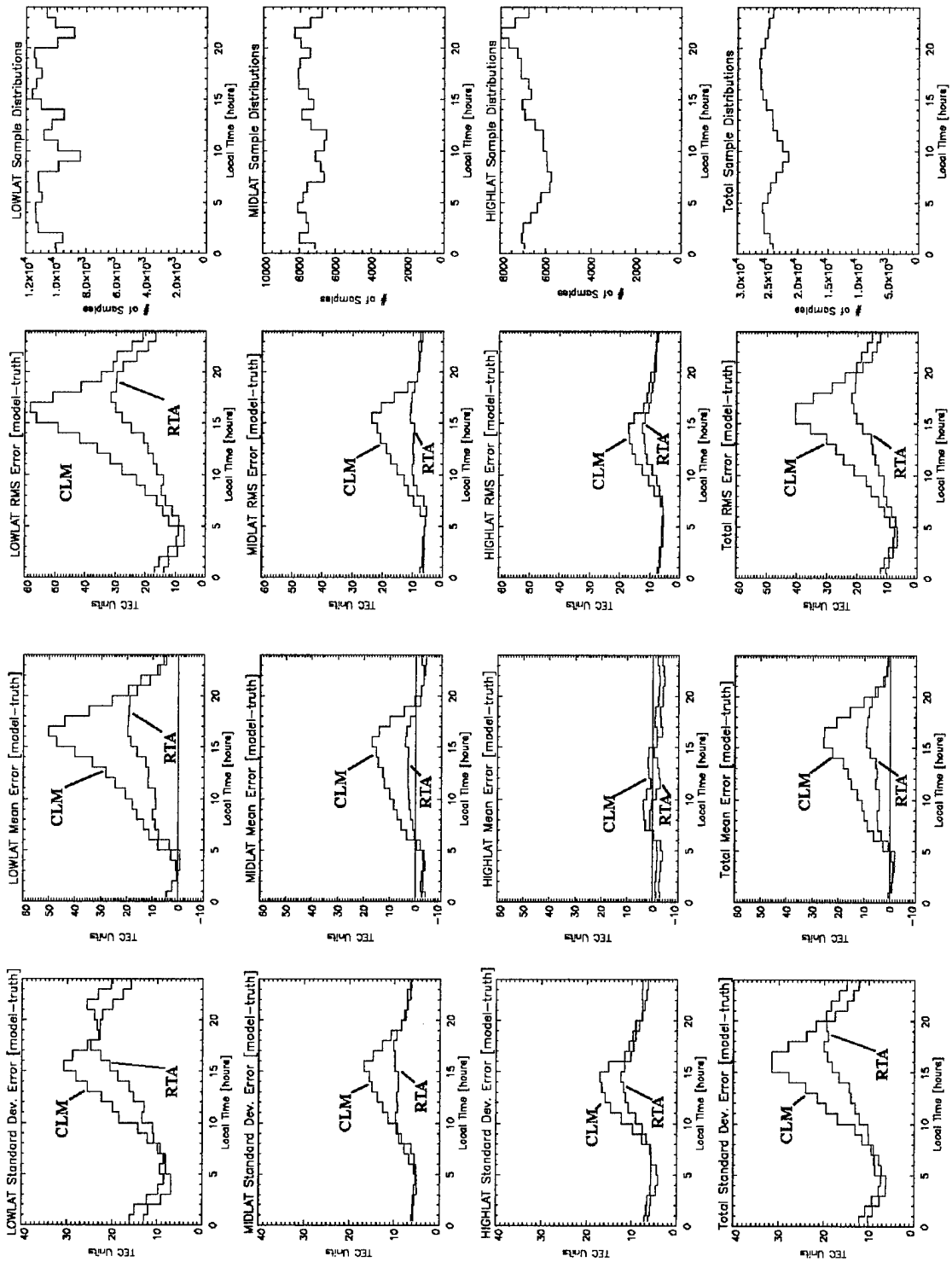

Figure 3.1: Model Error VS Local Time (CLM=Climatology, RTA=Real Time Adjustment)

The first thing to take note of is the uniformity in the sampling of local times in the distribution plots. There is a slight dip in the total number of samples around 10 LT but it is not enough to affect the results. In the error plots you can clearly see the time of day when the GPS data will really help improve the climatology. The LOWLAT model showed the largest improvement in TEC. There is an average improvement of 5.4 TEC units (RMS error) in the nighttime and a 17.4 TEC units (RMS Error) improvement during the daytime. In the MIDLAT model there is 1 TEC unit (RMS Error) of improvement during the night and an improvement of 8.7 TEC units (RMS Error) during the daytime. The HIGHLAT model showed an improvement of .9 TEC units (RMS Error) during the nighttime and an improvement of 4.2 TEC units (RMS Error) during the daytime. Overall there is a considerable improvement in all three models during the daytime when the ionospheric TEC values are the largest and there is also an improvement in the nighttime TEC when the ionospheric TEC values are the smallest. Overall, the largest improvements occurred primarily in the LOWLAT region during the daytime.

3.2 Distance From Station

The next set of distributions were distance from station VS TEC error. In Figure 3.2 these distributions were plotted for the entire time period (day 35 – day 200). The data were binned in 100km sections where 0km to 100km is the first of the 70 bins.

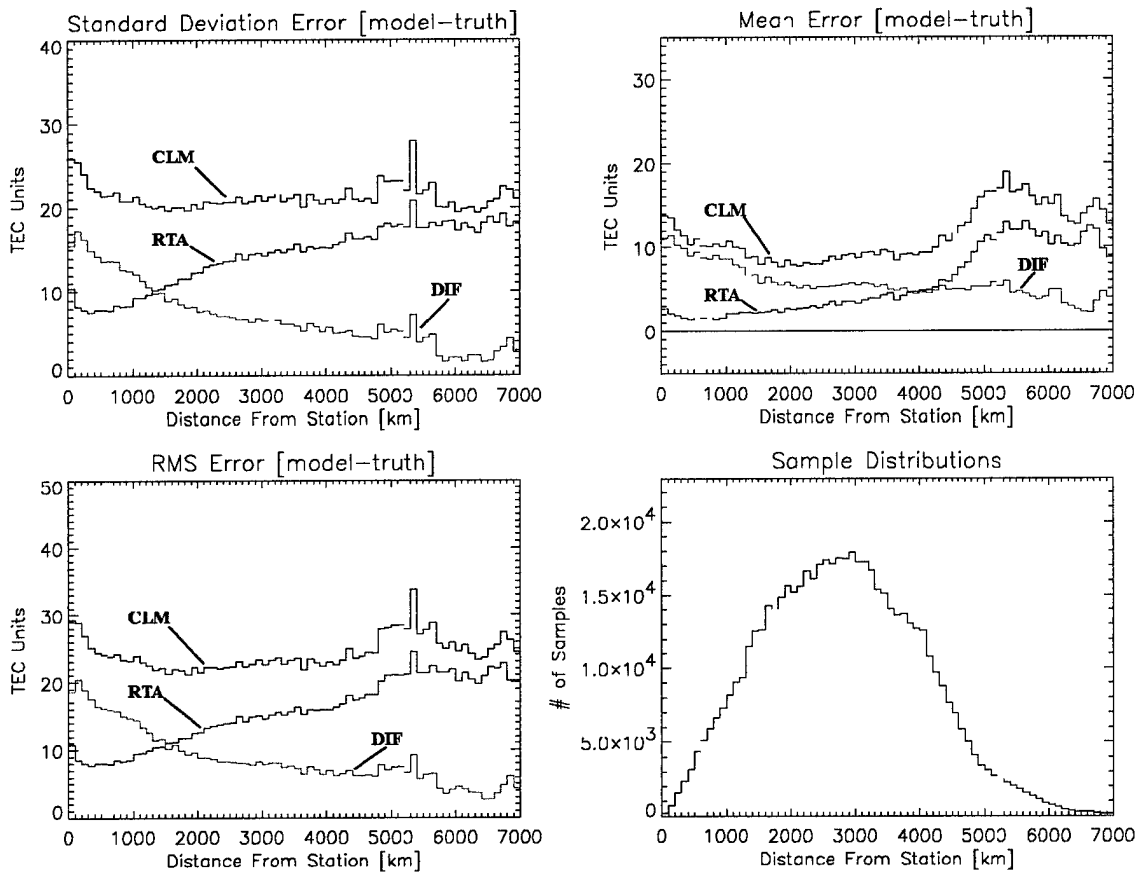

Figure 3.2: Distance From Station Verses Error (CLM=Climatology, RTA=Real Time Adjustment, DIF = CLM - RTA which is the improvement over climatology)

By looking at the sample distributions you can see that there are relatively few samples near the stations. This is primarily due to the fact that the majority of the stations are several kilometers inland. As for the error, the red histogram plot shows the improvement over climatology. This plot shows the extent to which the driver stations affect the model output as a function of distance. You can see that the GPS data overall has a positive effect and that the largest improvement happens near the station. However, there is a slight inconsistency in these plots is with the error that is very close to the stations

which can be seen in the first three bins (0km to 300km). In both the climatology (CLM) and real time adjustment (RTA) histogram plots there is a slight increase in the errors that was not expected. To determining what was going on in this region the spatial distribution of the errors larger than 20 TEC units were plotted on a global map (Figure 3.3).

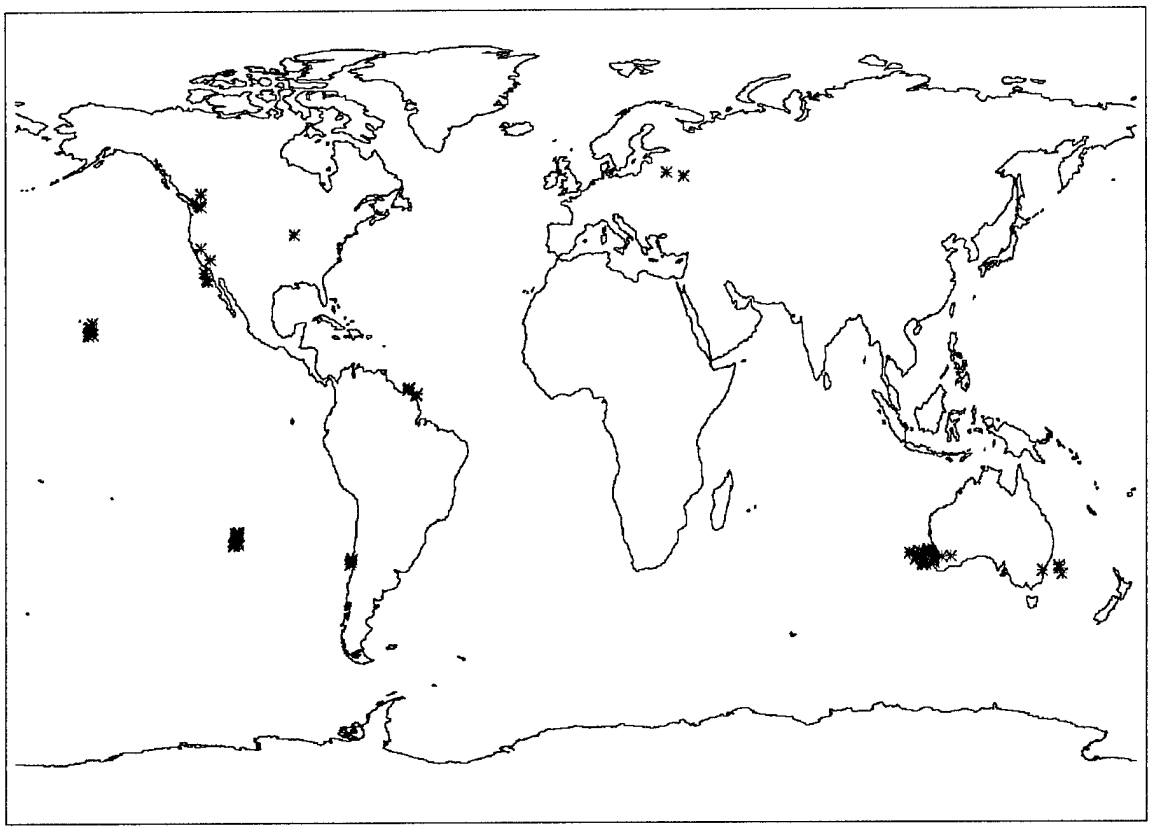

Figure 3.3: Distribution of TEC error larger than 20TEC units from 0-300km.

Figure 3.3 shows that the majority of the GPS stations did play some part in the large errors. However, there is a considerable amount of error associated with the station PERT in Australia. This station potentially does have some problems and is being looked at it more closely (Decker, personal communication). Another factor to take into consideration in the 0 to 300km region is the fact that the distance calculation is calculated from TOPEX data position to the station location and not the actual location of the GPS data given to PRISM. The actual data location can be up to 300km away from GPS receiver

for a GPS satellite elevation angel of 45 degrees. It is only when the elevation angle is 90 degrees (GPS satellite overhead) that the data location matches the station location (see figure 2.1 for the geometry).

3.3 Kp Distributions

The final analysis performed was to examine the errors as a function of magnetic activity. To do this the error distributions from the previous analysis (Error VS Distance From Station) were subdivided into thirteen ten day periods (see appendix D). This division permits sampling at all local times. Three hour Kp data were obtained from NOAA's National Geophysical Data Center. In figure 3.4, the three hour Kp values are plotted and are divided into thirteen plots that correspond to the thirteen data periods.

By examining these 10 day distributions and taking note of the general level of magnetic activity for that period there was a small trend. In periods where there was a small amount of magnetic activity, the errors were generally smaller than those with large amounts of activity. This can be seen by comparing the following two ten day time periods (Figures 3.5 & 3.6). The first period is of day 101-112 which has several times of high Kp and the second period is of day 161-173 which has relitivly low Kp for the entire period.

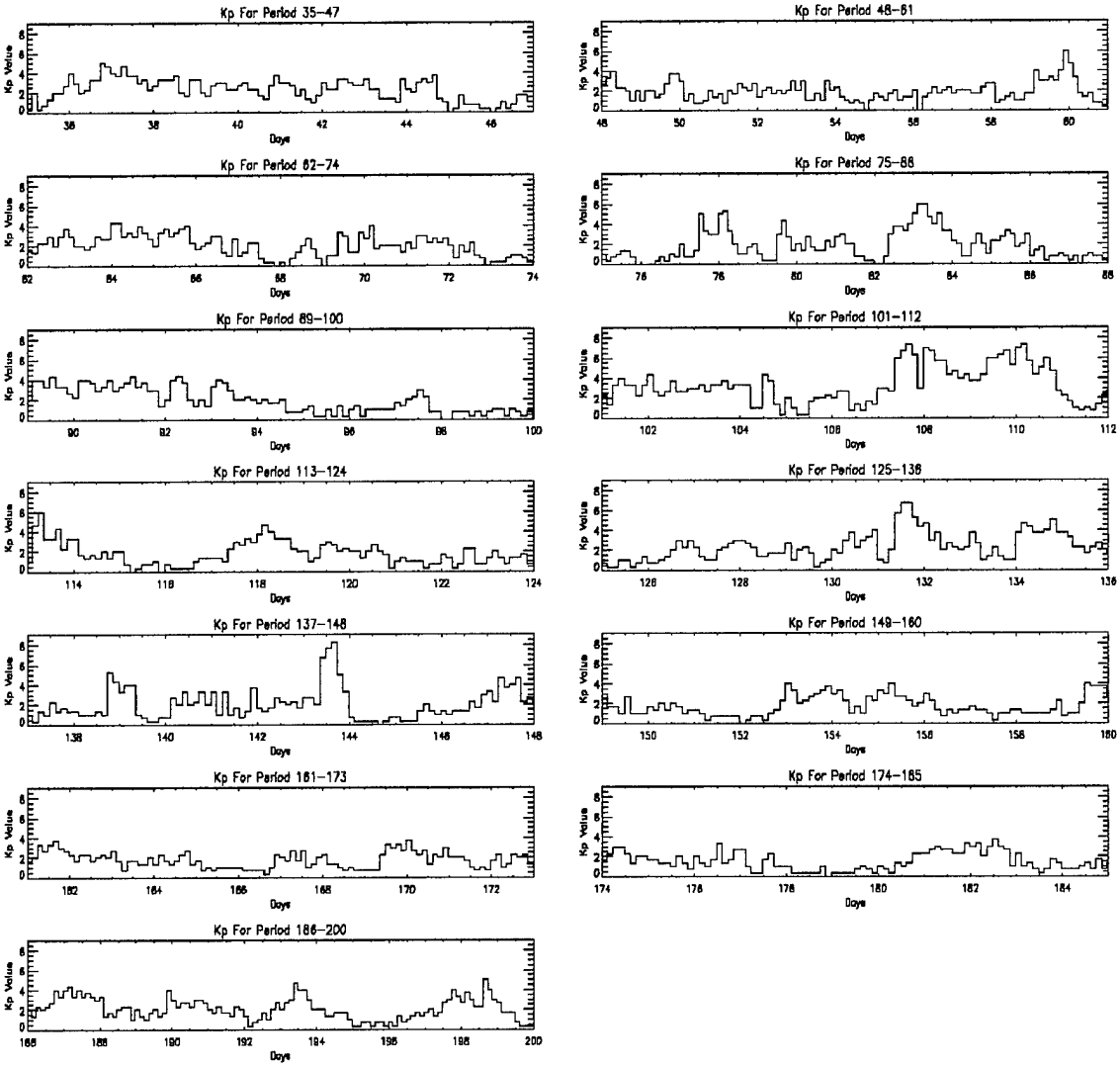

Figure 3.4: Three-Hour Kp Values.

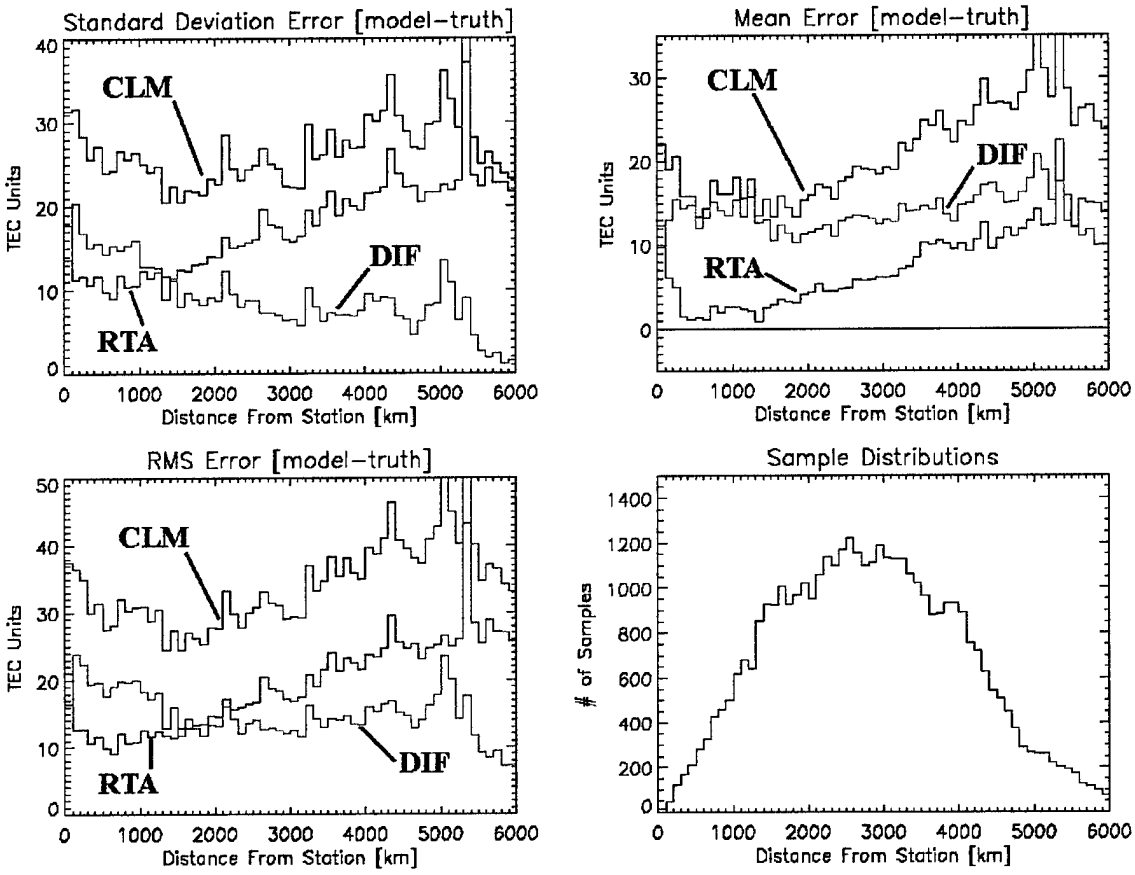

Figure 3.5: Error VS Distance From Station for period 101-112. (CLM = Climatology, RTA=Real Time Adjustment, DIF = CLM - RTA which is the improvement over climatology)

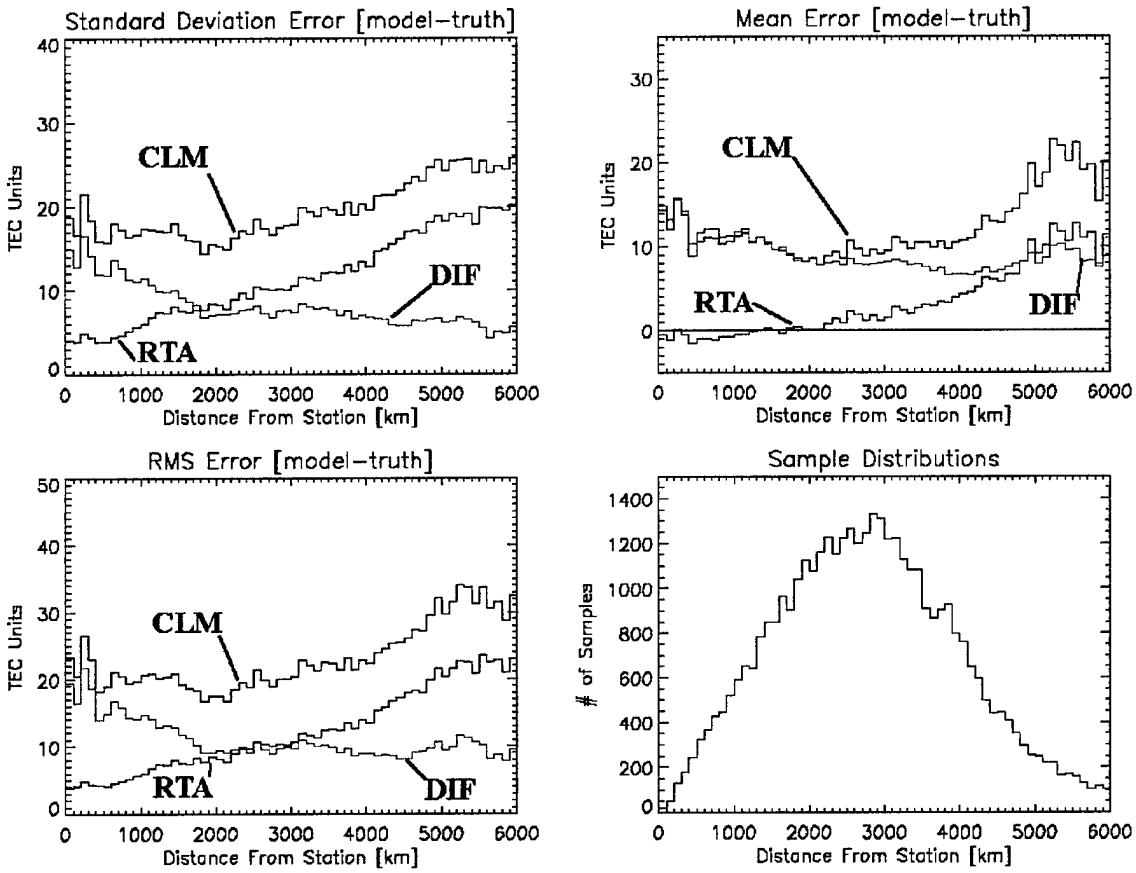

Figure 3.6: Error VS Distance From Station for period 161-173.

(CLM=Climatology, RTA=Real Time Adjustment, DIF = CLM - RTA which is the improvement over climatology)

The first thing to notice from these plots is how the climatology varied. When the Kp was high the climatology RMS error was on average 32.6 TEC units but for low Kp the average RMS error was 21.2 TEC units. Another trend was the level of error for the RTA PRISM run. For the high Kp period it was evident that GPS data did improve the climatology RMS on average by 14.3 TEC units and the low Kp period had an overall RMS improvement of 10.4 TEC units. However, even though the high Kp period showed the greatest improvement, the

RMS errors for this period were on average 18.2 TEC units where as the low Kp period error was only 10.8 TEC units. To examine the effect of Kp and its effect on the overall error a second more detailed analysis was performed.

3.4 Second Kp Analysis

Errors were binned by Kp instead of days, into three. The first bin is for minimum Kp with values equal to 0 to less than 3, the second bin is for moderate Kp with values from equal to 3 to less than 6, and the third for high Kp with values from equal to 6 to equal to 9. In Figure 3.7 the error distributions of the three bins are plotted with respect to local time. In appendix E these error are further broken down into the individual model components in PRISM (LOWLAT, MIDLAT, HIGHLAT).

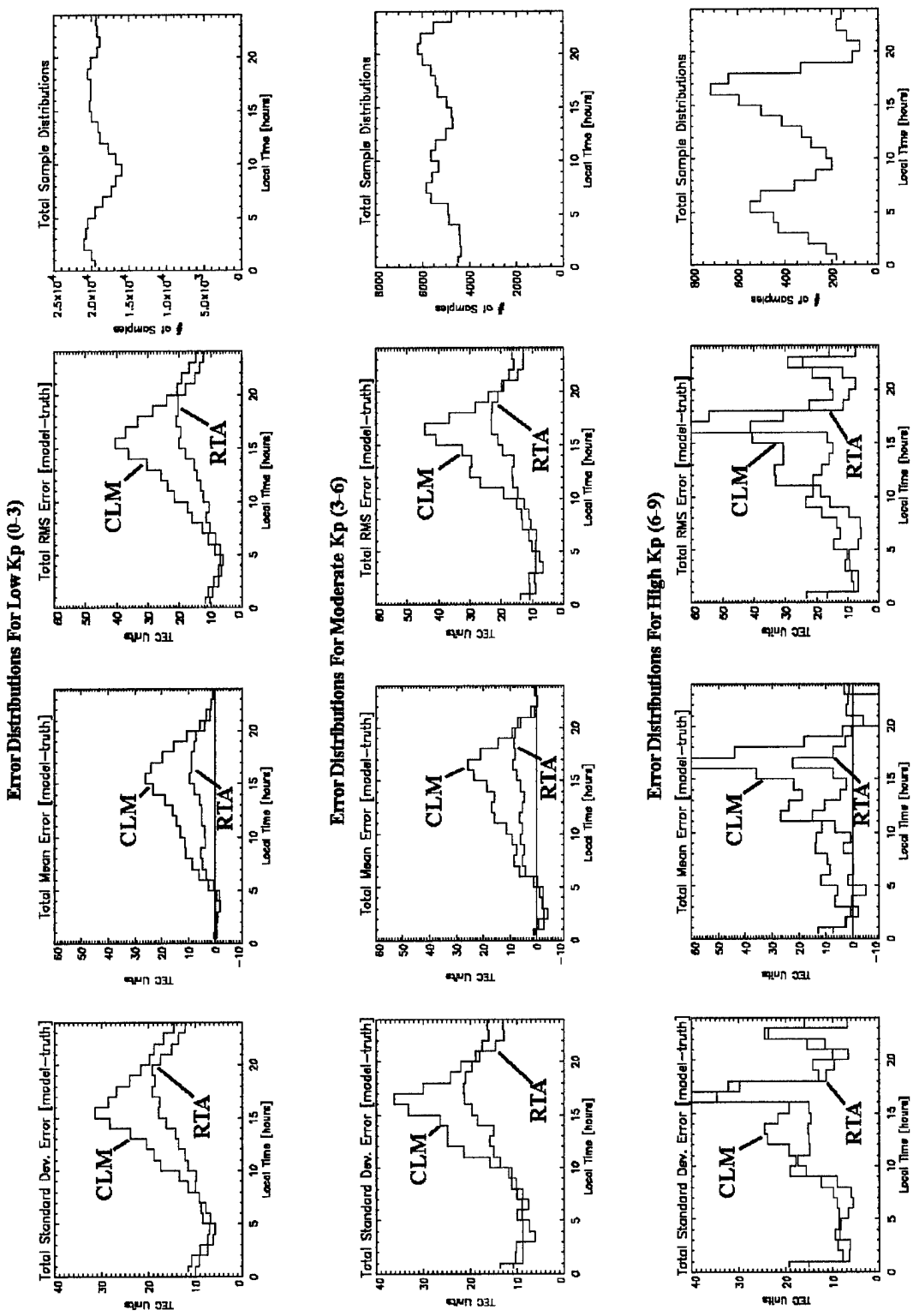

Figure 3.7: Errors by Magnetic Activity VS Local Time. (RTA=Real Time Adjustment, CLM=Climatology)

These distributions look very similar to the previous local time distributions, but there are some small differences. For instance there is a noticeable difference between the low Kp and mid Kp errors around nine local time. As Kp increases there is an increase in the level of error. Also, there is a slight increase in the overall error as the magnetic activity increases. To better see the differences Figure 3.8 puts all the RMS summary errors onto two plots, one for climatology (CLM), and the other for the real time adjustment (RTA).

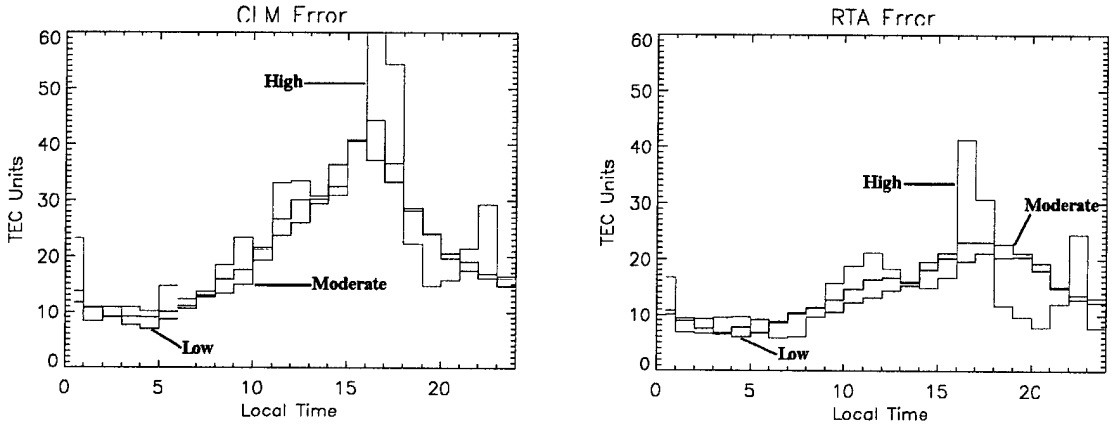

Figure 3.8: RMS Errors (Low=Low Kp, Moderate=Moderate Kp, High=High Kp)

From this figure you can clearly see that the error does increase with increasing Kp between low and moderate values. However, the high Kp is very sporadic showing improvements during some times (example: local time 18-22) and large errors during others (example: local time 16-17). This variation is probably due to the few number of samples at high Kp values. Table 3.2 below shows the number of total samples in each of the three distributions.

Kp	# of Samples	% of total samples
Low	459,758	77.5%
Moderate	125,288	21.1%
High	8,194	1.4%

Table 3.2: Kp Sample Distributions

Chapter 4

Summary & Conclusions

4.1 Summary

PRISM was developed for the Department of Defense to provide an accurate, real time specification of the ionosphere on a global scale. The climatology portion of PRISM PIM (Parameterized Ionosphere Model) requires the following indices to generate an output: Universal Time (UT), Geomagnetic Activity (Kp); Inerplanetary Magnetic Field (IMF) components (By, Bz); and the 10.7 cm solar flux (F10.7). If real time data are available, PRISM uses a Real Time Adjustment (RTA) algorithm to adjust the climatology by using weighting functions. These RTA data can be obtained from three sources: TEC data from GPS satellites, in situ measurements by DMSP, and ionospheric soundings made by the Digital Ionospheric Sounding (DISS) network. The real time input parameters include: Total Electron Content (TEC); ion drift velocities; in situ number density; ion/electron temperatures; fractional He^+, H^+, O^+ content; ionospheric layer critical frequencies (foF2, foF1, and foE); and peak electron density heights (hmF2, hmF1, and hmE).

The objective of this study was to validate PRISM when driven with and without Global Positioning Satellite (GPS) TEC data. In this study PRISM was run twice (Run 1= No GPS data CLM run, Run 2=With GPS data RTA run) at hourly intervals during the period of February 4th 2002 (day 35) – July 19 2002

(day 200). This large period would provide a validation of PRISM that takes into account both the seasonal and geomagnetic variations. It should be noted that a few days and hours were removed from this period due to gaps in the GPS data but this did not adversely affect the results.

The data used for the validation is vertical TEC data from the TOPEX/Poseidon satellite. This satellite has an orbit of 1336 km and an inclination of 66 degrees. This provides worldwide (over-ocean) coverage of vertical TEC within a longitude range of 0 to 360 degree and a latitude range of –66 to 66 degrees. The vertical TEC measurements are taken every second however for this study data were averaged over 12 seconds to reduce noise in the data and reduce the number of comparisons. This 12 second data are then compared to the two PRISM runs (CLM & RTA) and the errors were analyzed.

4.2 Conclusion

In this study 593,240 vertical TEC measurements were compared to the two PRISM runs for a total of 1,186,480 comparisons. The first analysis of the errors was to look at how the overall error varied with local time. In Figure 4.1, the errors are summarized for the entire period. In this figure there are three sets of distributions. The first two bars of all local time combined, the second two are of the day time local times which range from 7:00LT to 19:00LT, and the last two are of night time local times which range from 20:00LT to 6:00LT.

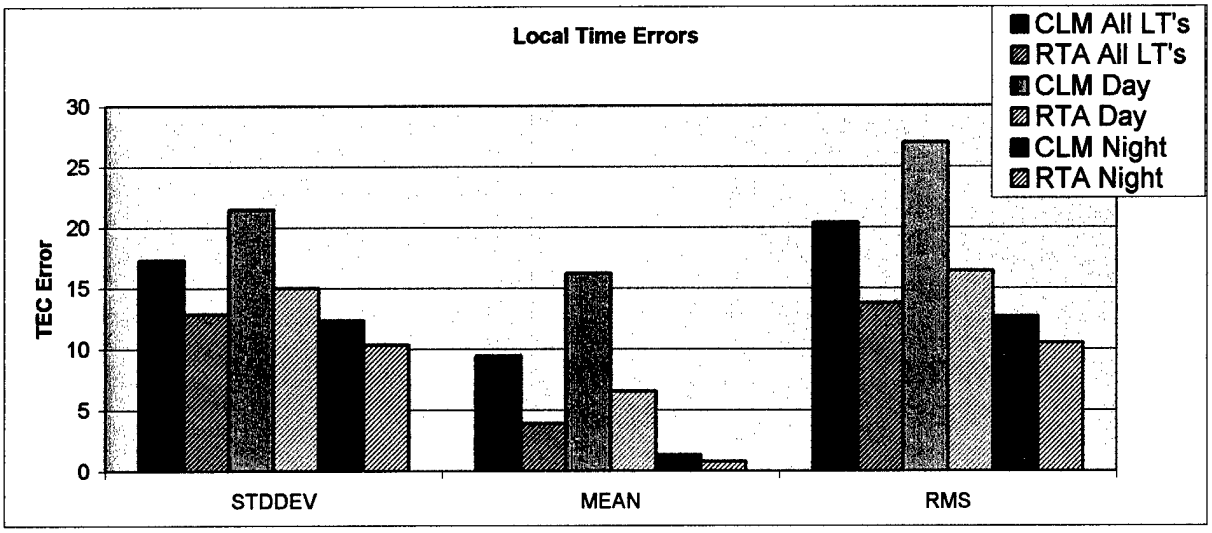

Figure 4.1: Total Error VS Local Time.

Figure 4.1 illustrates how the GPS data improve the climatology by 6.7 TECU RMS. Separating the errors by day and night you can see that the largest improvement of 10.6 TECU RMS is during the daytime when the TEC is the largest, and the smallest improvement of 2.1 TECU RMS happens during the nighttime when the TEC is the lowest.

The second error analysis evaluated the error changes with distance from the station. These errors were divided into 13 ten-day periods to help aid in seeing the seasonal and magnetic variations. Figure 4.2 summarizes the errors by these periods.

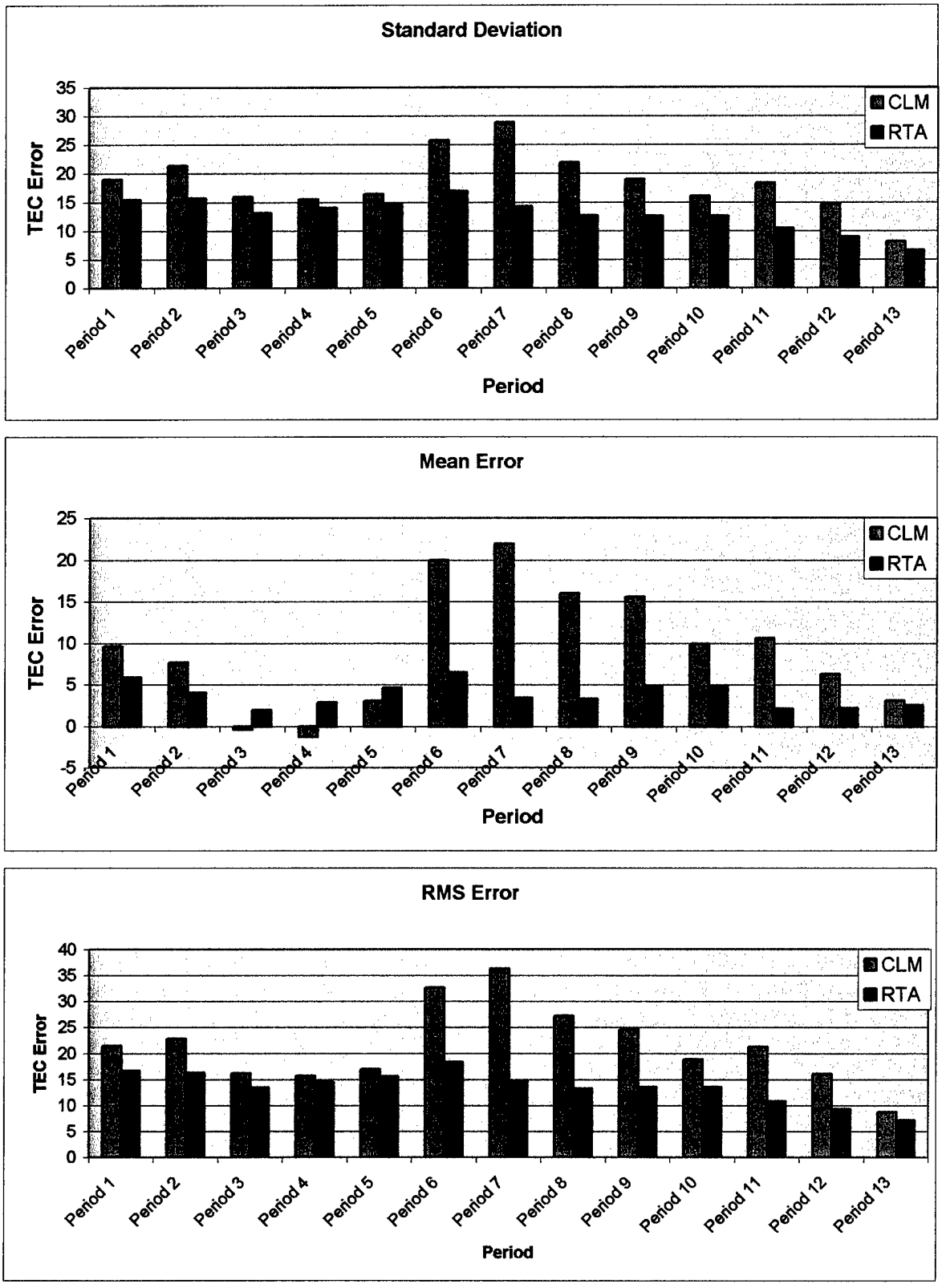

Figure 4.2: Summary Errors for the Thirteen Periods (10 days each)

From this distribution it is clear that error does vary as a function of time period or that it has a seasonal component. To explore this further a plot was made of how the daily TEC varied as a function of time. Figure 4.3 shows the daily TEC was plotted along a single meridian (zero longitude) for all latitudes and times. The TEC data are obtained by interpolating 1 degree TEC values along this meridian throughout the CLM PRISM runs.

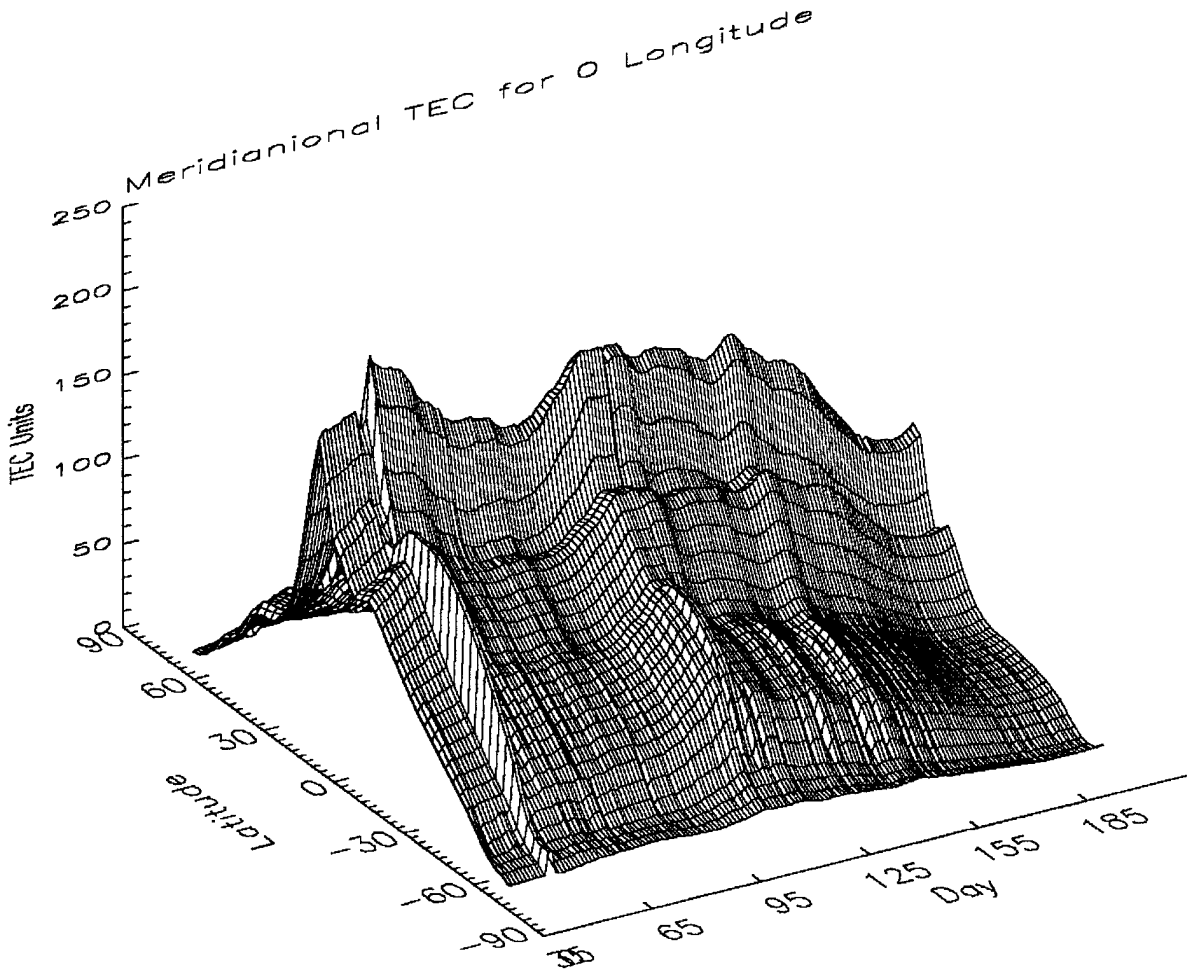

Figure 4.3: Daily TEC Along a Single Meridian (zero longitude).

When comparing Figure 4.3 with the errors in Figure 4.2, the size of the error is directly proportional to the daily maximum of TEC. So relatively speaking, the higher the daily maximum in TEC the higher the error in TEC.

The third analysis evaluates the error variation occurring with different magnetic activity. In this analysis there was a small trend as Kp increases. As the Kp ranges from low to moderate there was a slight increase in the overall error, which was on the order of a few TEC units. High Kp values perform much worse that both the moderate and low Kp the majority of times, but there were a few times where it did much better (see Fig 3.8). Since the high Kp samples only made up 1.4% of the total distribution and that the latitudes above 66 degrees were not sampled, nothing conclusive can be said about this.

Finally, the error within the three different models within PRISM (LOWLAT, MIDLAT, HIGHLAT) are summarized. The figures (Figures 4.4 & 4.5) below shows the overall errors for the model and how each of the models in PRISM contributed to the total error.

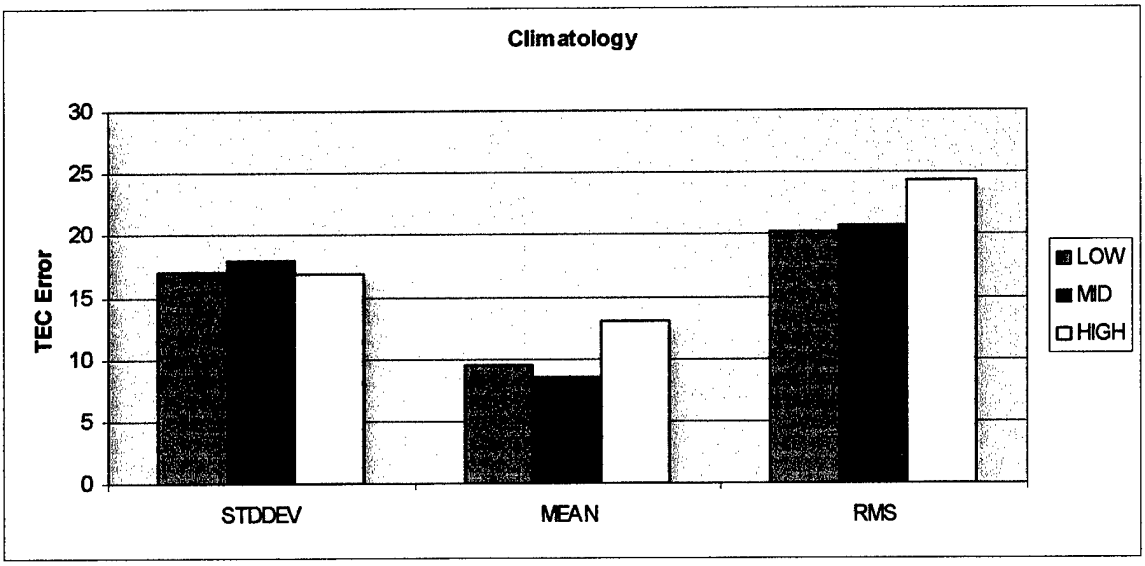

Figure 4.4: Climatology Error by PRISM Model (LOWLAT, MIDLAT, HIGHLAT)

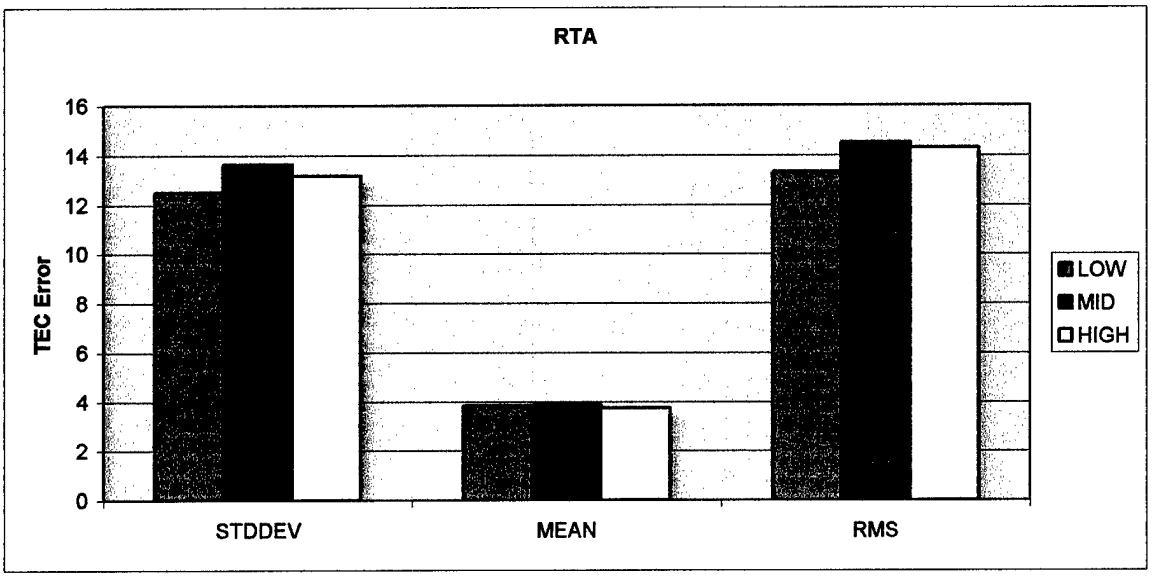

Figure 4.5: Real Time Adjustment (RTA) Error by PRISM Model (LOWLAT, MIDLAT, HIGHLAT)

Here you can see the overall error contribution by the three different models. These figures show that when PRISM is given driver data the error of all three models is reduced from 20 to 24 TECU to 13 to 14 TECU.

Having an accurate real time specification of the ionosphere is an essential first step to being able to forecast the ionosphere. This thesis did a thorough analysis of the real time ionosphere specification by PRISM using the same input parameters currently in use by the Air Force Weather Agency (AFWA). The intent was to make this performance analysis a useful resource to AFWA. This work also laid down the benchmark for the next generation models to be compared to. Using this validation data set and the algorithms developed in this research, furture models can be compared to PRISM to determine their improvement in accuracy. The benefits of having an accurate specification and forecast of the ionosphere would be to greatly enhance the capabilities of many DoD systems. Improvements could be made to remote sensors affected by the ionosphere which include inaccurate position readings from GPS satellites, corrections could also be made for high frequency communication disturbances, and it would be possible to predict communication outages. This knowledge would serve as a force multiplier for commanders allowing them to maximize the use of their resources and plan for possible problems caused by space weather.

Appendix A. Sample TEC GPS Driver Data Plots for PERT

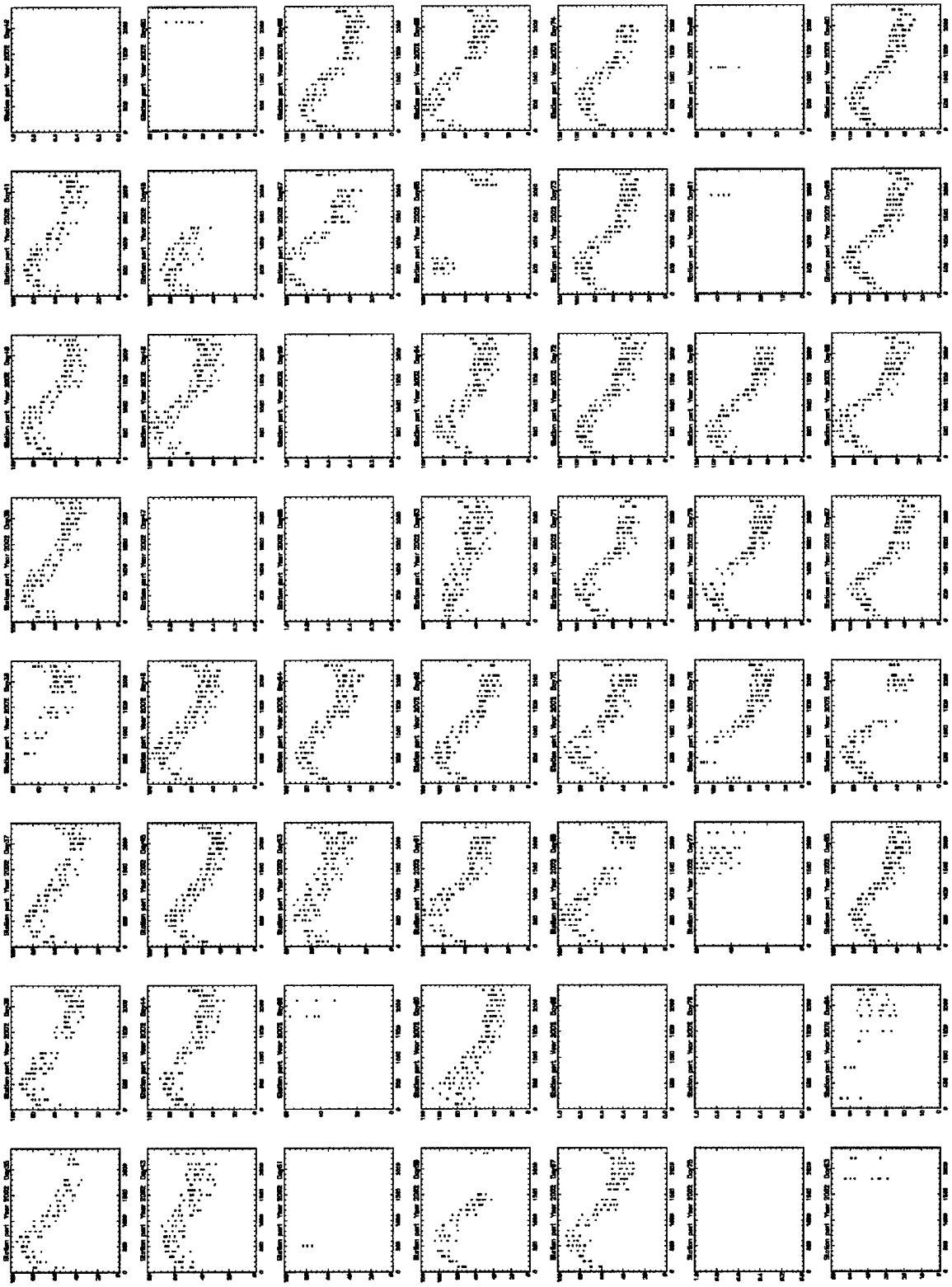

PERT Station Plot Days 33-90

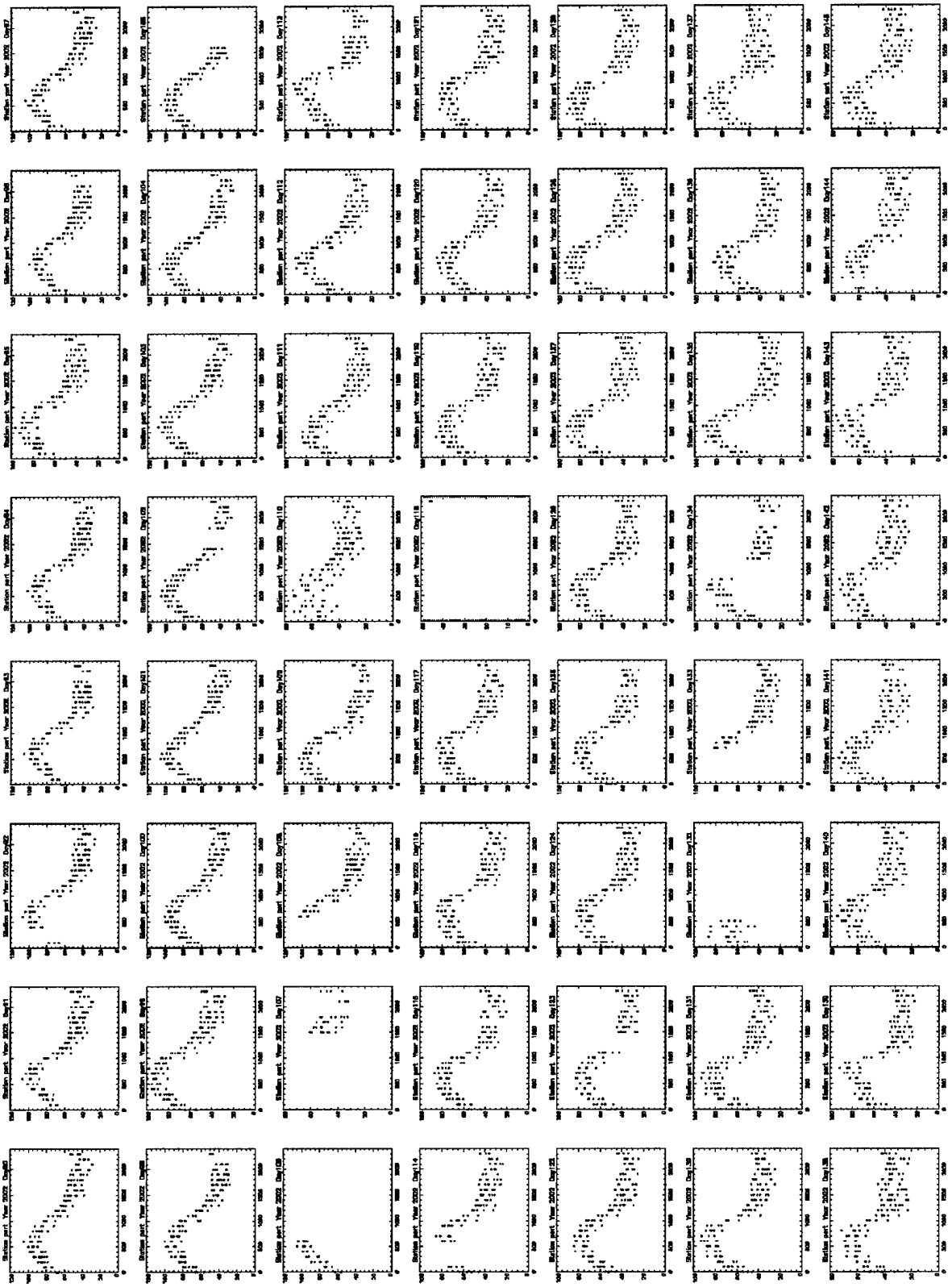

PERT Station Plot Days 90-145

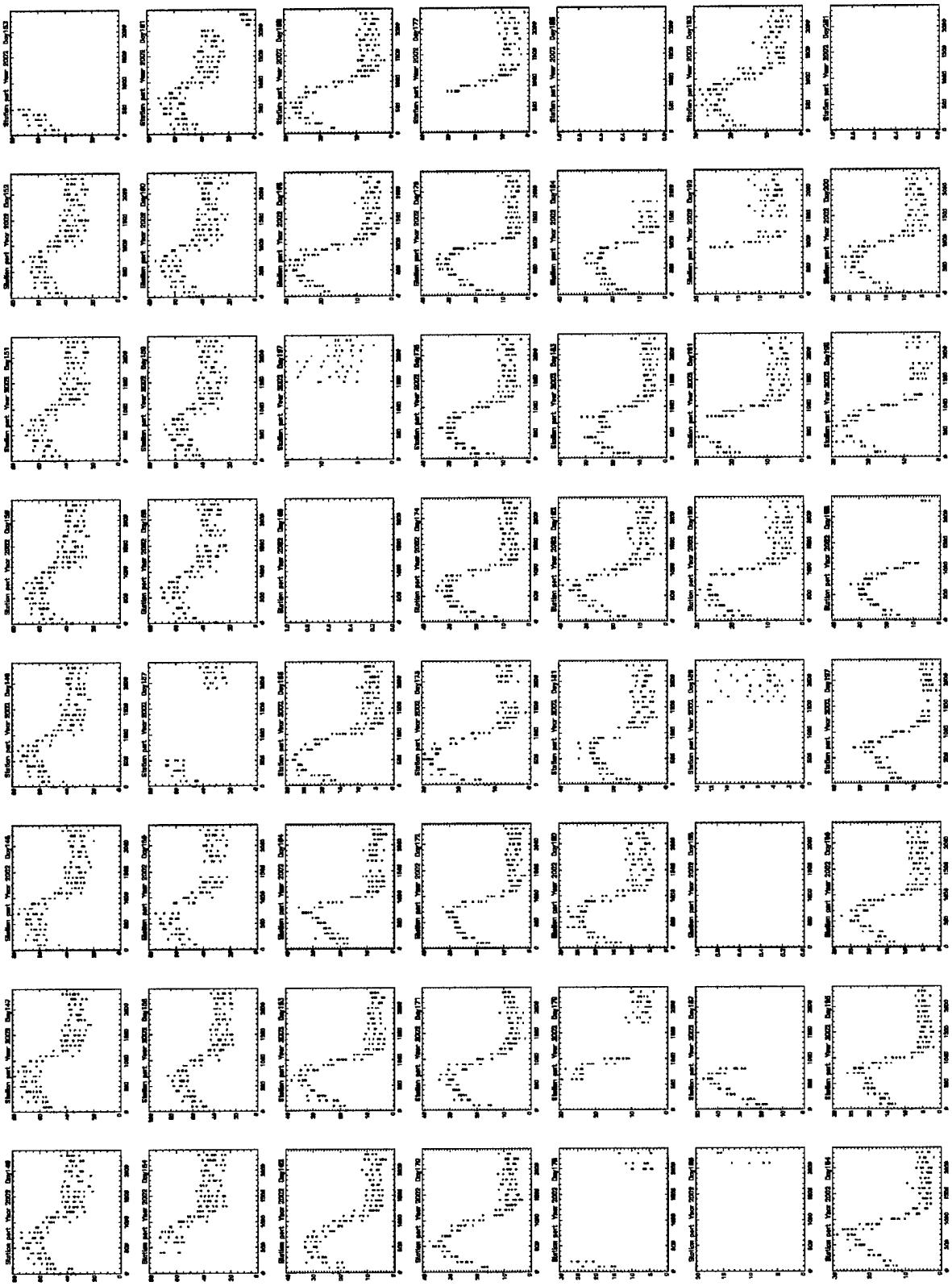

PERT Station Plot Days 146-200

Appendix B: Main Analysis Program

```
;*************************************************************************
;************************** MAIN PROGRAM *********************************
;*************************************************************************
;IDL program that reads 24 PRISM files into a 3d array.
;Modified to loop over several times.
;Modified to check station availability.
;Creates a validation file containing all arrays created.
;MAIN LOOP
FOR DAYI=35,250 DO BEGIN
GET_FILE:
;***************For a standard input*******************
TEC3D=FLTARR(24,46,91)
TEC3D_clm=FLTARR(24,46,91)
TEC3D_rta=FLTARR(24,46,91)
daystart=DAYI
I=daystart
;FOR I=daystart,daystart DO BEGIN  ;DAY loop
file_day=string(I,'(I3.3)')
file_day=strcompress(file_day,/remove_all)
FOR TYPE=0, 1 DO BEGIN  ;RTA CLM Loop
FOR II=0,23 DO BEGIN  ;HOUR loop
;BAD hour adjustment
;;IF (II EQ 18) THEN BEGIN
;;II=II+1
;;ENDIF
file_hour=string(II,'(I2.2)')
file_hour=strcompress(file_hour,/remove_all)
IF (TYPE EQ 0) THEN BEGIN
typestring='CLM'
ENDIF
IF (TYPE EQ 1) THEN BEGIN
typestring='RTA'
ENDIF
FILE='E:\'+typestring+'\d'+file_day+'h'+file_hour+'\data.in'
;***************Start of the program******************
FILE=STRCOMPRESS(FILE,/REMOVE_ALL)
GET_LUN,LUN
;;;;;;;;;;;;;;;;;;;;;;;;;
START:
OPENR,LUN,FILE, ERROR = err
; If err is nonzero, something happened. Print the error message to
; the standard error file (logical unit -2):
IF (err NE 0) THEN BEGIN
CLOSE,LUN
        IF (II EQ 23) THEN BEGIN
        I=I+1
        II=0
        ENDIF
        IF (II LT 23) THEN BEGIN
        II=II+1
        ENDIF
```

```
file_day=string(I,'(I3.3)')
file_day=strcompress(file_day,/remove_all)
file_hour=string(II,'(I2.2)')
file_hour=strcompress(file_hour,/remove_all)
FILE='E:\RTA\d'+file_day+'h'+file_hour+'\data.in'
GOTO, START
ENDIF
PRINT,'Reading data...Please wait...'
FILE1='99'
YEAR=0
DAY=0
UT=0.
F10P7=0.
KP=0.
SSN=0.
SDUM="
READF,LUN,SDUM
READF,LUN,SDUM
READF,LUN,YEAR,DAY,UT,F10P7,KP,SSN
UT=UT/3600.
; Read the primary coordinate system type, output grid type, and plasmasphere
; flag from the PIM output file
IDUM=0
READF,LUN,SDUM
READF,LUN,SDUM
READF,LUN,IDUM
CRDTYP=IDUM MOD 10
GRDTYP=(IDUM MOD 100)/10
IF(GRDTYP NE 0) THEN BEGIN
  CLOSE,LUN
  FREE_LUN,LUN
  PRINT,'File "'+FILE+'" contains the wrong type of output grid for RECCCRIT.'
  READ,'Do you want to try another file (Y/[N])? ',SDUM
  IF STRUPCASE(STRMID(STRCOMPRESS(SDUM,/REMOVE_ALL),0,1)) EQ 'Y' THEN
BEGIN
    GOTO,GET_FILE
  ENDIF ELSE BEGIN
    GOTO,END_PULLIAM
  ENDELSE
ENDIF
; Read grid information from the PIM output file
SLAT=0.
SLON=0.
ELAT=0.
ELON=0.
NLAT=0
NLON=0
DLAT=0.
DLON=0.
READF,LUN,SDUM
READF,LUN,SDUM
READF,LUN,SLAT,ELAT,SLON,ELON,NLAT,NLON,DLAT,DLON
; Read the output data type from the PIM output file
```

```
DATTYP=0
READF,LUN,DATTYP
IF (DATTYP NE 0) AND (DATTYP NE 2) THEN BEGIN
  CLOSE,LUN
  FREE_LUN,LUN
  PRINT,'File "'+FILE+'" contains the wrong type of output data for RECCCRIT.'
  READ,'Do you want to try another file (Y/[N])? ',SDUM
  IF STRUPCASE(STRMID(STRCOMPRESS(SDUM,/REMOVE_ALL),0,1)) EQ 'Y' THEN
BEGIN
    GOTO,GET_FILE
  ENDIF ELSE BEGIN
    GOTO,END_PULLIAM
  ENDELSE
ENDIF
; Read critical frequencies and heights and TEC from the PIM output file
IF DATTYP EQ 2 THEN BEGIN
  NALT=0
  READF,LUN,NALT,FORMAT='(29X,I6)'
  READF,LUN,SDUM
  ALT=FLTARR(NALT)
  READF,LUN,ALT
  EDP=FLTARR(NALT)
ENDIF
GLAT=FLTARR(NLAT,NLON)
GLON=FLTARR(NLAT,NLON)
MLAT=FLTARR(NLAT,NLON)
MLON=FLTARR(NLAT,NLON)
MLT=FLTARR(NLAT,NLON)
FOF2=FLTARR(NLAT,NLON)
HMF2=FLTARR(NLAT,NLON)
FOF1=FLTARR(NLAT,NLON)
HMF1=FLTARR(NLAT,NLON)
FOE=FLTARR(NLAT,NLON)
HME=FLTARR(NLAT,NLON)
TEC=FLTARR(NLAT,NLON)
TEC2=FLTARR(NLON,NLAT)
DUM1=FLTARR(5)
DUM2=FLTARR(7)
FOR ILAT=0,NLAT-1 DO BEGIN
  FOR ILON=0,NLON-1 DO BEGIN
    READF,LUN,SDUM
    READF,LUN,DUM1
    GLAT(ILAT,ILON)=DUM1(0)
    GLON(ILAT,ILON)=DUM1(1)
    MLAT(ILAT,ILON)=DUM1(2)
    MLON(ILAT,ILON)=DUM1(3)
    MLT(ILAT,ILON)=DUM1(4)
    IF DATTYP EQ 2 THEN BEGIN
      READF,LUN,SDUM
      READF,LUN,EDP
    ENDIF
    READF,LUN,SDUM
    READF,LUN,DUM2
```

```
    FOF2(ILAT,ILON)=DUM2(0)
    HMF2(ILAT,ILON)=DUM2(1)
    FOF1(ILAT,ILON)=DUM2(2)
    HMF1(ILAT,ILON)=DUM2(3)
    FOE(ILAT,ILON)=DUM2(4)
    HME(ILAT,ILON)=DUM2(5)
    TEC(ILAT,ILON)=DUM2(6)
    TEC2(ILON,ILAT)=DUM2(6)
    TEC3D(II,ILAT,ILON)=DUM2(6)
    IF (ILON EQ 0) THEN BEGIN
    TEC3D(II,ILAT,90)=DUM2(6)
    ENDIF
  ENDFOR
ENDFOR
CLOSE,LUN
FREE_LUN,LUN
END_PULLIAM:
PRINT,'FINISHED'
ENDFOR  ;Hour loop
IF (TYPE EQ 0) THEN BEGIN
TEC3D_clm=TEC3D
ENDIF
IF (TYPE EQ 1) THEN BEGIN
TEC3D_rta=TEC3D
ENDIF
ENDFOR  ;TYPE Loop  RTA CLM
;**********Station Availability program*********
daystart=I
station1=''
time=fltarr(10000)
latitude=fltarr(10000)
longitude=fltarr(10000)
vtec=fltarr(10000)
station=strarr(10000)
slat=fltarr(10000)
slon=fltarr(10000)
day=fltarr(10000)
f=0l
file_day=string(daystart,'(I3.3)')
file_day=strcompress(file_day,/remove_all)
FOR II=0,23 DO BEGIN  ;HOUR loop
file_hour=string(II,'(I2.2)')
file_hour=strcompress(file_hour,/remove_all)
FILE='E:\PRISM\no_gt_2002\rta\d'+file_day+'\d'+file_day+'h'+file_hour+'.dat'
close,1
START1:
openr,1,FILE,ERROR = err  ;MUST PUT ERROR SKIP ROUTINE HERE
IF (err NE 0) THEN BEGIN
CLOSE,1
        IF (II EQ 23) THEN BEGIN
        I=I+1
        II=0
        ENDIF
```

```
        IF (II LT 23) THEN BEGIN
        II=II+1
        ENDIF
        ;Incase there is a missing file
        day1=FIX(FILE_DAY)
        vtec(F)=0
        day(F)=day1
        latitude(F)=0
        longitude(F)=0
        TIME(F)=0
        station1=strcompress(station1,/remove_all)
        station(F)=0
        slat(F)=0
        slon(F)=0
        F=F+1
file_day=string(I,'(I3.3)')
file_day=strcompress(file_day,/remove_all)
file_hour=string(II,'(I2.2)')
file_hour=strcompress(file_hour,/remove_all)
FILE='E:\PRISM\no_gt_2002\rta\d'+file_day+'\d'+file_day+'h'+file_hour+'.dat'
GOTO, START1
ENDIF
WHILE NOT EOF(1) DO BEGIN
day1=FIX(FILE_DAY)
readf,1,format='(5F9.3,A6,3f9.3)',dum,time1,lat1,lon1,vtec1,station1,dum,slat1,slon1
        vtec(F)=vtec1
        day(F)=day1
        latitude(F)=lat1
        longitude(F)=lon1
        TIME(F)=time1
        station1=strcompress(station1,/remove_all)
        station(F)=station1
        slat(F)=slat1
        IF (slon1 GT 180) THEN BEGIN
        newslon1=slon1-180
        lon1=-180+newslon1
        ENDIF
        slon(F)=lon1
        F=F+1
ENDWHILE
ENDFOR
G=F-1
latitude=latitude(0:G)
longitude=longitude(0:G)
vtec=vtec(0:G)
time=time(0:G)
station=station(0:G)
slat=slat(0:G)
slon=slon(0:G)
day=day(0:G)
;Plotting instructions
```

```
stationloop=['aoa1','areq','cic1','cro1','drao','eisl','gode','gol2','gold','guam','hrao','jplm','kiru','kour','k
okb','madr','mad2','madr','mcm4','mdo1','mkea','nlib','nya2','pert','pie1','pots','quin','sant','suth','tid
b','usud','zwen']
StationAvail=fltarr(n_elements(stationloop),24)
StationAvail_lat=fltarr(n_elements(stationloop),24)
StationAvail_lon=fltarr(n_elements(stationloop),24)
endofarray=n_elements(time)-1
FOR I=0,endofarray DO BEGIN
el1=time(I)
el1=el1/100
el2=station(I)
el3=slat(I)
el4=slon(I)
        FOR II=0, N_ELEMENTS(stationloop)-1 DO BEGIN
        IF (el2 EQ stationloop(II)) THEN BEGIN
        el1=fix(el1)
        StationAvail(II,el1)=[1]
        StationAvail_lat(II,el1)=[el3]
        StationAvail_lon(II,el1)=[el4]
        ENDIF
        ENDFOR
ENDFOR  ;End of Station Availiability
;ENDFOR   ;Day loop
;**********Read In TOPEX Data**********
;This program reads in one 12 second data file into arrays.
dum=''
Tday=fltarr(9000)
Tut=fltarr(9000)
Tlat=fltarr(9000)
Tlon=fltarr(9000)
Tlonconv=fltarr(9000)
Ttec=fltarr(9000)
Tloct=fltarr(9000)
TSTDDEV=fltarr(9000)
counter=0l
dayindex=FIX(daystart)
dayindex=string(dayindex,'(I3.3)')
dayindex=strcompress(dayindex,/remove_all)
file='E:\TOPEX Data\Processed_12_data\TOPEX_12s_'+dayindex+'.txt'
close,1
openr,1,file, ERROR = err
        IF (err NE 0) then begin
        print,'Could not find the TOPEX data FILE'
        print,file
        ENDIF
        readf,1,dum
        WHILE NOT EOF(1) DO BEGIN
        readf,1,year1,day1,ut1,lt1,lat1,lon1,tec1,stddev1
        Tday(counter)=[day1]
        Tut(counter)=[ut1]
        Tloct(counter)=[lt1]
        Tlat(counter)=[lat1]
        Tlon(counter)=[lon1]
```

```
        IF (lon1 GT 180) THEN BEGIN
        newslon1=lon1-180
        lon1=-180+newslon1
        ENDIF
        Tlonconv(counter)=[lon1]
        Ttec(counter)=[tec1]
        TSTDDEV(counter)=[stddev1]
        counter=counter+1
        ENDWHILE
Tday=Tday(0:counter)
Tut=Tut(0:counter)
Tloct=Tloct(0:counter)
Tlat=Tlat(0:counter)
Tlon=Tlon(0:counter)
Tlonconv=Tlonconv(0:counter)
Ttec=Ttec(0:counter)
TSTDDEV=TSTDDEV(0:counter)
;**********Interpolation**********
;This part fixes the removal of lon 360 from the PRISM output
;The array is FIXEDTEC(latitude=46, longitude=91)
;latitude  array(0)=-90 array(45)=90
;longitude  array(0)=0 array(90)=360
PRISMTECARR_clm=fltarr(counter+1)
PRISMTECARR_rta=fltarr(counter+1)
MAGLAT=fltarr(counter+1)
MAGLON=fltarr(counter+1)
interlat=(tlat+90)/4
interlon=tlon/4
        FOR III=0,counter DO BEGIN
        PRISMTEC1=interpolate(TEC3D_clm,[Tut(III)],[interlat(III)],[interlon(III)],/grid)
        PRISMTEC2=interpolate(TEC3D_rta,[Tut(III)],[interlat(III)],[interlon(III)],/grid)
        MAGLAT1=interpolate(MLAT,[interlat(III)],[interlon(III)],/grid)
        MAGLON1=interpolate(MLON,[interlat(III)],[interlon(III)],/grid)
        PRISMTECARR_clm(III)=PRISMTEC1
        PRISMTECARR_rta(III)=PRISMTEC2
        MAGLAT(III)=MAGLAT1
        MAGLON(III)=MAGLON1
        ENDFOR
;END of Interpolation
;**********Distance Calculation**********
;Calculates the distance to the nearest station.
distancearray=fltarr(n_elements(stationloop))
dis=fltarr(n_elements(ttec))  ;contains distances
disstation=strarr(n_elements(ttec))  ;contains closest station
disstationlat=fltarr(n_elements(ttec))
disstationlon=fltarr(n_elements(ttec))
FOR K=0,counter DO BEGIN  ;loop over every data point
discounter=n_elements(stationloop)-1
Tdislat=Tlat(K)
Tdislon=Tlonconv(K)
time=Tut(K)
timeround=round(time)
IF (timeround EQ 24) THEN BEGIN
```

```
timeround=23
ENDIF
        FOR KK=0, discounter DO BEGIN   ;Sets array to 20000km
        distancearray(KK)=20000
        ENDFOR
                FOR KKK=0, discounter DO BEGIN
                test=StationAvail(KKK,timeround)
                        IF (test EQ 1) THEN BEGIN

        dis1=MAP_2POINTS(StationAvail_lon(KKK,timeround),StationAvail_lat(KKK,timeroun
d),Tdislon,Tdislat,/meters)
                        dis1=dis1/1000
                        distancearray(KKK)=dis1
                        ENDIF
                ENDFOR
dis(K)=min(distancearray)
disstation1=STATIONLOOP(WHERE(DISTANCEARRAY EQ MIN(DISTANCEARRAY)))
disstation(K)=disstation1(0)
disstationlat1=slat(where(station EQ disstation1(0)))
disstationlat(K)=disstationlat1(0)
disstationlon1=slon(where(station EQ disstation1(0)))
disstationlon(K)=disstationlon1(0)
ENDFOR
;*****************End of distance calculation************************
;*******************Write Validation File*****************************
close,2
        writefile='ValidationDay1a_'+dayindex+'.txt'
        openw,2,writefile
        printf,2,'DAY UT   LT    LAT   LON    MLat   MLon  TTEC  STDDEV P_CLM
P_RTA  DIST   DSLat  DSLon  DStation'
                counter=counter-2
                        FOR W=0,counter DO BEGIN
                        days=day1
                                a=strcompress(days,/remove_all)
                        uts=tut(W)
                                b=strcompress(uts,/remove_all)
                        tlocts=tloct(W)
                                c=strcompress(tlocts,/remove_all)
                        tlats=tlat(W)
                                d=strcompress(tlats,/remove_all)
                        tlons=tlon(W)
                                e=strcompress(tlons,/remove_all)
                        maglats=maglat(W)
                                f=strcompress(maglats,/remove_all)
                        maglons=maglon(W)
                                g=strcompress(maglons,/remove_all)
                        ttecs=ttec(W)
                                h=strcompress(ttecs,/remove_all)
                        tstddevs=tstddev(W)
                                i=strcompress(tstddevs,/remove_all)
                        prism_clms=prismtecarr_clm(W)
                                j=strcompress(prism_clms,/remove_all)
                        prism_rtas=prismtecarr_rta(W)
```

```
        k=strcompress(prism_rtas,/remove_all)
diss=dis(W)
        l=strcompress(diss,/remove_all)
disstationlats=disstationlat(W)
        m=strcompress(disstationlats,/remove_all)
disstationlons=disstationlon(W)
        n=strcompress(disstationlons,/remove_all)
disstations=disstation(W)
        o=strcompress(disstations,/remove_all)
tot=a+' '+b+' '+c+' '+d+' '+e+' '+f+' '+g+' '+h+' '+i+' '+j+' '+k+' '+l+'
   $ '+m+' '+n+' '+o
printf,2,tot
ENDFOR
ENDFOR
END
```

Appendix C: Sample Validation File

DAY	UT	LT	LAT	LON	MLat	MLon	TTEC	STDDEV	P_CLM	P_RTA	DIST	DSLat	DSLon	DStation
35	1.15324	2.34969	-66.1400	17.9468	-60.6322	59.8250	29.9167	2.87107	22.6815	25.7079	3332.87	-77.8400	187.450	mcm4
35	1.15685	2.46357	-66.1200	19.6007	-60.9012	60.9984	29.1667	2.03443	22.6667	25.7810	3304.89	-77.8400	187.450	mcm4
35	1.16047	2.57718	-66.0811	21.2506	-61.1592	62.1903	27.0000	2.08167	22.6152	25.8540	3278.36	-77.8400	187.450	mcm4
35	1.16409	2.69036	-66.0235	22.8941	-61.4055	63.4004	28.8333	2.79384	22.5459	25.9354	3253.30	-77.8400	187.450	mcm4
35	1.16771	2.80295	-65.9473	24.5287	-61.6383	64.6204	27.8333	2.15381	22.4005	25.9035	3229.77	-77.8400	187.450	mcm4
35	1.17148	2.91942	-65.8481	26.2191	-61.8661	65.9028	27.1667	2.03443	22.1188	25.6283	3206.93	-77.8400	187.450	mcm4
35	1.17570	3.04871	-65.7139	28.0952	-62.1050	67.3575	27.1667	2.22985	21.7979	25.3188	3183.35	-77.8400	187.450	mcm4
35	1.17974	3.17123	-65.5622	29.8723	-62.3239	68.7693	26.8333	2.26691	21.5351	25.0788	3162.85	-77.8400	187.450	mcm4
35	1.18369	3.28928	-65.3938	31.5839	-62.5207	70.1620	24.7500	1.63936	21.2764	24.8462	3144.76	-77.8400	187.450	mcm4
35	1.18733	3.39686	-65.2195	33.1430	-62.6913	71.4626	24.4167	2.09993	21.0706	24.6660	3129.90	-77.8400	187.450	mcm4
35	1.19248	3.54638	-64.9439	35.3086	-62.9079	73.3230	26.0000	2.79881	20.7985	24.4368	3111.86	-77.8400	187.450	mcm4
35	1.19751	3.68912	-64.6429	37.3742	-63.0881	75.1620	27.2500	1.96320	20.5162	24.1452	3097.68	-77.8400	187.450	mcm4
35	1.20640	3.93339	-64.0351	40.9048	-63.3485	78.4940	27.3333	3.09121	20.0119	23.5669	3081.13	-77.8400	187.450	mcm4
35	1.21245	4.09395	-63.5751	43.2225	-63.5094	80.8470	29.5833	2.95687	19.7058	23.2624	3075.35	-77.8400	187.450	mcm4
35	1.21695	4.20956	-63.2065	44.8893	-63.5978	82.6155	26.5000	3.64005	19.4988	23.0633	3074.53	-77.8400	187.450	mcm4
35	1.22124	4.31709	-62.8342	46.4377	-63.6580	84.3209	27.9167	2.84190	19.3205	22.9007	3076.48	-77.8400	187.450	mcm4
35	1.22528	4.41593	-62.4681	47.8597	-63.6951	85.9408	30.8333	3.18416	19.1528	22.7484	3080.49	-77.8400	187.450	mcm4
35	1.22890	4.50220	-62.1273	49.0995	-63.7224	87.4172	30.0000	2.85774	19.0193	22.6233	3086.02	-77.8400	187.450	mcm4
35	1.23251	4.58651	-61.7745	50.3100	-63.7346	88.8496	28.5000	2.17945	18.8723	22.4958	3093.34	-77.8400	187.450	mcm4
35	1.23613	4.66888	-61.4105	51.4913	-63.7303	90.2520	29.3333	2.89636	18.7243	22.3472	3102.40	-77.8400	187.450	mcm4
35	1.23975	4.74933	-61.0355	52.6437	-63.7155	91.6658	29.9167	2.17786	18.5939	22.2137	3113.21	-77.8400	187.450	mcm4
35	1.24336	4.82786	-60.6500	53.7675	-63.6882	93.0896	29.5833	4.27119	18.4698	22.1005	3125.75	-77.8400	187.450	mcm4
35	1.24697	4.90451	-60.2543	54.8631	-63.6441	94.5149	29.9167	3.98870	18.3437	21.9833	3140.00	-77.8400	187.450	mcm4
35	1.25059	4.97930	-59.8490	55.9308	-63.5835	95.9413	30.8333	2.70288	18.2160	21.8627	3155.92	-77.8400	187.450	mcm4
35	1.25420	5.05228	-59.4344	56.9712	-63.5069	97.3690	30.9167	2.49861	18.1277	21.7787	3173.50	-77.8400	187.450	mcm4
35	1.25781	5.12347	-59.0108	57.9848	-63.4145	98.7977	32.8333	3.67045	18.0430	21.6976	3192.71	-77.8400	187.450	mcm4
35	1.26143	5.19290	-58.5787	58.9721	-63.3068	100.227	30.9167	3.59301	17.9594	21.6170	3213.51	-77.8400	187.450	mcm4
35	1.26504	5.26063	-58.1383	59.9338	-63.1842	101.658	31.3333	2.56038	17.8770	21.5369	3235.88	-77.8400	187.450	mcm4
35	1.26865	5.32668	-57.6901	60.8704	-63.0655	103.104	32.3333	2.68742	17.7936	21.5022	3259.78	-77.8400	187.450	mcm4
35	1.27226	5.39111	-57.2343	61.7826	-62.9302	104.519	30.2500	4.58485	17.7049	21.4749	3285.18	-77.8400	187.450	mcm4
35	1.27588	5.45394	-56.7713	62.6710	-62.7804	105.924	29.7500	2.24072	17.6219	21.4460	3312.04	-77.8400	187.450	mcm4
35	1.27949	5.51523	-56.3014	63.5362	-62.6164	107.321	27.5833	2.53174	17.5447	21.4152	3340.33	-77.8400	187.450	mcm4
35	1.28310	5.57503	-55.8248	64.3789	-62.4387	108.710	27.4167	3.20048	17.4768	21.3665	3370.02	-77.8400	187.450	mcm4
35	1.28671	5.63336	-55.3418	65.1997	-62.2476	110.090	26.3333	4.08928	17.4182	21.2861	3401.06	-77.8400	187.450	mcm4
35	1.29032	5.69027	-54.8528	65.9993	-62.0437	111.462	26.2500	2.20322	17.3643	21.1918	3433.41	-77.8400	187.450	mcm4
35	1.29393	5.74582	-54.3579	66.7783	-61.8273	112.825	27.5000	3.17543	17.3150	21.0861	3467.04	-77.8400	187.450	mcm4
35	1.29754	5.80003	-53.8574	67.5374	-61.5925	114.155	27.6667	3.54338	17.2667	20.9785	3501.92	-77.8400	187.450	mcm4
35	1.30114	5.85295	-53.3516	68.2770	-61.3293	115.422	24.7500	3.63146	17.2082	20.9136	3538.00	-77.8400	187.450	mcm4
35	1.30475	5.90462	-52.8406	68.9980	-61.0547	116.704	25.2500	3.16557	17.1499	20.8821	3575.24	-77.8400	187.450	mcm4
35	1.30836	5.95508	-52.3247	69.7008	-60.7689	117.974	24.6667	2.13437	17.0913	20.8390	3613.62	-77.8400	187.450	mcm4
35	1.31197	6.00437	-51.8041	70.3860	-60.4723	119.231	24.3333	3.51979	17.0324	20.7846	3653.09	-77.8400	187.450	mcm4
35	1.31557	6.05253	-51.2790	71.0543	-60.1653	120.476	26.6667	2.05480	16.9733	20.7188	3693.61	-77.8400	187.450	mcm4
35	1.31918	6.09959	-50.7495	71.7062	-59.8481	121.710	25.0833	3.32812	16.9143	20.6420	3735.17	-77.8400	187.450	mcm4
35	1.32279	6.14560	-50.2159	72.3422	-59.5244	122.953	25.5000	1.97906	16.8675	20.5643	3777.70	-77.8400	187.450	mcm4
35	1.32639	6.19058	-49.6782	72.9629	-59.1903	124.149	25.5833	3.22641	16.9366	20.6098	3821.20	-77.8400	187.450	mcm4
35	1.33000	6.23458	-49.1368	73.5687	-58.8428	125.294	26.0833	3.27766	17.0772	20.7389	3865.61	-77.8400	187.450	mcm4
35	1.33360	6.27761	-48.5917	74.1602	-58.4846	126.425	26.6667	3.34996	17.2184	20.8695	3817.57	-31.8000	115.720	pert
35	1.33721	6.31973	-48.0431	74.7378	-58.1162	127.541	27.0833	1.38193	17.3605	21.0021	3761.06	-31.8000	115.720	pert
35	1.34081	6.36095	-47.4910	75.3021	-57.7377	128.644	26.5833	2.72208	17.5037	21.1365	3705.17	-31.8000	115.720	pert
35	1.34441	6.40131	-46.9358	75.8535	-57.3497	129.733	27.6667	3.06413	17.6482	21.2730	3649.94	-31.8000	115.720	pert
35	1.34801	6.44084	-46.3774	76.3924	-56.9522	130.809	29.5833	3.14797	17.8024	21.4223	3595.40	-31.8000	115.720	pert
35	1.35162	6.47957	-45.8160	76.9192	-56.5397	131.849	29.4167	2.56445	18.0193	21.6433	3541.59	-31.8000	115.720	pert
35	1.35522	6.51751	-45.2517	77.4344	-56.1069	132.829	28.0000	1.35401	18.3719	22.0180	3488.53	-31.8000	115.720	pert
35	1.35882	6.55471	-44.6847	77.9383	-55.6670	133.798	28.4167	2.36144	18.7505	22.4233	3436.26	-31.8000	115.720	pert
35	1.36242	6.59118	-44.1151	78.4314	-55.2203	134.754	29.7500	3.26917	19.1547	22.8588	3384.82	-31.8000	115.720	pert
35	1.36602	6.62696	-43.5428	78.9140	-54.7667	135.700	29.7500	3.00347	19.5843	23.3241	3334.23	-31.8000	115.720	pert
35	1.36962	6.66206	-42.9682	79.3865	-54.3067	136.634	28.2500	3.11247	20.0387	23.8187	3284.55	-31.8000	115.720	pert
35	1.37322	6.69650	-42.3912	79.8492	-53.8405	137.557	29.0833	3.20048	20.5178	24.3422	3235.81	-31.8000	115.720	pert
35	1.37681	6.73031	-41.8119	80.3025	-53.3497	138.481	31.2500	2.12623	21.0488	24.9285	3188.05	-31.8000	115.720	pert
35	1.38041	6.76352	-41.2304	80.7466	-52.8303	139.368	29.7500	2.34965	21.6123	25.5503	3141.33	-31.8000	115.720	pert
35	1.38401	6.79614	-40.6468	81.1819	-52.3066	140.242	31.5833	3.22641	22.1882	26.1863	3095.68	-31.8000	115.720	pert
35	1.38776	6.82951	-40.0368	81.6262	-51.7568	141.138	31.0000	2.94392	22.8010	26.8632	3049.33	-31.8000	115.720	pert

Appendix D: Ten Day Distance Error Distributions

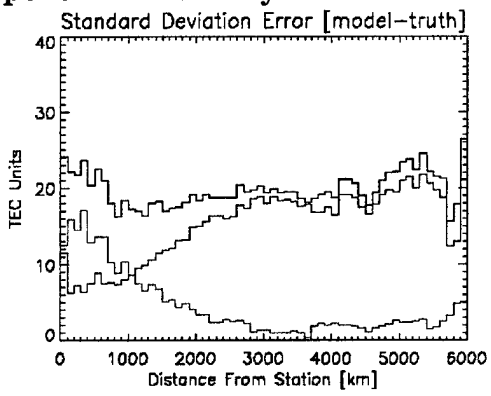

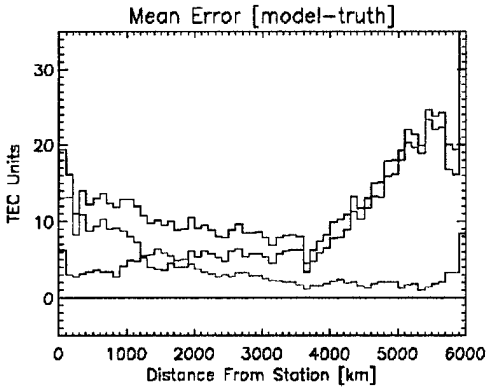

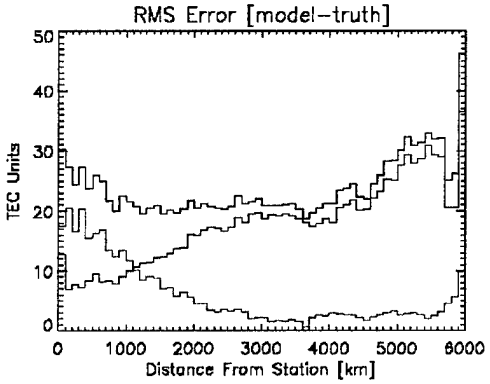

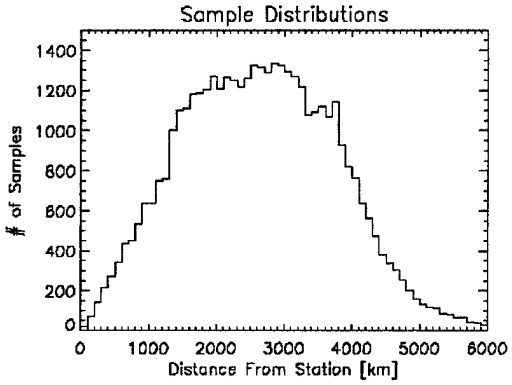

Period 35-47

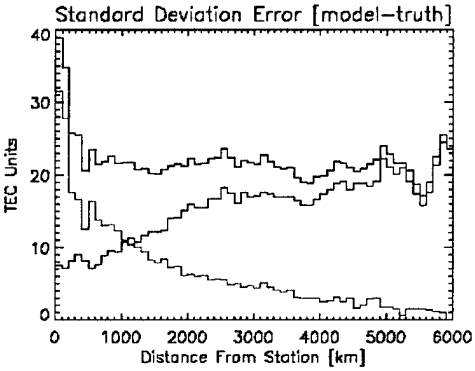

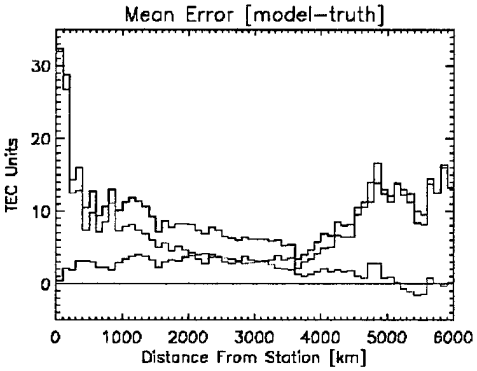

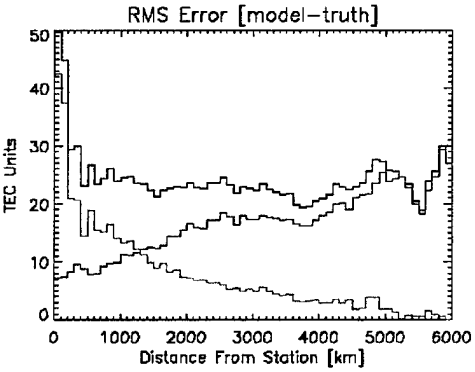

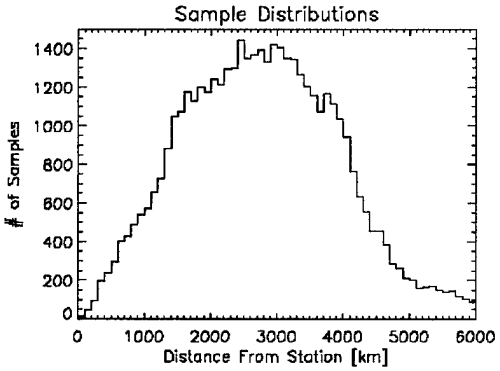

Period 48-61

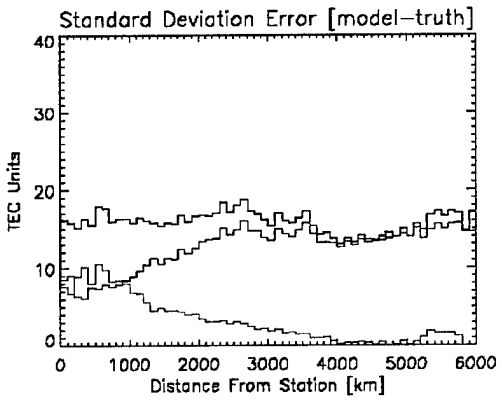

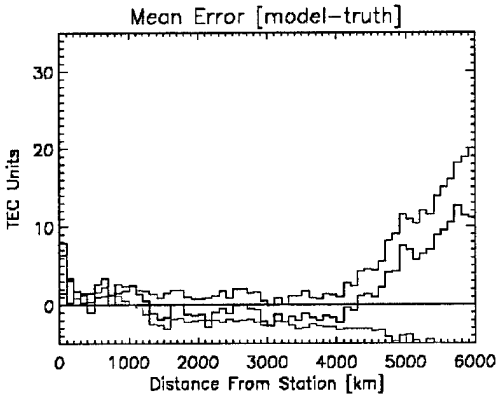

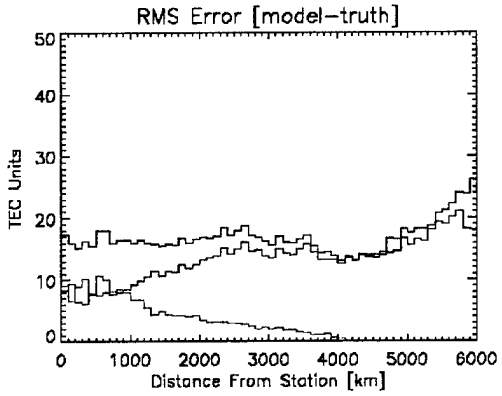

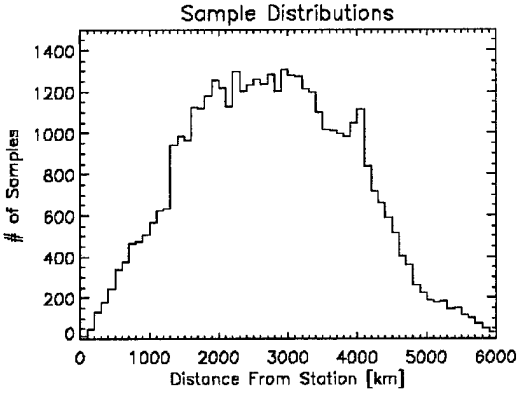

Period 62-74

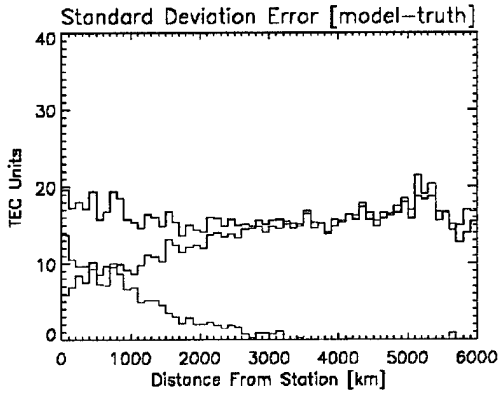

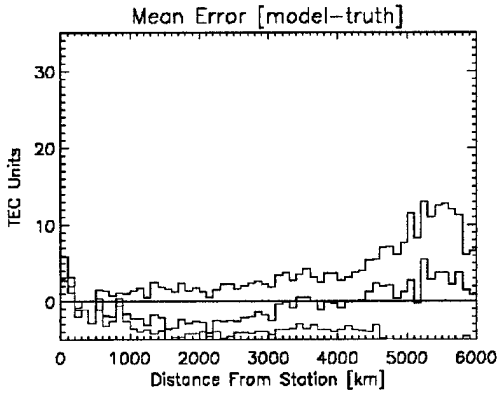

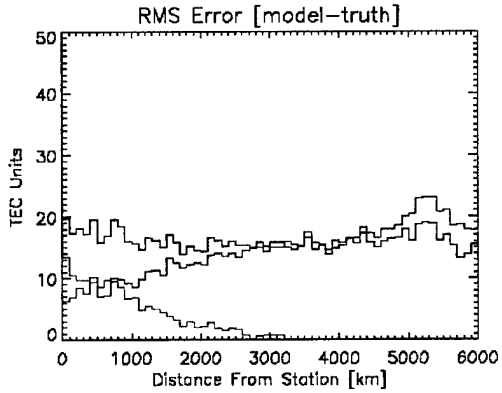

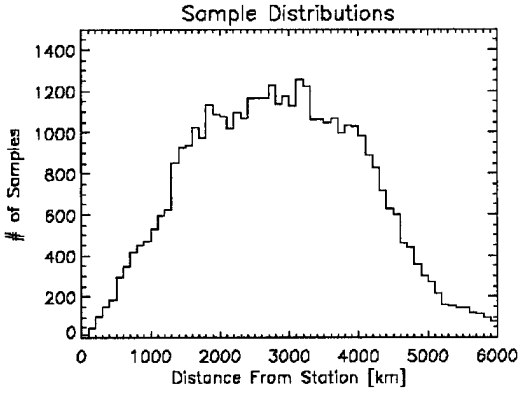

Period 75-88

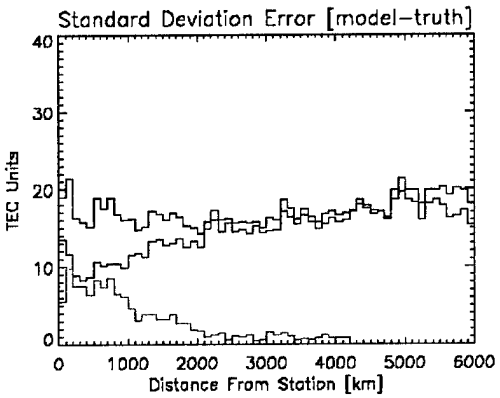

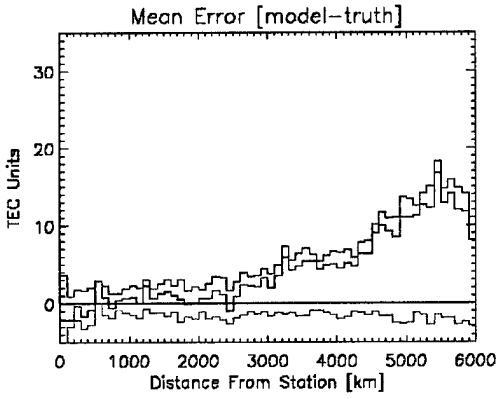

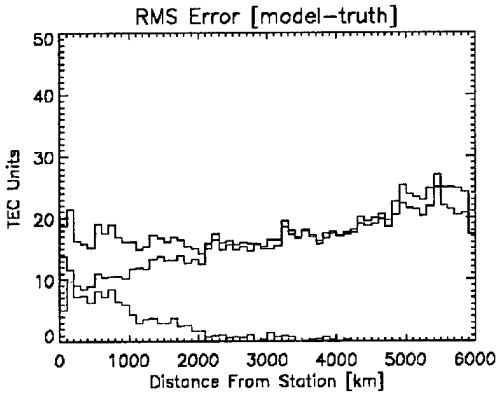

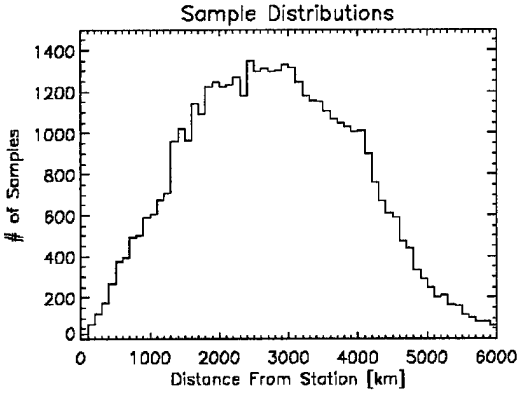

Period 89-100

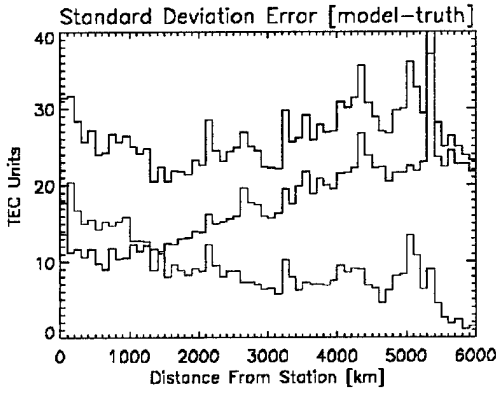

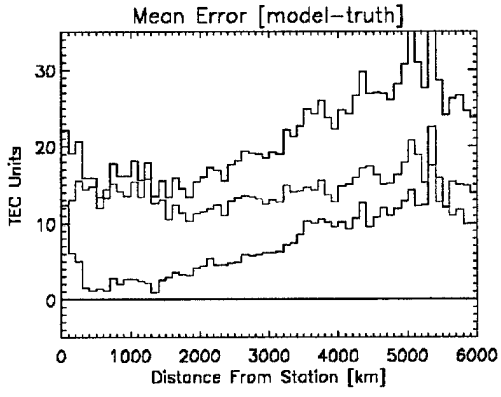

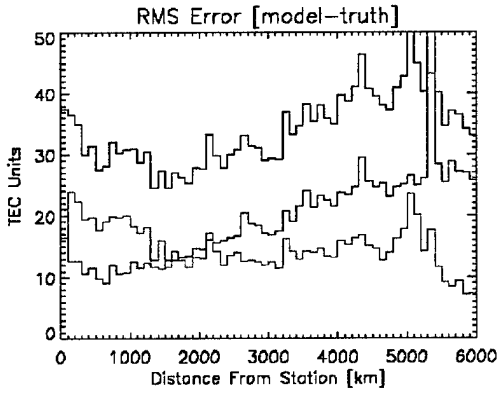

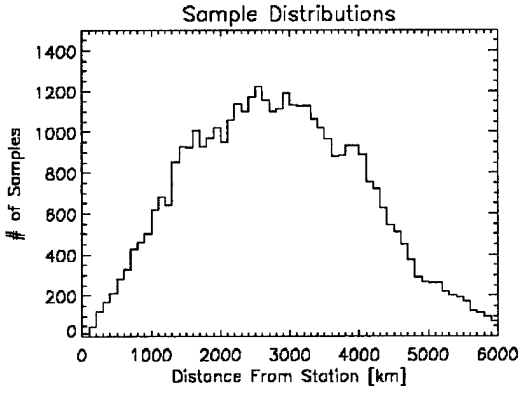

Period 101-112

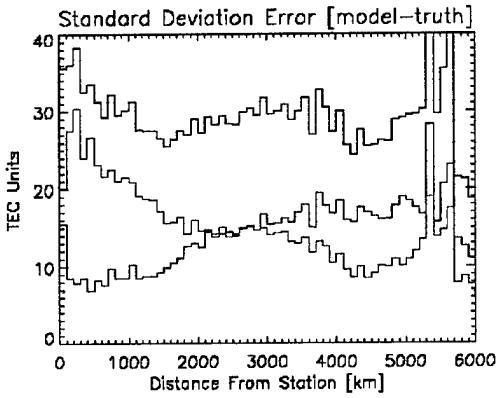

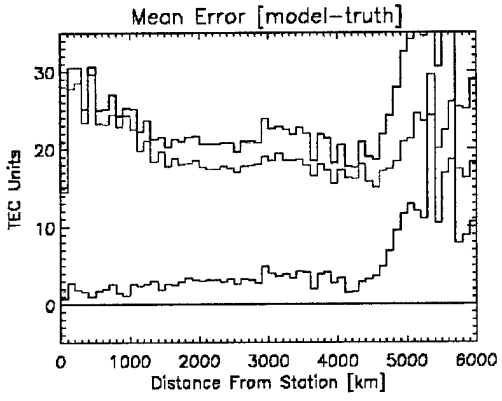

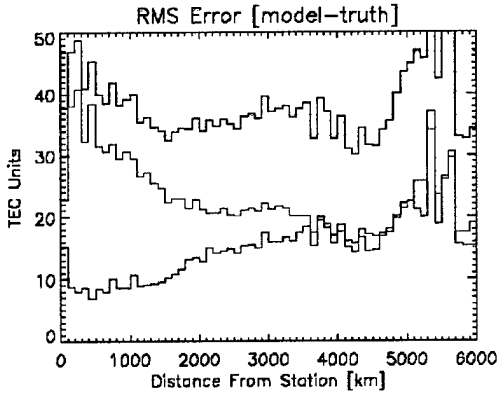

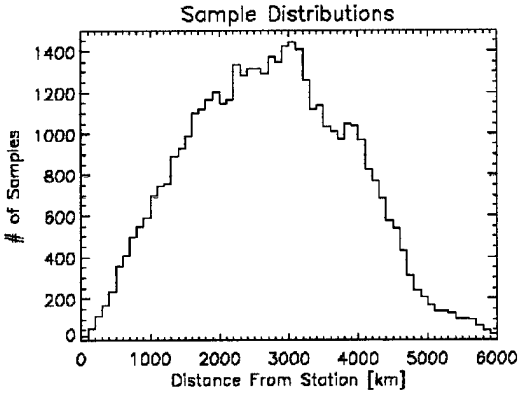

Period 113-124

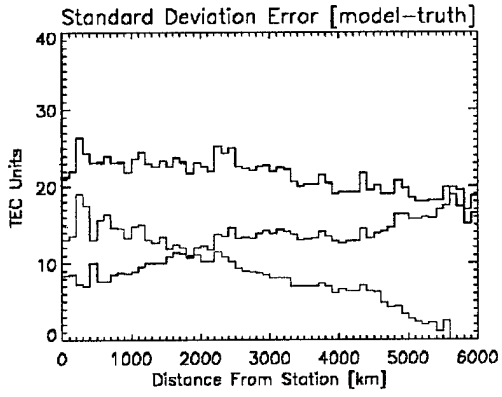

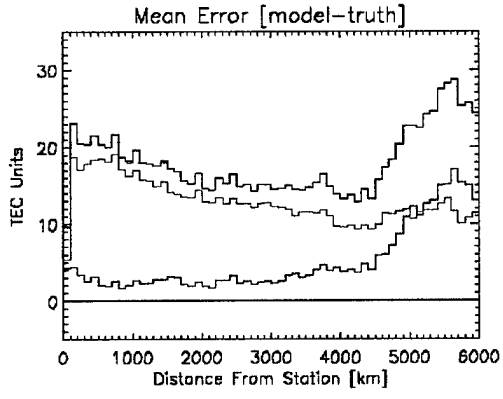

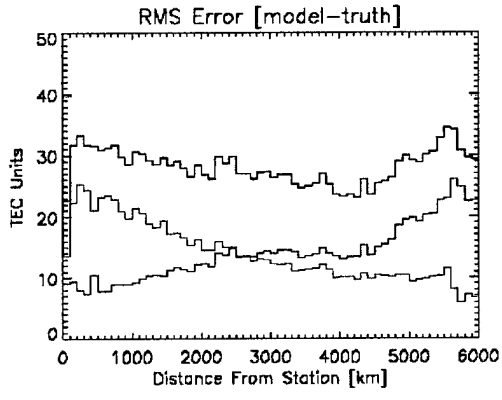

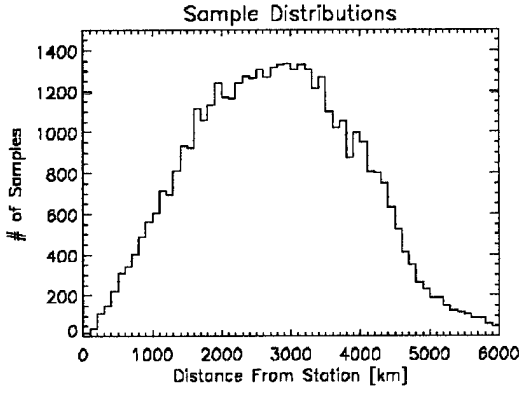

Period 125-136

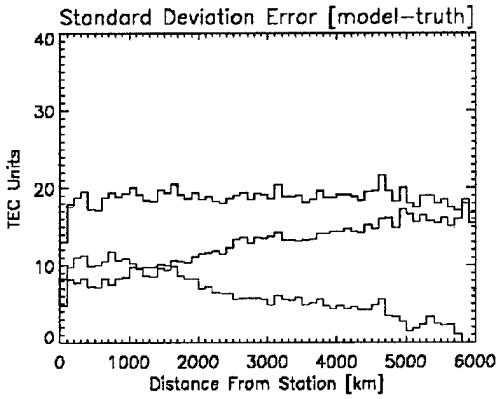

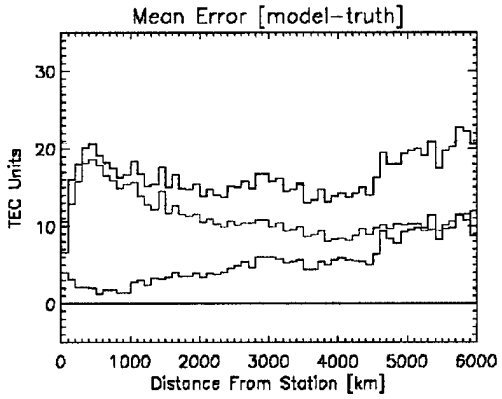

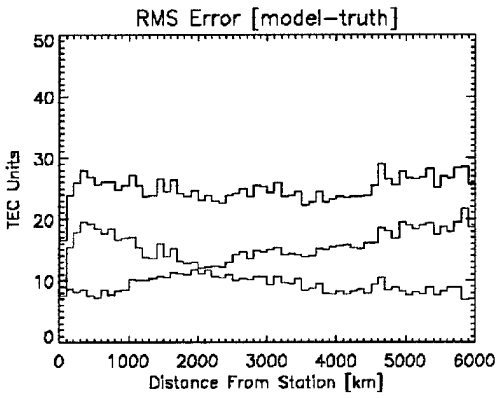

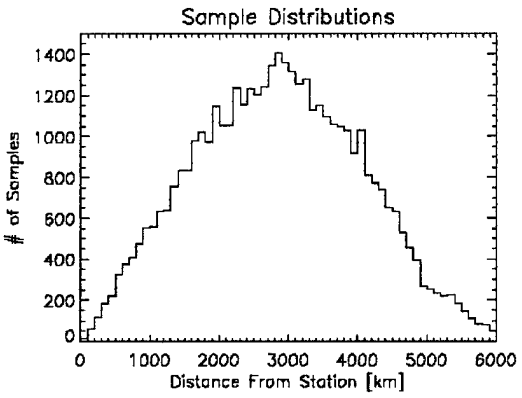

Period 137-148

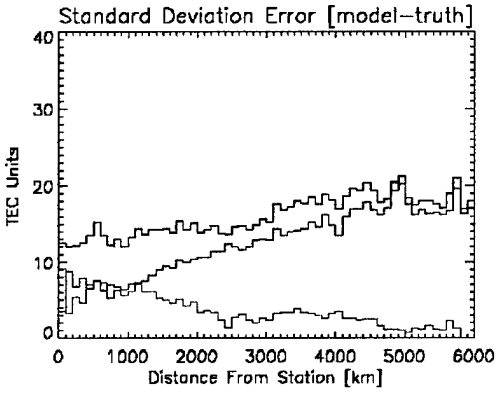

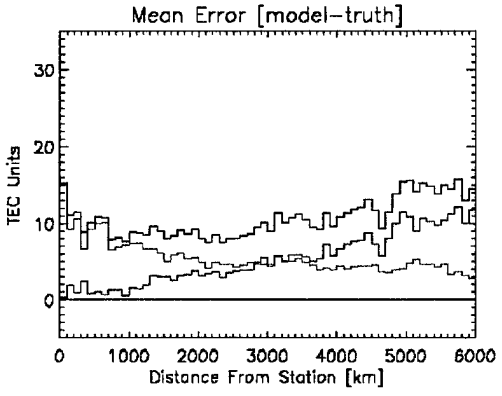

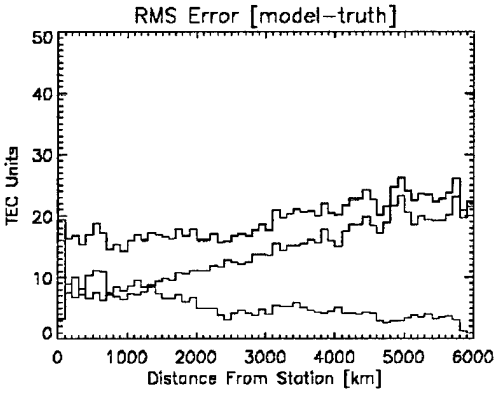

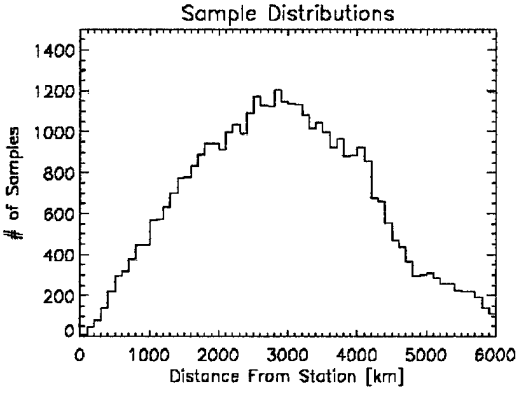

Period 149-160

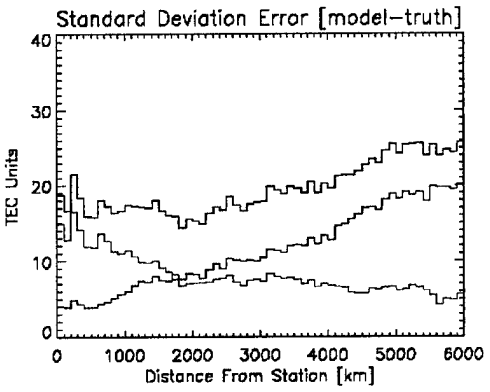

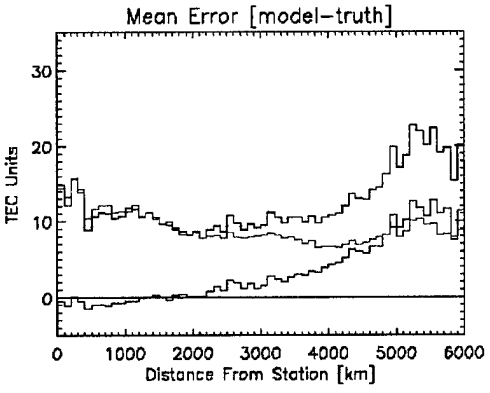

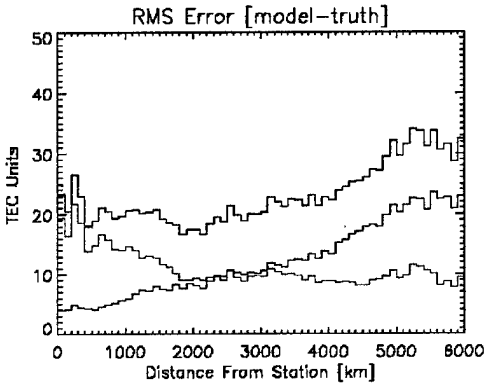

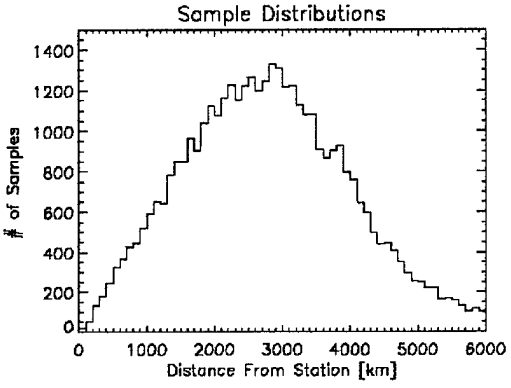

Period 161-173

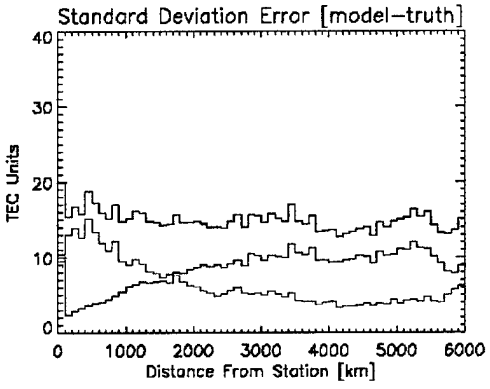

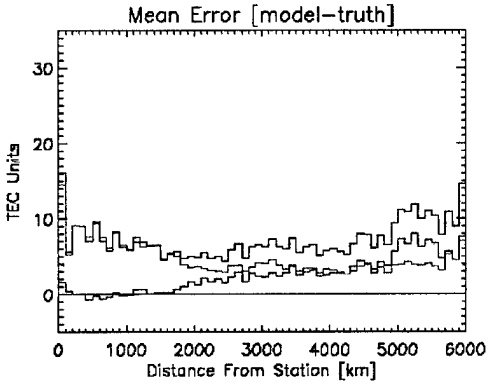

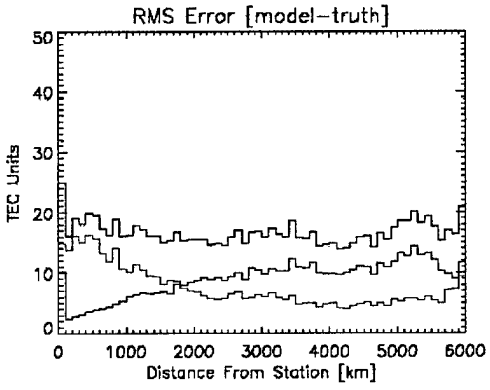

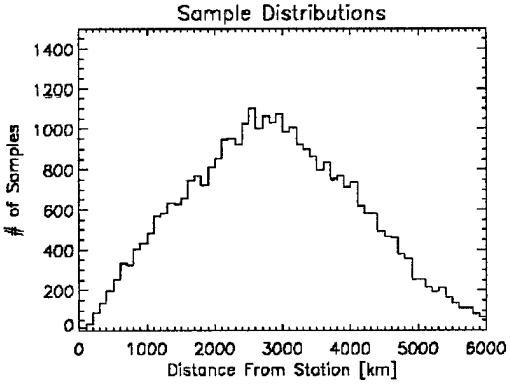

Period 174-185

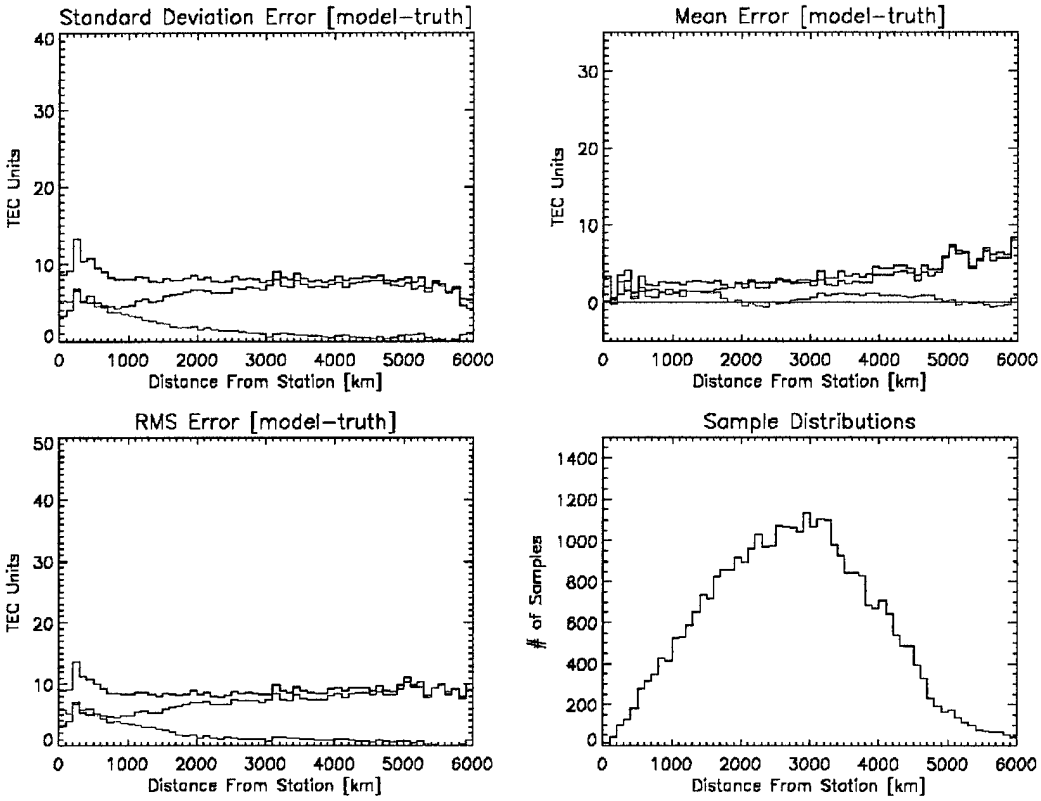

Period 186-200

Appendix E: Local Time Error Distributions by Kp

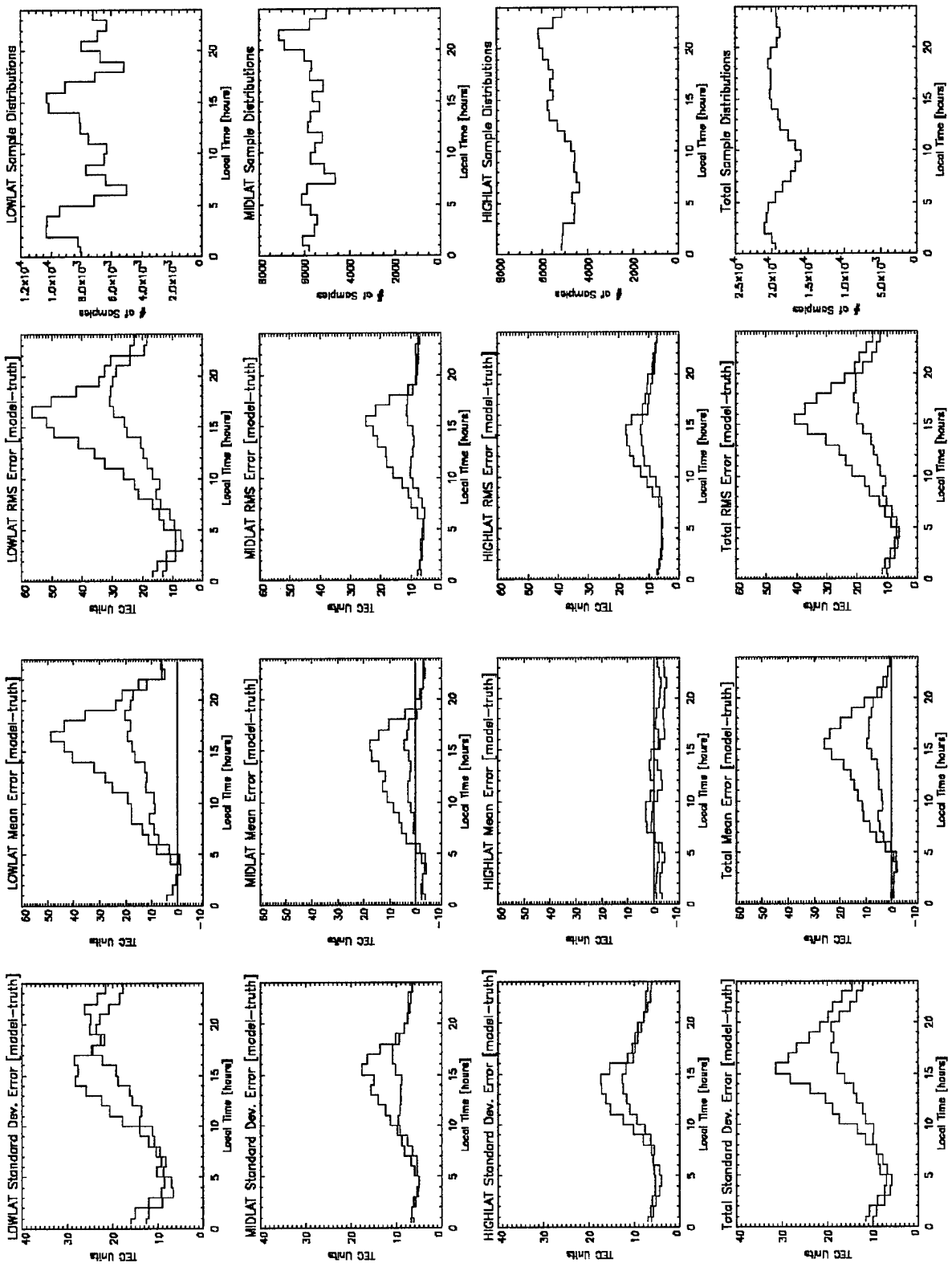

Kp Distributions for Low Kp (0-3)

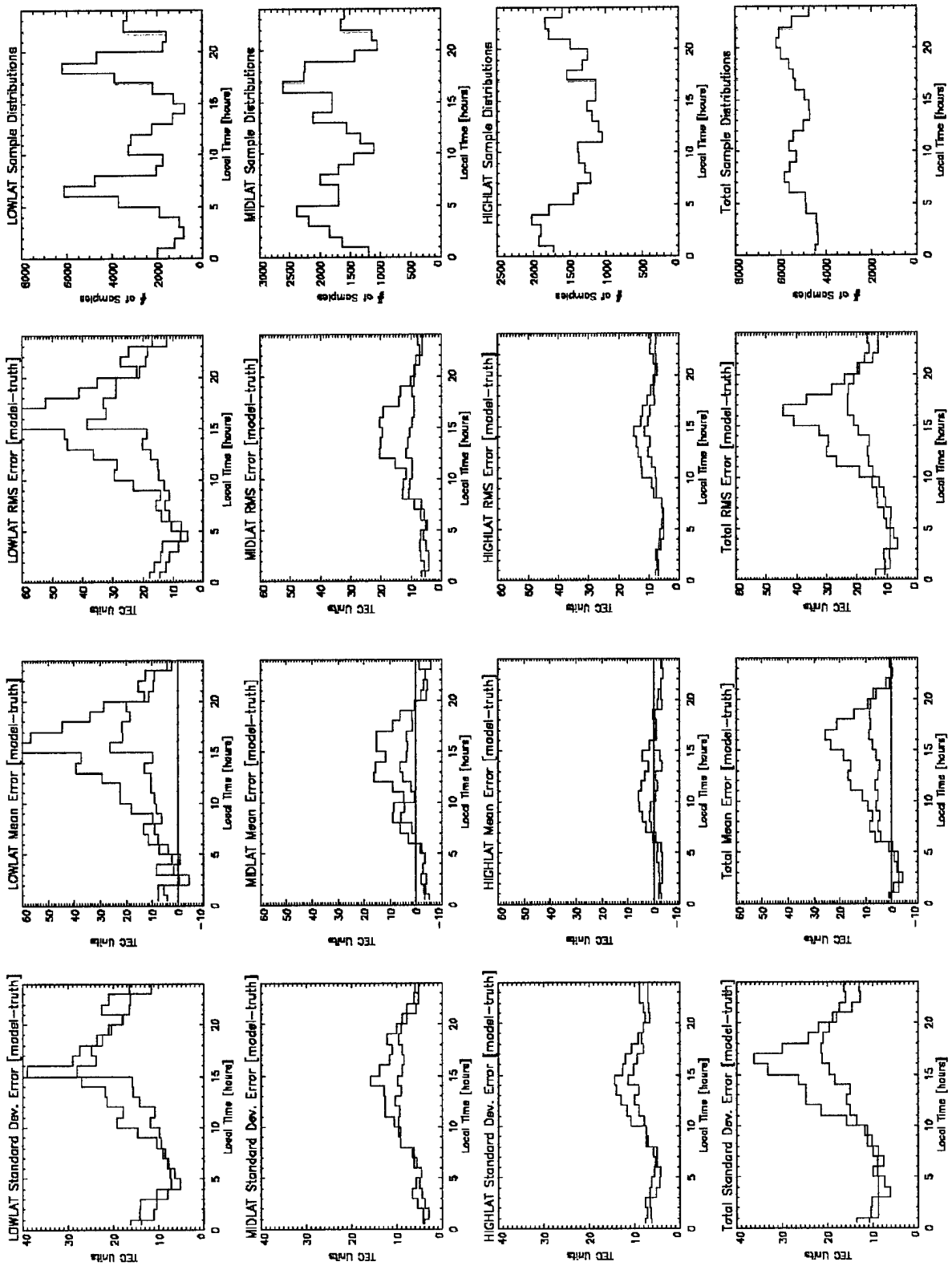

Kp Distributions for Moderate Kp (3-6)

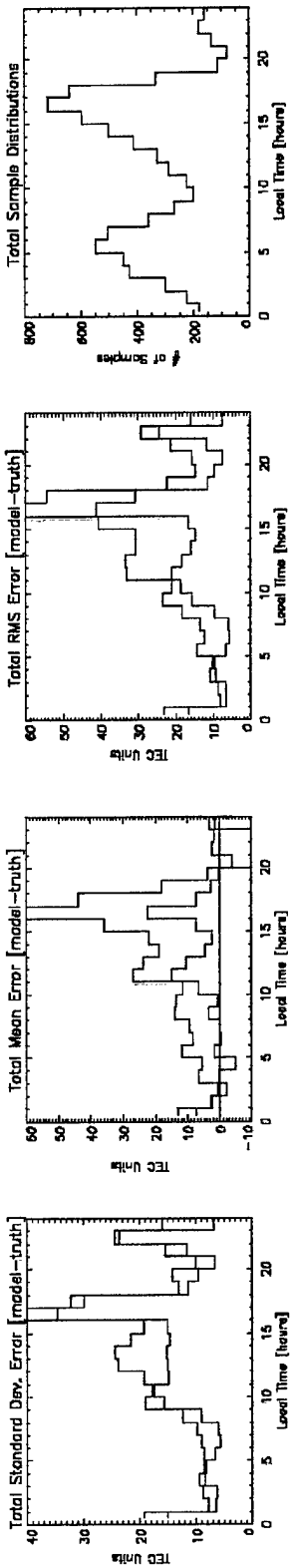

Kp Distributions for Moderate Kp (6-9)

Appendix F: Sample PRISM Output

```
YEAR   DAY  UT (sec)  F10.7  Kp   Solar Sunspot Number
-------------------------------------------------------
2002    35      0.0      210.0  2.0   196.00
  0
    Latitude     Longitude     Latitude  Longitude Latitude Longitude
 Starting Ending  Starting Ending     Step  Step      Delta  Delta
 -90.00   90.00   0.00  356.00     46    90       4.00   4.00
Number of altitude points =    50
  Altitudes
   90.00   95.00  100.00  105.00  110.00
  115.00  120.00  125.00  130.00  135.00
  140.00  145.00  150.00  160.00  170.00
  180.00  190.00  200.00  210.00  220.00
  230.00  240.00  250.00  260.00  270.00
  280.00  290.00  300.00  320.00  340.00
  360.00  380.00  400.00  450.00  500.00
  550.00  600.00  650.00  700.00  750.00
  800.00  850.00  900.00 1000.00 1100.00
 1200.00 1300.00 1400.00 1500.00 1600.00

-90.00  0.00 -74.50  17.30  20.28 CAP
Densities
7.83E+02 2.18E+03 6.05E+03 1.55E+04 2.50E+04
3.43E+04 4.43E+04 5.67E+04 7.09E+04 8.38E+04
9.54E+04 1.06E+05 1.16E+05 1.33E+05 1.48E+05
1.61E+05 1.73E+05 1.85E+05 1.97E+05 2.11E+05
2.26E+05 2.42E+05 2.60E+05 2.83E+05 3.07E+05
3.31E+05 3.53E+05 3.72E+05 3.92E+05 3.96E+05
3.84E+05 3.63E+05 3.37E+05 2.70E+05 2.12E+05
1.68E+05 1.33E+05 1.07E+05 8.77E+04 7.48E+04
6.37E+04 5.44E+04 4.64E+04 3.37E+04 2.45E+04
1.78E+04 1.30E+04 9.43E+03 6.86E+03 4.99E+03
  FoF2, HmF2,   FoF1, HmF1,   FoE, HmE   TEC
  5.65 339.54   0.00   0.00   1.42 110.00  15.62
```

Appendix G: A sample of a PRISM TEC RTA output.

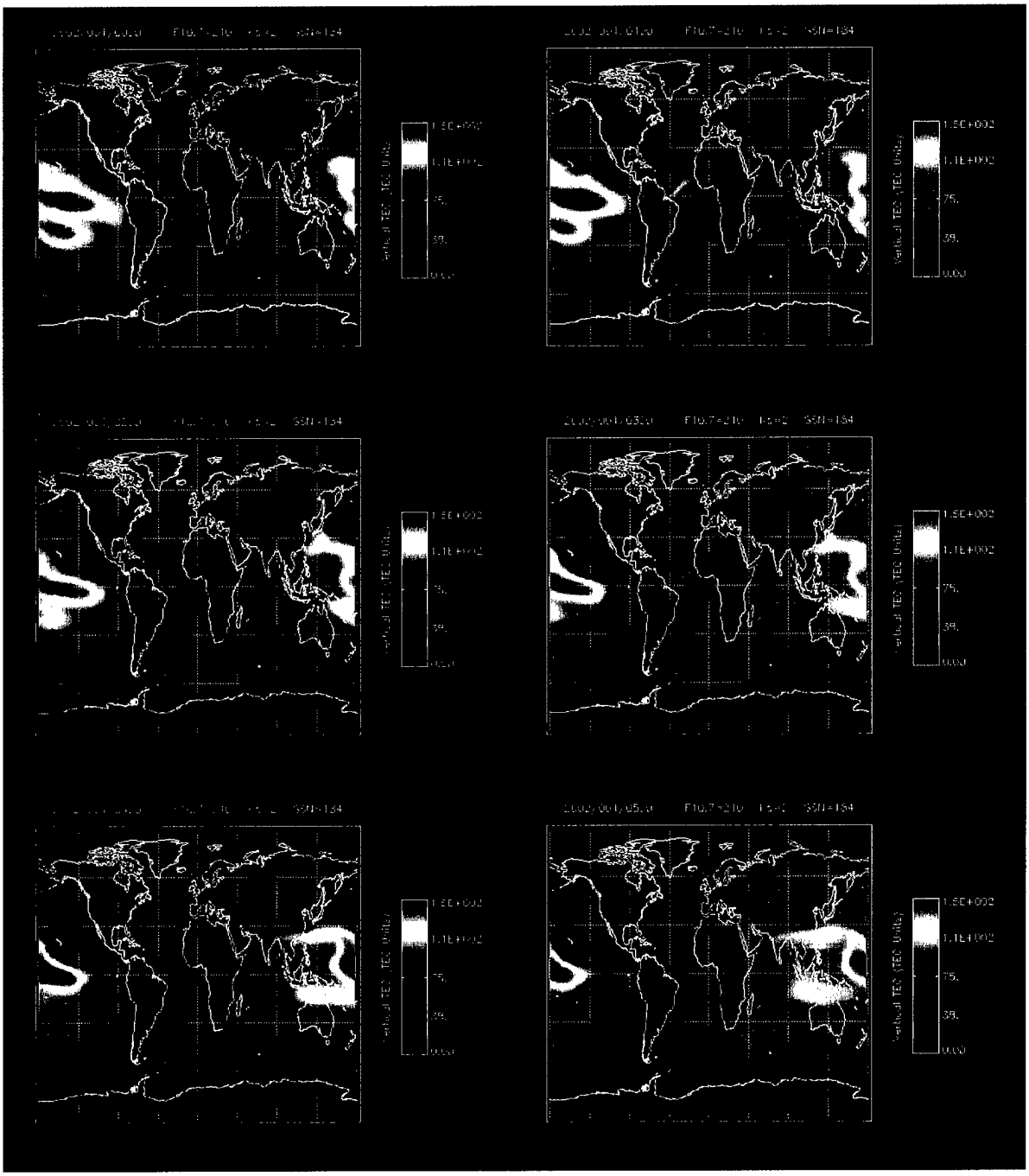

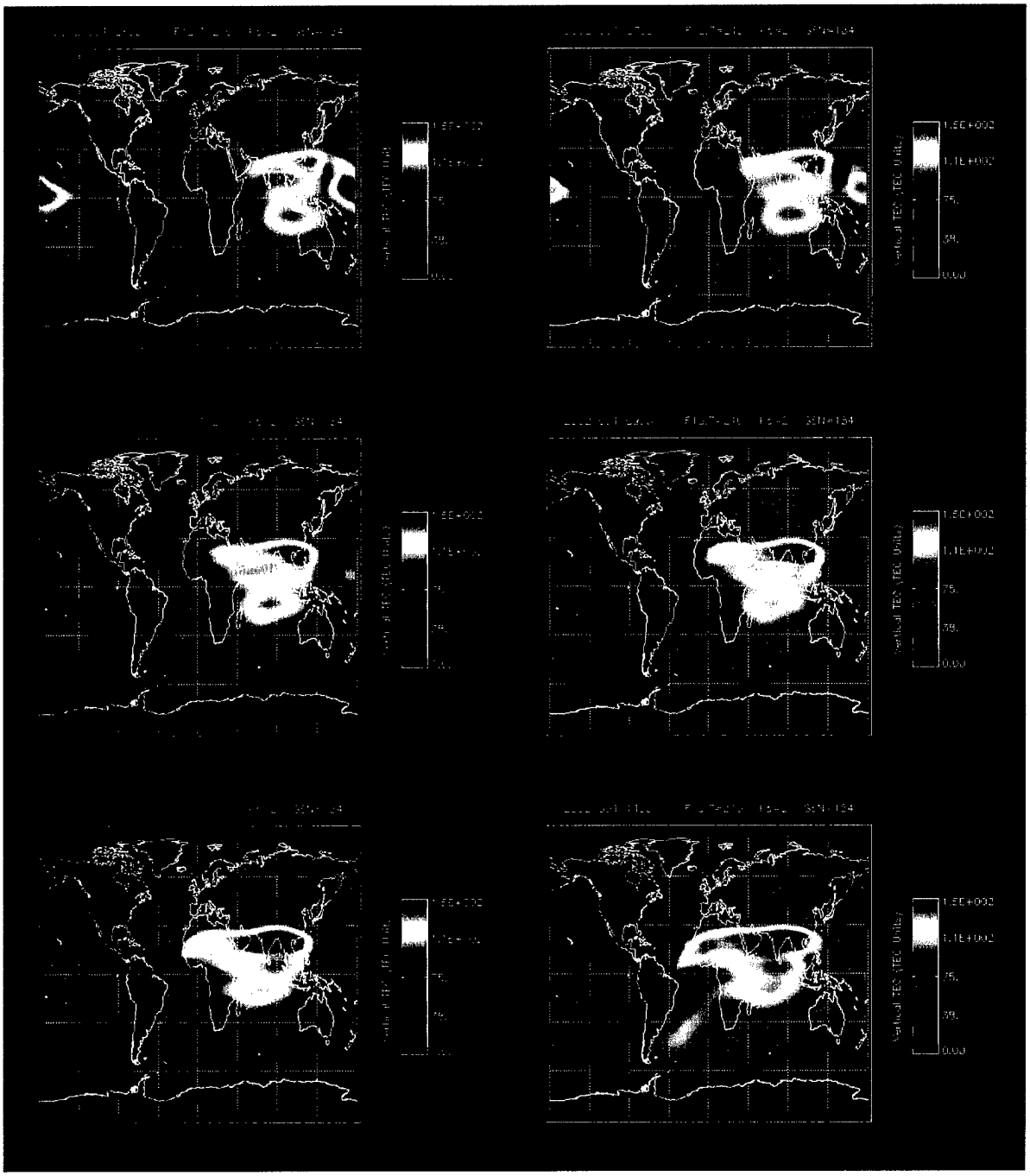

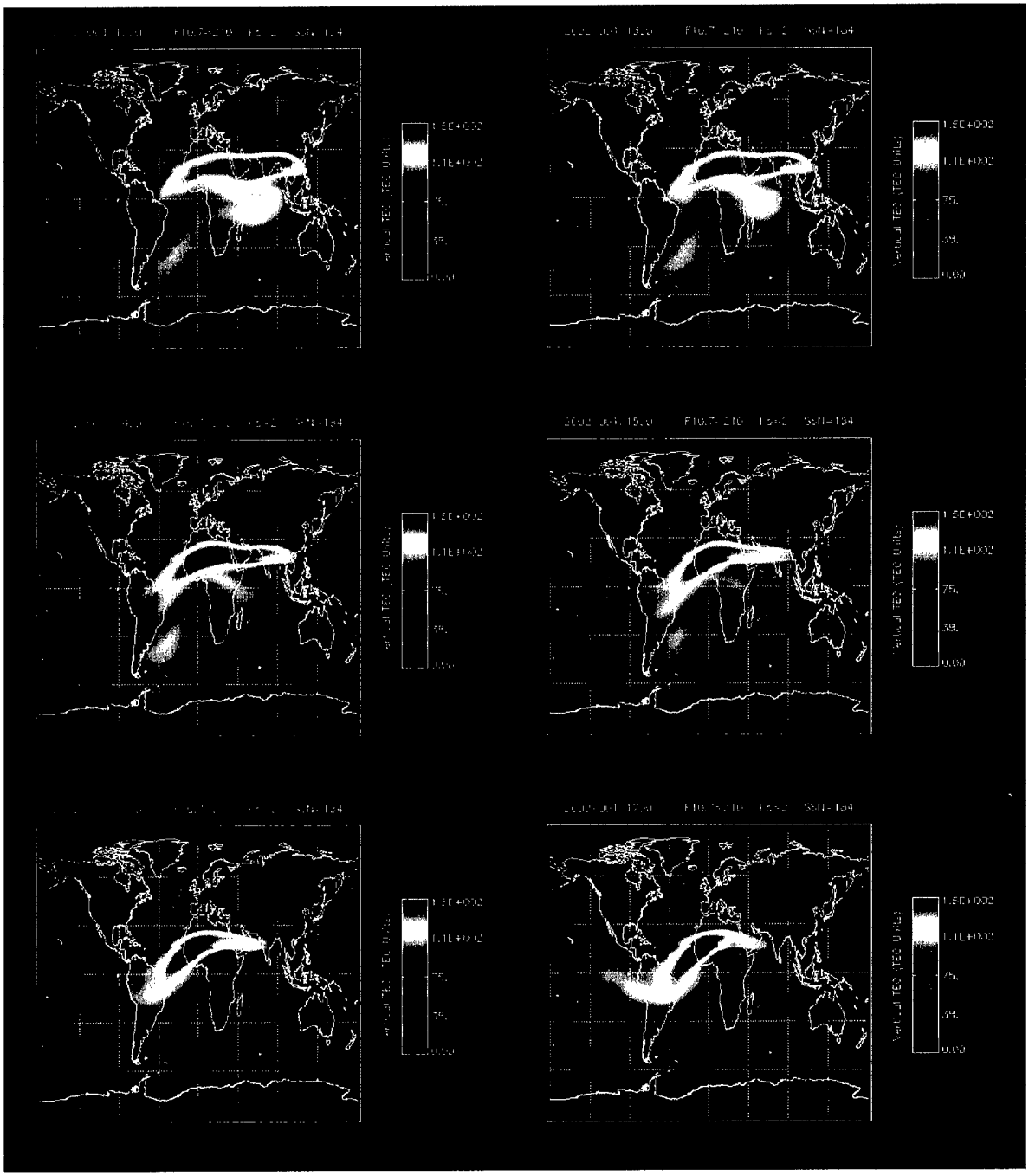

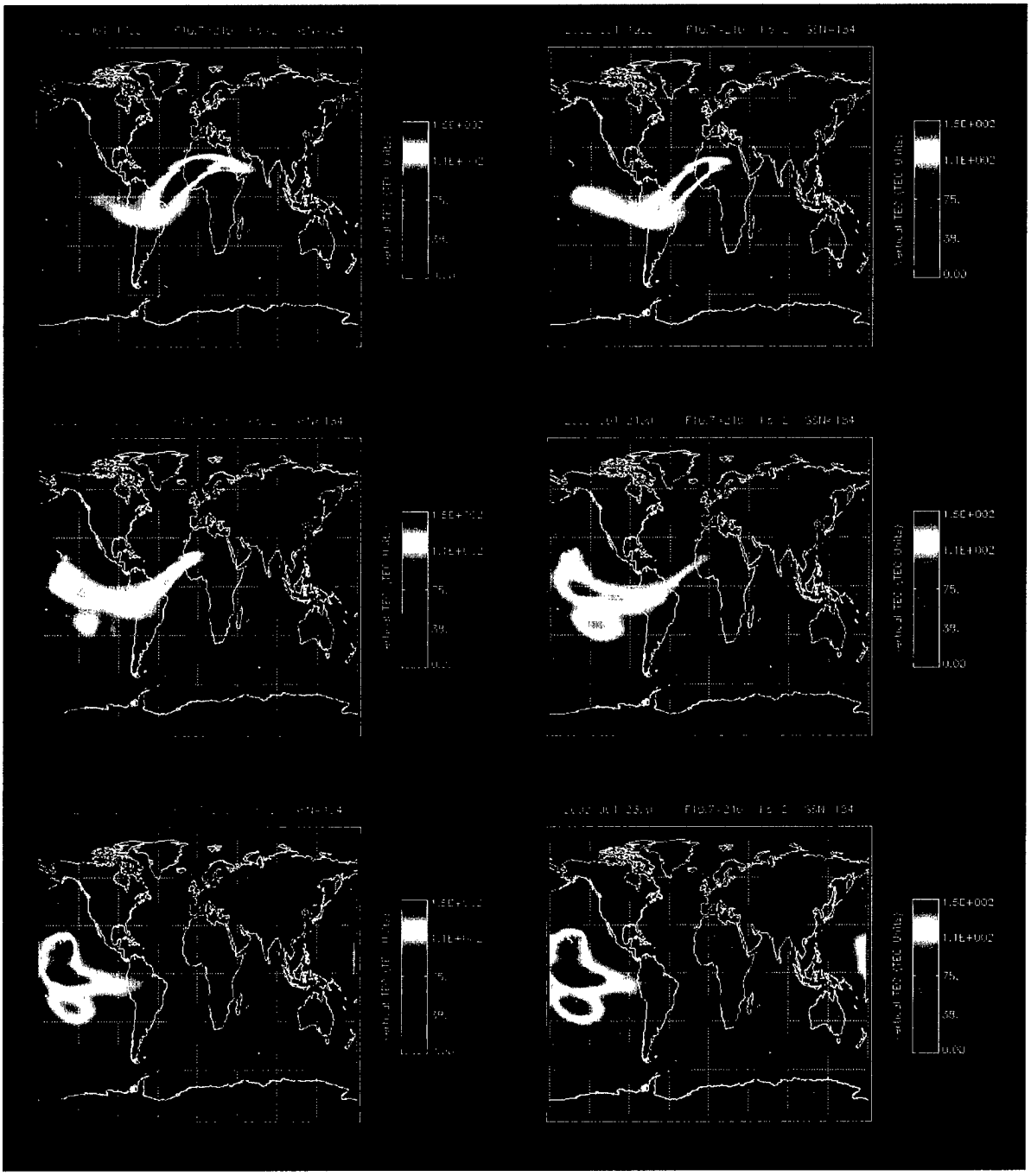
1.5E+002
1.1E+002
75.
38.
0.00

References

Anderson, D. N., A Theoretical study of the ionospheric F-Region equatorial anomaly, II, Results in the American and Asian sectors, Planet. *Space. Sci.*, 21, 421-442, 1973.

Brace, L. H., and R. F. Theis, Global empirical models of ionospheric electron temperature in the upper F-region and plasmasphere based on in-situ measurements form the Atmosphere Explorer-C, ISIS 1, and ISIS 2 satellites, *J. Atmos. Terr. Phys.*, 43, 1317,1981.

Callahan, P., TOPEX GDR user's handbook, JPL D-8944, Rev. A, internal document, pp.3-9, Jet Propulsion Lab, Pasadena, CA, 1993.

Canck, Marcel H. De, Ionosphere – The Earth's Atmosphere, AntenneX Online Issue No. 63, July 2002.

Daniell, Robert E., L. D. Brown, Parameterized Real-Time Ionospheric Specification Model PRISM Version 1.5, Contract F19628-89-C-0005, Newton, MA, Computational Physics Inc., 31 Mar 1995.

Decker, D. T., C. E. Valladares, R. Sheehan, Su. Basu, D. N. Anderson, and R. A. Heelis, Modeling daytime F layer patches over Sonderstrom, *Radio Science*, 29, 249-268, 1994.

Hardy, D. A., M. S. Gussenhoven, R. R. Raistrick, and W. J. McNeil, Statistical and functional representation of the pattern of auroral energy flux, number flux, and conductivity, J. *Geophys. Res.*, 92 12275-12294, 1987.

Hargreaves, J. K., The Solar-Terrestrial Environment, Cambridge, Cambridge University Press, 1992.

Hedin, A. E., Empirical global model of upper thermosphere winds based on Atmospheric and Dynamics Explorer satellite data, *J. Geophys. Res.*, 93, 9959-9978, 1988.

Heppner, J. P., and N. C. Maynard, Empirical high latitude electric field models, *J. Geophys. Res.*, 92, 4467-4489, 1987.

Ho, C. M., B.Wilson, A. Mannucci, U. Lindquister and D. Yuan, A Comparative Study of Ionospheric Total Electron Content Measurements Using Global

Ionospheric Maps of GPS, TOPEX Radar, and the Bent Model, *Radio Science*, Vol 32, Number 4, pg 1499-1512, 1997.

Imel, D. A., Evaluation of TOPEX/Poseidon dual-frequency ionosphere correction, *J. Geophysics res.*, 99, 24895, 1994.

Jasperse, J. R., The photoelectron distribution function in the terrestrial ionospherem in Physics of Space Plasmas, Scientific Publishers, Cambridge, MA, pp. 53-84, 1982.

Jursa, Adolph S., Department of the Air Force, Handbook of Geophysics and the Space Environment, Air Force Geophysics lab, Air Force Systems Command, 1985.

Mannucci, A., B. Wilson, and D. Yuan, Monitoring Ionospheric Total Electron Content Using the GPS Global Network and TOPEX/Poseidon Altimeter Data, Proceddings of the Beacon Satellite Symposium, University of Wales, Aberystwyth, 1994.

Pulliam, R., W. Borer, D. Decker, P. Doherty, Operational Ionosphere Model Validation, Proceedings of the American Institute of Aeronautics and Astronautics Space 2000 Conference & Exposition, Paper #A00-42948, Long Beach, CA, Sep 2000.

Rasinkangas, R. Textbook on Space Physics, International Space Physics Educational Consortium, November 1998.

Strickland, D. J., D. L. Brook, T. P. Coffey, and J. A. Fedder, Transport equation techniques for the deposition of auroral electrons, *J. Geophysics Res.*, 81, 2755-2764, 1994.

Tascione, Thomas F., Introduction to the Space Environment, 2nd Edition, Malabar, FL, Krieger Publishing, 1992.

Vladimer, J. A., P. Jastrzebski, M. C. Lee, P. H. Doherty, D. T. Decker, D. N. Anderson, Longitude structure of ionospheric total electron Content at low latitudes measured by the TOPEX/Poseidon satellite, *Radio Science*, vol. 34, Number 5, 1239-1260, 1999.